Induced polarization and Resistivity measurements on a suite of near surface soil samples and their empirical relationship to selected measured engineering parameters

Johnmary Kiberu

March, 2002

Induced polarization and Resistivity measurements on a suite of near surface soil samples and their empirical relationship to selected measured engineering parameters

by

Johnmary Kiberu

Thesis submitted to the International Institute for Geo-information Science and Earth Observation in partial fulfilment of the requirements for the degree in Master of Science in *Applied Geophysics*.

Degree Assessment Board

Thesis advisor	Dr. Jean. Roy
Thesis examiners	Dr. Ir. Slob (**External Examiner, TU Delft**)
	Prof. C. Reeves (**Chairman**)
	Prof. F. Van der Meer (**Member**)
	Ir. Sporry (**Member**)

INTERNATIONAL INSTITUTE FOR GEO-INFORMATION SCIENCE AND EARTH OBSERVATION

ENSCHEDE, THE NETHERLANDS

Disclaimer

This document describes work undertaken as part of a programme of study at the International Institute for Geo-information Science and Earth Observation (ITC). All views and opinions expressed therein remain the sole responsibility of the author, and do not necessarily represent those of the institute.

Abstract

Time–domain induced polarization (IP) and resistivity laboratory measurements were performed on 43 natural soil samples obtained from Antequera (Spain), Nairobi (Kenya) and Enschede (The Netherlands). Soils are polarizable when they contain clay minerals, which are the main causes of swelling and shrinking. These two effects are a major concern for foundation engineering because they cause extensive damage to structures. Therefore, there is a need to develop a technique that would be able to identify, at the outset of an investigation, those soils that posses undesirable expansion characteristics.

Clayey soils exhibit membrane polarization which is due to ion accumulations and variation in ion mobility within the pore passages. The use of IP was an attempt to identify clay minerals. The following parameters were measured: Chargeability (m) and resistivity (ρ) using a transmitter and receiver. Soils were saturated with distilled water and emphasis was given to the analysis of m as a function of water content. The relationship of m to particle size distribution was illustrated by use of triangular plots.

The laboratory results showed that the IP response was dependant on the amount of water and cation exchange capacity (CEC), which is directly related to clay minerals. Decay curve analysis was performed in terms of 3 exponential decays and the respective amplitudes (Aj) were found to be statistically dependant on water content. However, the ratios of Aj did not show any dependency on water content, and were therefore, used to differentiate soil samples according to their origin.

Keywords

Induced polarization, time domain, chargeability, decay curve analysis, resistivity, cation exchange capacity, grain size, porosity, water content

Acknowledgements

I would wish to express my thanks and gratitude to my supervisor: Dr. Jean Roy who proposed this project and guided me up to the final handing in of this thesis. His critical comments and helpful suggestions contributed to enrich my thesis.

All the staff of Applied Geophysics division of ITC Enschede are greatly acknowledged. Prof. Dr. C. Reeves, Dr. S. Barritt, Ir. R. Sporry and Mr. W. Hugens are thanked for their support and encouragement.

I would wish to extend my thanks to the Head of Geology Department, Makerere University; Dr. Andrew Muwanga, for giving me permission to attend this course. All the staff of ITC and DISH hotels are appreciated for ensuring the optimum academic environment that has helped me in the completion of the study period. The Netherlands government is thanked for awarding me a scholarship that enabled me to attend this course at ITC.

The research would not have taken foot without the help of Mr. Patrick Kariuki who provided me with the necessary data and the soil samples. I thank Drs. B. de Smeth for the advice he offered during the experiment and for the permission to use the Chemistry Laboratory.

To my classmates, without you, life would have been hard for the 18 months. I would lie to express my sincere appreciation and gratitude to Mr. John Kironde for the relentless help, he has offered me by staying and keeping a keen eye on the property at home. Thank you very much for your prayers and encouraging words.

My gratitude to the computer cluster manager, secretary and ITC reproduction department for their assistance at all moments.

Contents

List of Tables

List of Figures

Chapter 1

Introduction

1.1 Introduction

The use of Induced electrical Polarization (IP) technique over the past 30 years has proven to be one of the most successful geophysical methods in providing in situ information about rock mineralogy especially in search for disseminated minerals with electronic conductivity. For this case, the technique is being applied to quite a new field, which concerns materials that do not contain conductive minerals but rather clay minerals. The method has been used, though rarely in the fields of hydrogeology (Vacquier et al., 1957), (Marshall and Madden, 1959), oil and gas field exploration (Sternberg and Oehler, 1990) and in environmental studies such as mapping of polluted land areas (Towel et al., 1985). However, it is worth noting that previous IP studies of non metallic earth materials have focused on clay mineral soils, sandy and shaly sediments containing clay minerals (Klein and Sill, 1982). Laboratory studies on the electrical characteristics of such soils is able to show diagnostic signatures of what they consist and thus, hopefully, can lead to a proper classification of soil material in terms of clay presence and other materials.

Polarization is a geophysical phenomenon which measures the slow decay of voltage in the ground after the cessation of an excitation current pulse (time domain method) or low frequency variation of the resistivity of the earth (frequency domain method) (Sumner, 1976). In simple terms, the IP effect reflects the degree to which the subsurface is able to store electric charge, analogous to a leaky capacitor. It occurs when an electric current passes through a rock/soil. If the current is interrupted, a difference in potential, which decays with time is observed. The rate of decay of this potential (induced polarization potential) depends on the lithology of the rock, its pore geometry and degree of water saturation. Schlumberger (1920) noted that this phenomenon was taking place in the bulk volume of the rock and not on the field electrodes used to measure it. The dependency of polarizability of rocks/soils upon their

lithological composition and hydrogeological properties favors the application of the IP method for hydrogeological (groundwater) and engineering geologic investigations.

This study is based on laboratory induced polarization and resistivity measurements on a suite of near surface soil samples from Spain, The Netherlands and Kenya. The empirical relationship between electrical IP measurements and the measured engineering parameters will be a subject of interest in the analysis of the results. For this research, the engineering parameters are taken to be CEC, clay content, porosity and grain size, however the results will be compared with other engineering parameters from the main soil swelling project[1]. These near surface natural soils rarely contain conductive particles (e.g graphite), and their electrical properties are attributed to the presence of clay minerals. Soils that contain clay minerals and change volume with water content are termed as swelling soils. An attempt to use this technique on soil samples in the laboratory, will hopefully provide a low cost non–invasive means of studying swelling soils for engineering purposes and to asses the suitability of the sub surface. This may ultimately decrease the cost of evaluation and help to make the right decision at such an important stage in decision making for an engineering programme.

The IP effect in earth materials having non metallic minerals is usually referred to as membrane polarization. This requires the presence of particles such as clays, with a negative surface charge, which in the presence of an electrolyte like water, attracts cations and forms an electrical double layer on the particle surface. The volume property of soil related to this phenomenon is the Cation Exchange Capacity (hereafter referred to as CEC) (Olhoeft, 1985) which is proportional to the surface charge density and the specific surface area of the solid phase (Bolt and Bruggenwert, 1978) and mostly related to clay minerals. This property supports the alternative procedure of IP in trying to detect clay minerals apart from the other conventional laboratory techniques like Xray diffraction.

The study will attempt to relate polarizability and resistivity parameters obtained from Induced electrical polarization measurements with other properties measured through other techniques and these include CEC, clay content, clay mineralogy, particle size, and water content. All soils that show a membrane type of polarization have their own characteristic sets of electrochemical reactions. These reactions are the basis of the IP technique in volume characterization and evaluation.

[1]PhD program involved in mapping swelling clays

1.2 Problem definition

A systematic and thorough laboratory study, which is the purpose of this study, is needed to understand the effects of clay within the soil samples on induced electrical polarization laboratory measurements. The swelling behavior of soils, which is caused by presence of clay minerals, is a destructive phenomenon from an engineering point of view and given its widespread distribution within the soils, a solution to this problem has to be sought. However the problem of identifying, at the outset of an
investigation, those soils likely to possess undesirable swelling characteristics remains one of the most troublesome phases of the subject.

In a separate project, a study of this behavior by the Ground & Space-based shortwave infrared (SWIR) reflectance spectrometers to identify clay minerals is under way. These methods are designed for a low–cost large scale mapping. However, for foundation engineering, it requires volume characterizations which involve taking measurements on soils in situ. In many parts of the world, the possibility of damage to structures due to the swelling of clays constitutes a severe problem in design and construction. Owing to the serious economic implications as a result of this phenomenon there is a need for an in-situ information provider and in this context, the technique of induced electrical polarization will be used in an attempt to identify clay minerals and provide information for volume investigations.

The IP technique in this research assumes the measurement of both resistivity ρ and the polarizability η. This procedure will provide a convenient means of examining the dependence of IP response on variables such as grain size, clay type (mineralogy), cation exchange capacity, and water content. The swelling potential of clay minerals is directly linked to their ability to adsorb water and also depends on the clay type. Therefore, this experimental investigation is focused on natural soil samples that consist of phyllosilicates (clays). The fact that clay minerals have the ability to conduct electricity through ion exchange reactions with pore fluids e.g. water in soil samples, will provide the basis of evaluating the potential role of induced polarization technique in swelling potential evaluation.

This project is run as a component in support of a wider project[2] to detect the swelling potential of clays by low cost non–invasive means. Swelling soils and expansive clays are major hazards because they cause extensive damage worldwide every year. Houses, offices, schools and factories are always subject to structural damage once constructed on such soils.

[2]PhD program involved in mapping swelling clays

1.3 Objectives of the research

The main objectives of this research project are the following:

- Study the technique of IP and concentrate on its possible application to the clay swelling potential mapping.
- Observe the inter-relationship between variables such as IP response, resistivity, water content, CEC and grain size.
- Attempt to identify all sources of error encountered in the experiment in an effort to improve the IP technique in this field of application.
- Attempt to quantify the Cation Exchange Capacity (CEC) and acquire information about the nature of the clay mineralogy in the soil samples by the IP technique.

1.4 Research Questions

1. Is there any relationship between the amount of water in the soil samples with the chargeability and resistivity values so obtained?
2. Can the IP technique be used to differentiate between different soil types according to their electrical response?
3. Does the geological and geographical background of the soil samples have an effect on their electrical and water adsorption behaviors?
4. Is there any relationship between the granulometrical composition of soils and their polarizability?
5. Is there any effect on the polarizability of soil samples based on the preparation methods (remoulding, re–sampling and saturation)?
6. Can the analysis of the exponentials of the individual decay curves obtained lead to parameters related to granulometry and water content?
7. Is it possible to use the IP technique to quantify CEC given other data such as clay content and water content? Can it also identify the clay minerals?

1.5 Hypothesis

- By measuring the IP response when the water content and granulometric distribution (including clay content) are provided by other means, the IP technique can be used to quantify CEC.

1.6 Sources of Data and Information

1.6.1 Literature

The time domain electrical induced polarization technique has been used in the study of chargeability of fine sediments and soils. Some literature on the time domain technique was obtained from the library to support this research and notably papers from journals.

The software programs used in this research are categorized into two:

- Data Processing
  - SPSS
- Data documentation and presentation
  - MSword, Grapher, MsPowerpoint,and LaTex

1.6.2 Data

Ancillary data was obtained from the main swelling project (Mr. Patrick Kariuki[3]). This included a set of data about particle size analysis and cation exchange capacity values (CEC). These data sets covered soil samples from **Spain and Kenya**, no data set was available for samples from **The Netherlands**. Therefore, the laboratory study with samples from The Netherlands involved water content determination and chargeability measurements.

A particle size distribution (PSD) analysis is a necessary index test for soils because it represents the relative proportions of different sizes of particles. From this it is possible to tell whether the soil consists of predominantly gravel, sand, silt or clay sizes and to a limited extent which of these sizes ranges is likely to control the engineering properties.

There are mainly two procedures of carrying out a particle size analysis. The first one is sieving which is used for gravel and sand size (coarse) particles that can be separated into different size ranges with a series of sieves of standard aperture. The

[3]PhD student, Earth System Analysis Department

second procedure is the sedimentation which is suitable for small size particles like clay and silt (Head, 1992). Measurements in this case are made either by sampling a suspension of soil particles in water by means of special pipette or by determining the density of the suspension using a special hydrometer (the hydrometer method). The data on particle size analysis for clay and silt fractions in this research was obtained by the sedimentation procedure and in particular by means of a special pipette. The sedimentation procedure is based on the fact that largest particles fall more quickly through water than smaller ones. Thus, if a suspension is made up of clay and silt in water, the silt will settle out more quickly than the clay and by measuring the speed at which the suspension as a whole settles out, it is possible to determine the distribution of particle sizes.

The CEC expresses the number of positive charges from the ions that neutralize the negative charge of soil particles. It was determined through chemical means by the following procedure. The soil samples were percolated with ammonium acetate and the bases were measured in the percolate. The samples were then subsequently percolated with sodium acetate, made by mixing dilute solution of Na (1000mg/l) with 25 ml of IM NH_4OAc solution, where the excess salt was then removed and the adsorbed sodium exchanged by percolation with ammonium acetate. However, there are two procedures for doing this:
1. Percolation tube procedure
2. Mechanical extractor procedure. For this study, the method used was the percolation tube procedure (Reeuwijk, 1995). For Na measurements, 12.5 ml of 2%Cs suppressant was added to the sodium acetate solution to overcome ionization interference, before mixing it with the soil samples. Exchangeable Na was then measured by flame emission spectrophotometry (FES) at a wavelength of 589.0 nm. The sodium in this percolate is a measure for CEC.

In addition, information about geology, location, depth at which the soils where collected and other relevant short descriptions were also made available.

1.7 Research methodology

The general research methodology was designed to make an effort to fulfill the objectives. The main induced polarization data was treated in collaboration with other data obtained from the swelling clay project. The methodology for the research work is graphically summarized in the flow–chart (Figure 1.1). The dotted line separates the data obtained from the swelling clay project (Particle size analysis and CEC) and that obtained through this research.

- Step 1
  Literature review: This involved collecting published material through literature search tools from the Library about the subject of Induced Polarization. This was done before the IP instrumentation was obtained.

- Step 2
  Set up of measuring apparatus: This involved the modification of the ITC–IP transmitter by installing a new current regulator and a crystal timer. The building up of the non polarizable potential electrodes was done and the IP sample holder put back in service after cleaning and lubrication. The Elrec–6 receiver was acquired on rental basis from IRIS France. Designing and cutting the sample tubes from the Polyvinyl (PVC) tubes was done together with the purchase of the red caps to be used for preventing soil spill over.

- Step 3
  Sample preparation: Though the samples were already collected from the field, there was a need to prepare them. This involved putting them in specially prepared sample polyvinyl chloride (PVC) tubes and saturating them with water. The sample tubes were labelled using numbers (1,2...43) and then weighed.

- Step 4
  Data acquisition: This involved taking weights of the soil samples with their containers every day. Secondly, calibrating the IP Transmitter before IP measurements. The same procedure was followed with the Elrec–6 IRIS receiver. The IP measurements were made in the time domain mode.

- Step 5
  Data Processing: This involved the use of Grapher , Excel and SPSS softwares for data analysis. Decay curve decomposition was done using non linear least squares fitting algorithms. Graphical displays were used to relate the IP response (Chargeability) with water content, CEC, resistivity and particle size. MSWord, MSPowerpoint and LaTex were used for data documentation and presentation.

- Step 6
  Data interpretation: This was based on the results obtained (i.e IP response dependence on clay content, clay mineralogy, and moisture content). After the experimentation research, conclusions and recommendations were given.

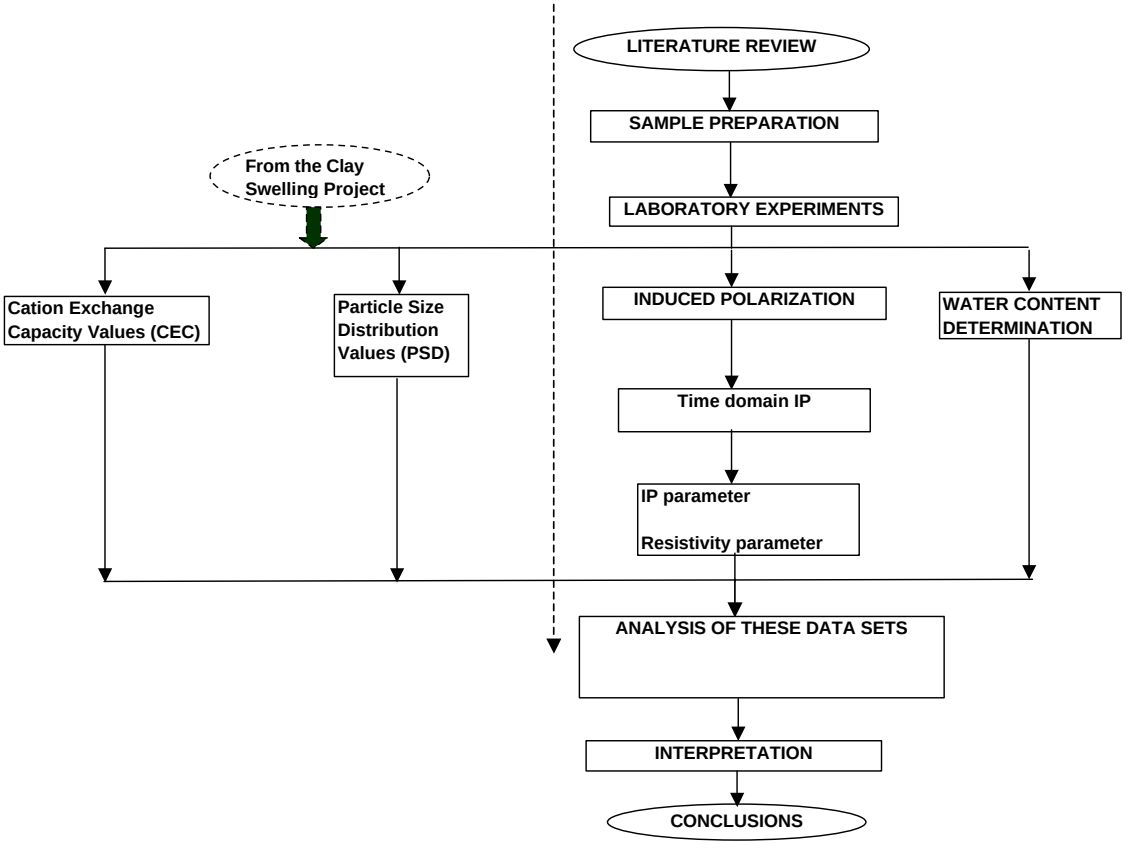

Figure 1.1: Research methodology flow chart

Chapter 2

Background to the research

2.1 Introduction

Work on the use of remote sensing techniques to identify clay minerals, notably, Space and Ground based shortwave infrared reflectance spectrometry techniques, which have the discriminatory capacity to identify clay minerals has been reported by Van der Meer (1999). Basically these techniques allow the measurement of distinctive spectra of smectite, illite and kaolinite (here listed from high to low swelling potential). Such work aims at low cost, large scale mapping of clay mineralogy however a certain proportion of coverage of the soil response would be masked especially for areas in or near urban areas, or under conditions of thick and dense vegetation. Each of these techniques essentially provides surface measurements , however, for foundation engineering, information about in situ properties of soils is required for volume characterizations and also for ground truthing and calibration of satellite–borne sensor data.

Standard geotechnical engineering practice for the delineation of areas of high swelling potential builds on extensive laboratory analysis including x-ray diffraction analysis for identifying clay mineralogy and Atterberg limits for deriving the swelling index, which are both labour intensive and expensive, and do not provide in situ measurements and results.

The swelling of clay minerals in soils is caused by the chemical attraction of water, where water molecules are incorporated in the clay structure in between the clay plates. When more water is available, the clay plates are further separated, destabilizing the mineral structure and hence causing expansion. There are factors that are involved in clay swelling and these include: type and amount of clay particles in soils, clay particle size, soil moisture content and structure. It is these factors that lead to the possible use of geophysical techniques including the IP technique that may decrease the amount of labour and money when undertaking such characterizations

that can provide a tool that may contribute to the mapping of a worldwide economic problem.

2.2 The use of geophysical techniques: electric properties and the IP technique

The technique of Induced Polarization was used in studies of Schlumberger (1920) who observed a voltage transient after a cut–off of direct current pulse that had been fed into the ground. In an attempt to describe the observed phenomenon, he attributed the transient voltage to an electrical polarization of the ground and thus used the same phenomenon in exploiting and locating unexposed ores.

The polarization phenomenon was previously studied in detail by Wait (1959a) and its modern development stems largely from the work done by Bleil (1953). In addition, Vacquier et al. (1957) and Marshall and Madden (1959) described, respectively, the time domain IP measurements on artificial clay sand mixtures and a theoretical model for membrane (clay) polarization. Ogilvy and Kuzmina (1972) described additional time domain measurements on artificial mixtures, while Roy and Elliot (1980) used horizontal layers of varying clay sand composition to model negative apparent chargeabilities due to geometric effects. Vanhala and Soininen (1995) carried out laboratory measurements using spectral induced polarization on soil samples in order to assess the effect of mineralogy, grain size distribution, moisture content and electrolyte composition on the resistivity of soil material.

Rocks, which contain clay mineralogy often display electrical properties which can not be predicted by the bulk electrical properties of the constituents (Cohen, 1981). Interactions between clay minerals and ground water can produce polarization phenomena and decreases in resistivity.

The electrical properties of minerals as they pertain to IP create three main classes: insulators, electronic conductors (sulphides, oxides and graphite) and lastly ion exchangers (clays). The two basic electrical properties are taken as resistivity ρ measured in Ohm.m and the dielectric behaviour. Resistivity is a measure of the opposition to flow of charge in a material and the dielectric behaviour refers to a substance that exhibits a polarization due to charge separation in an electric current.

Electrical resistivity is a physical property of soils and rocks that depends directly on the pore fluid's electrical resistivity and saturation, as well as the clay content. When clay is present, the resistivity becomes frequency dependant because of a fundamental charge storage mechanism that introduces a capacitive-like element in the equivalent circuit representation of the ground.

Vacquier et al. (1957) studied the membrane polarization effect in groundwa-

ter prospecting, and found that the ratio of two chargeability values measured at different times after cut–off of the current pulse, i.e., a quantity roughly dependant on the relaxation time, could be related to the grain size of the sediment. Marshall and Madden (1959) presented a membrane–polarization model which, although an ultimate simplification for sediment texture, gave qualitatively correct predictions of how grain size affects the phase spectrum of the sediment.

Polarization is caused by concentration gradients that develop at zone boundaries in response to current flow in clay rock materials. Keller and Frischknecht (1966) gave a qualitative development of this concept based on anion blockage to demonstrate that theoretically there is a peak polarization response for different clays and their concentrations. Variation in the intensity of polarization implies that clay content is also changing from place to place in the rock.

The dependency of resistivity on clay type and content has been examined to be able to predict porosity and hydrocarbon saturation from well logs. Waxman and Smits, 1968; Waxman and Thomas, 1974 assumed that the resistivity of rocks is frequency dependant, which is true at low frequencies, and therefore presented a semi empirical model for describing the dependence of resistivity on clay content, expressed as CEC per unit volume.

Vacquier et al. (1957) found that the chargeability of sand–clay mixtures was proportional to the constituent clay and its ionic exchange characteristics. The importance of rock texture for the IP effect is manifested by a weak IP in compact clays (low CEC), and a strong IP in sediments with disseminated clay particles (high CEC) on the surface of larger grains. Increased electrolyte salinity (ion concentration) and electrical conductivity decrease the IP effect (Klein and Sill, 1982).

Parkhomenko (1971) noted that for a fixed clay content, the chargeability of a rock is greater for clays having higher ion exchange capacities, however, this applies only in the active part of the IP response i.e to the left of the IP response drop, following the IP peak response in the bell–shaped IP response curve. However, this does not apply in the case of massive or pure clay. She observed that the largest induced polarization effects are obtained for clay contents in the range 3–10%. Higher or lower clay contents will give rise to a lower induced polarization. She also noted that induced polarization increases with increasing water content until an optimum saturation is reached beyond which IP decreases. The salinity and composition of the electrolyte have a profound influence upon the mode of occurrence of this maximum. With increasing concentration the maximum IP response is depressed and shifts slightly towards lower water contents. In a study with shaly sands, Ogilvy and Kuzmina (1972) demonstrated the occurrence of a maximum IP response for an optimum water content.

Illiceto et al. (1982) presented data to the effect that the maximum IP response

for an optimum water content occurred within the range $0.2 < \mathrm{Sw} < 0.6$ (where Sw is water saturation) for clean sands. When the finer (< 74 μm) fraction was washed out, this maximum shifted to lower values of Sw. When working with fine sediments, they found that the ratio A2/A3 using a decay model:

$$V(t) = A1e^{-t/T1} + A2e^{-t/T2} + A3e^{-t/T3} \tag{2.1}$$

with T1<T2<T3, was useful for lithotype identification, because for each lithotype (clays, loams, silts and sands), the ratio was falling in distinct ranges and it was statistically independent of water content.

Fraser and Ward (1965) worked with sandstone samples and observed that the IP effect was increasing with the degree of saturation almost linearly. He further observed that it was approaching zero at very small saturation. Keller and Frischkneit, 1966 and Ogilvy and Kuzmina, 1972 studied the effect of grain size parameters on the IP response. They have reported that induced polarization is low in the extreme cases of clean gravels or pure shales but that the IP effect attains a maximum value at some intermediate grain size. Dakhnov (1962) noted with the fully saturated reservoir rock that the induced polarization response was approximately proportional to the specific surface area of the constituent grains. It must be noted that specific surface area increases with a decrease in grain size.

Laboratory measurements on soil samples showed that their frequency dependant electrical response (FDER) can be used to estimate hydraulic conductivity and porosity using inversion and regression models, and in that regard
Boadu and Seabrook (2000) used a double Cole–Cole model. The FDER resistivity and phase spectra of a soil contains valuable information about its porosity, hydraulic conductivity, texture and fluid properties. The transport properties of soils and rocks such as fluid flow permeability and electrical conductivity, are important in near–surface environmental and engineering applications (Mazac et al., 1985). According to basic laboratory measurements on a variety of shaly sands, silts and clays, it is showed that the main feature of their conductivity spectra in the frequency range between 10^{-3} and 10^{3} Hertz is nearly a constant phase angle (Borner et al., 1996). Wet porous soils are generally very heterogeneous multi phase systems with a complicated internal structure whose electrical and hydraulic properties depend on the pore space geometry and also related to the microstructure of the pore space.

Polarization and the complex nature of electrical rock conductivity are attributed to zones of unequal ionic transport properties along the pore channels caused by charged interfaces and constrictions. Interactions at and near the contact area of the solid and liquid phases are the main causes of the formation of an electrical double layer. Various electrical phase boundary phenomena are of special interest, because they result in a dispersion of the electrical conductivity in the frequency

range (1mHZ to 10kHz) (Olhoeft, 1985). Using Induced polarization measurements, the complex electrical rock properties such as frequency effect or phase angle can be obtained. They depend on pore space structure and microstructure of the internal rock boundary layer. Therefore, they contain information about internal surface area, rock porosity, rock permeability and fluid properties.

Draskovits and Smith (1990) worked with data from drill hole geophysical and lithology well logs. They observed that coarse sand and gravel were characterized by high resistivity and low polarizability. Maximum polarizability was associated with silty beds having medium apparent resistivities whereas clay lithologies were indicated by low resistivities and low polarizabilities.

2.2.1 Position of the IP technique among other geophysical methods

The IP technique is a galvanic linear electrical method in which polarization of the ground is made by a physical electrical contact of an electrode also known as an ohmic contact. The essence of the IP technique is derived from the measurement of the slow decay of voltage in the ground following the cessation of an excitation current pulse (time domain method) or variations of the resistivity of the earth as a function of frequency (frequency domain method). This leads to classifying the technique, amongst other geophysical methods under galvanic electrical techniques (Figure 2.1).

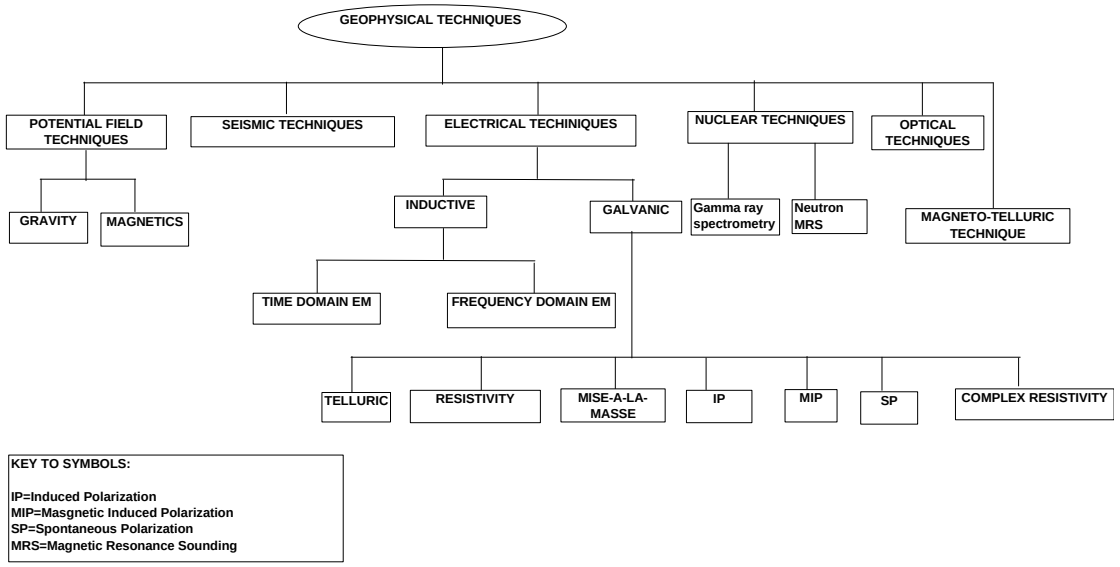

Figure 2.1: Position of the IP amongst other geophysical techniques

2.3 General characteristics of clays

Clays are one of the oldest ceramic raw materials and are recognized by certain properties. When they are mixed with water, they form a coherent, sticky mass, that is readily mouldable and if dried, becomes hard, brittle and retains its shape. Clays may take on various forms where they can easily be recognized as the sticky, tenacious constituent of soils and can also occur as rocks, which owing to compression, are so hard and compacted that penetration and action of water are very slow processes (Worrall, 1968). The commonest impurities in natural clays are quartz and micaceous material but minor impurities such as hydrated iron oxide, ferrous carbonate and pyrites also occur.

The basic building blocks of clay minerals are the tetrahedral layer and the octahedral layer. The tetrahedral layer is composed of either Si or Al in tetrahedral coordination (4 oxygens) with oxygen. The tetrahedral layer is obtained by joining Si tetrahedra (Figure 2.2) at their basal oxygens. The octahedral layer is composed of cations in octahedral co–ordination (6 oxygens) with oxygen and can be obtained by linking the Al octahedra (Figure 2.3) by the side or edge oxygens. Whether a cation is in tetrahedral or octahedral co–ordination with oxygens depends on the size of the cation. The cation is stable in a particular environment, as long long as it is able to keep the oxygen anions from touching, thereby preventing repulsive forces from destabilizing the structure. For example, Si is so small that only 4 oxygens are able to fit around it and the most stable arrangement of these oxygens is in tetrahedral co–ordination. Cations such as Mg^{2+}, Fe^{2+} and Fe^{3+} are larger and thus able to accommodate 6 oxygens in their co-ordination environment. Aluminium size is in between Si and Fe/Mg, therefore it has the ability to fit in either octahedral or tetrahedral co-ordination.

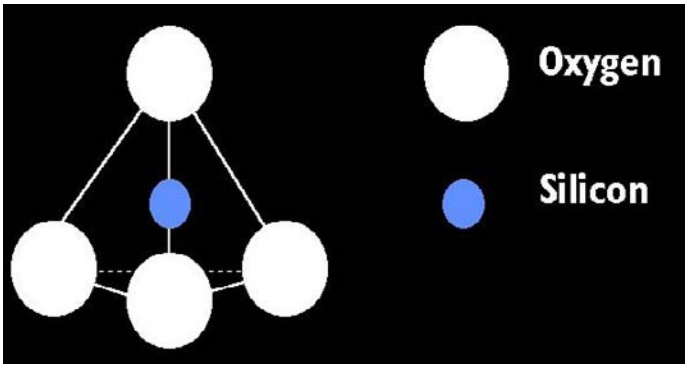

Figure 2.2: The silicon tetrahedron (after Bioag, 2001)

Charge development within the clay structure develops under the following con-

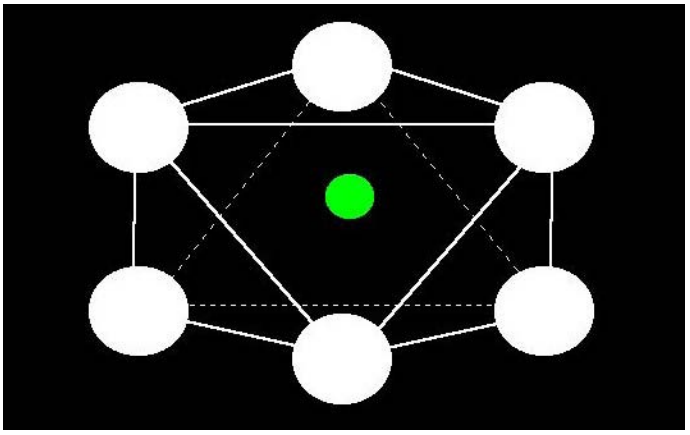

Figure 2.3: The Aluminium octahedron (after Bioag, 2001)

ditions. If an Al tetrahedra substitutes for a Si tetrahedra in the tetrahedral layer, excess negative charge will develop because of the difference in charge of the two cations i.e Al^{+3} and Si^{+4}. Due to this charge difference, the negative charge (-2) on the oxygens that is being shared between the Al and Si tetrahedral is not satisfied.

2.3.1 Formation and types of clay minerals

Clay minerals form at the expense of primary rock forming minerals. Primary minerals are unweathered minerals with relatively large crystals which formed under constant conditions. Examples include Mica, quartz, muscovite and feldspar. Secondary minerals are highly weathered clay minerals with tiny crystalline structure which formed under conditions of intense weathering.

Clays are formed from three distinct processes:

1. **Alteration**
   Chemical and physical changes of primary mineral, however, with light changes in structure
   Primary minerals $\rightarrow$ intermediate minerals $\rightarrow$ secondary minerals
   Muscovite + $H_2O \rightarrow$ vermiculite + K^+
   Vermiculite + $H_2O \rightarrow$ Montmorillonite + Mg^{2+}

2. **Recrystallization**
   Solubilizsed aluminium and silicon oxides from weathering clays recrystallize to form kaolinite (Grim, 1968).

3. **Weathering of clays to form other types of clay**
   Illite $\rightleftharpoons$ Montimorrilonite + K^+

Montmorillonite $\rightarrow$ Kaolinite + SiO_x
The longer or the more intense the weathering process, the more the silica that is lost and the lower Si:Al ratio.
For example, Vermiculite: 2Si:1Al layer (youngest)
Kaolinite: 1Si:1Al layer (more weathered)
Fe and Al oxides: no silica at all (highly weathered)

Clay minerals include kaolinite with a 1:1 type lattice, low CEC (3–15 meq/100g), low surface area (15 m^2/g) and a low shrink–swell capacity. Its structure is shown in Figure 2.4. Illite has got a 2:1 type lattice, medium CEC (10–40 meq/100g), medium surface area (80 m^2/g) and a medium shrink–swell ability. Lastly, montmorillonite with a 2:1 type lattice, high CEC (80–150 meq/100g), high surface area , high shrink–swell capacity. It structure is shown in Figure 2.5. The CEC values are quoted from Keller and Frischknecht, 1966.

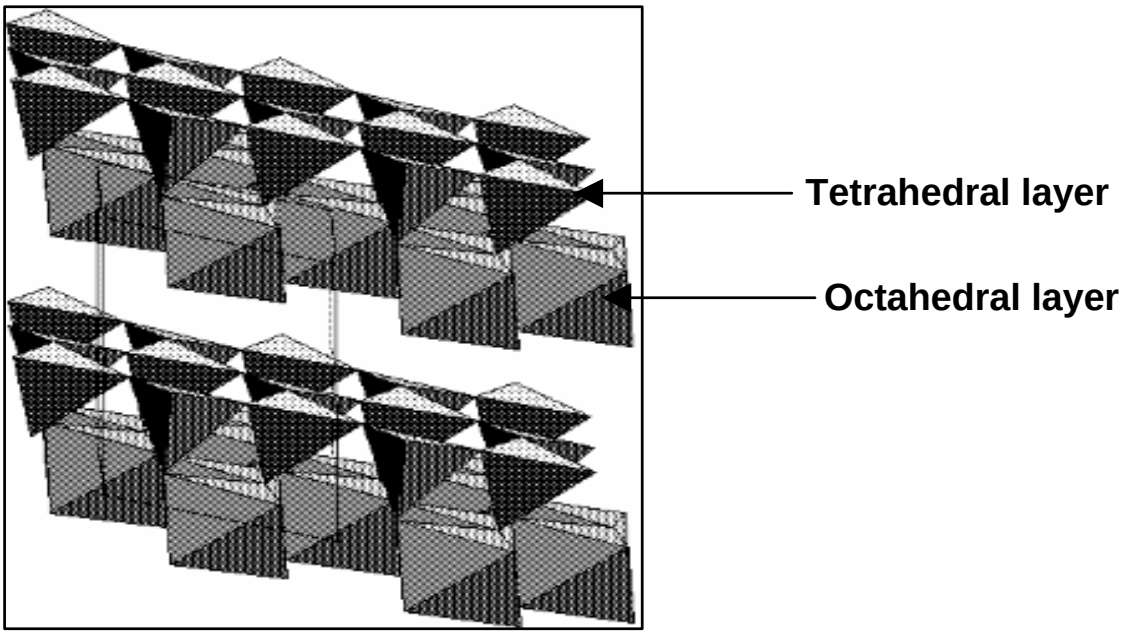

Figure 2.4: 1:1 type clay-kaolinite (Sherman, 1997)

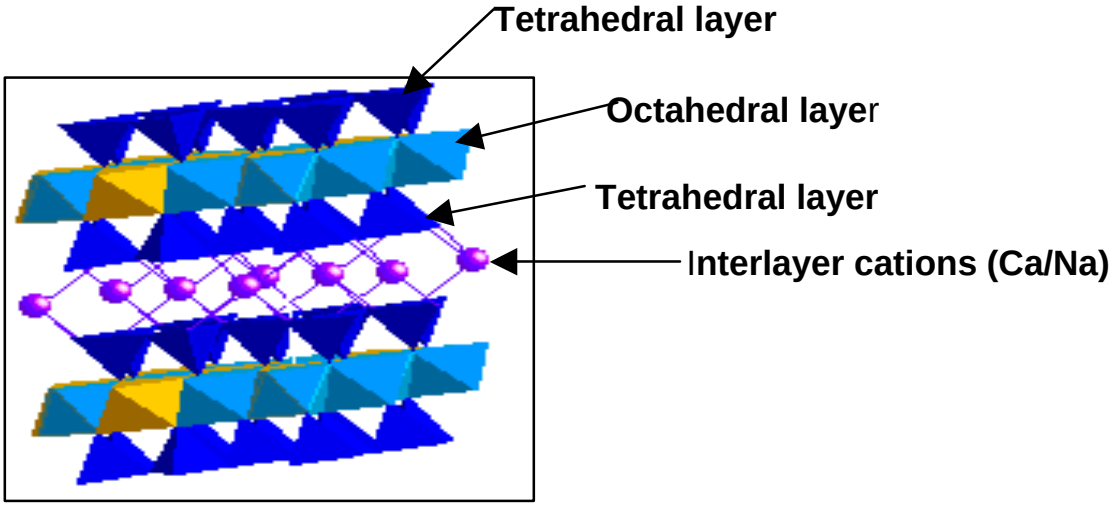

Figure 2.5: 2:1 type clay-montmorillonite (Sherman, 1997)

These minerals give rise to the CEC

2.3.2 Cation exchange capacity (CEC)

This is the total number of positive charges from exchangeable cations that neutralize the negative charges on the soil particles. The exchangeable cations are ions that neutralize the negative charge of the soil particles and exchange or equilibrate readily with others in the soil solution. Soils that contain clays have cations such as Ca, Mg, H, K and Na, which are loosely held to the surface and can subsequently be exchanged for other cations or essentially go into solution should the clay be mixed with water hence the reason why they are called exchangeable ions. The CEC is quantified in meq/100 g i.e the weight of ions in milliequivalents adsorbed per 100 grams of clay. The cation exchange capacity is a typical property of clayish material because it relates to the clay mineral structure and is the basis for the electrical behavior of such soils.

There are three main sources of the exchange capacity:

1. **Isomorphous substitution**
   This involves mainly the substitution of Al^{3+} for Si^{4+} in the tetrahedral sheet and Mg^{2+} or Fe^{+2} for Al^{3+} in the octahedral sheet. This is the major source of clay exchange capacity, except for the kaolin minerals (Mitchel, 1993). However, isomorphic substitution of Fe^{+3} for Al^{+3} in the octahedral layer does not give rise to charge because both cations have a charge of +3.

2. **Broken bonds**

These occur along particle edges and on non–cleavage surfaces and may provide exchange sites. They are the major source of the exchange capacity of kaolinite.

3. **Replacement**
   Ionized hydrogen from OH groups is replaced by another type of cation (Bioag, 2001).

Earlier research work done in the field of electrical induced polarization on rocks and soils shows that more work is needed to understand this phenomenon. Materials that contain clay minerals such as montmorillonite, illite and kaolinite give IP response due to their ability to have exchangeable cations in their lattice. A brief description of the formation of clay minerals and the causes of the cation exchange capacity have been indicated. Therefore, a detailed theoretical basis of the IP technique and its link to the structural characteristics of the clays needs to be given attention, which is the subject of the next chapter.

Chapter 3

Physicochemical basis of the Induced Polarization method

3.1 Introduction

The information discussed in this chapter provides the physical and chemical background of the Induced polarization technique.

3.2 Electrochemical nature

Empirical studies of the IP properties of mineralized rocks or synthetic ore samples have been done to investigate effects of certain changes in the solution chemistry (Henkel and Collins, 1961). Diffusion processes involve the motion of ions in solution resulting from the presence of a concentration gradient whereas the reactions between ions in solution are referred to as chemical reactions. In the earlier studies conducted by Marshal and Madden (1959) , it was indicated that diffusion processes seemed dominant in the frequency range of interest for field measurements however these studies were unable to identify any of the chemical reactions involved. In view of the fact that chemical environments can undergo tremendous variations in nature, a possibility exists that the IP phenomenon may also be very variable because of the chemical environmental factors.

A study conducted by Angoran and Madden (1977) was directed at identifying the processes that control the IP phenomenon and understanding how these processes are effected by the chemical environment. Therefore, an investigation of the effect of the in situ chemistry on the induced polarization phenomena was carried out by means of laboratory studies of the electrode impedances of metallic and sulfide minerals. However, the reaction rate theory shows that this effect is largely due to the

impedance associated with the diffusion of ions involved in the charge transfer reaction to and from the reaction sites. The conclusion from the laboratory study was that the impedance is inversely proportional to the concentration of the reacting ions and inversely proportional to the square root of the frequency. The basic parameter of concern in this study is the **electrode impedance**.

3.3 Electrode impedance

This is the total resistance to the flow of alternating current across the interface between an electrode and an electrolyte; includes solution resistance, capacitances in the fixed and diffuse layers, and warburg impedance. However the interpretation of this impedance requires the assumption of a particular model electrical equivalent circuit. When metallic or any other conducting minerals are part of the electric current paths in an otherwise ionic conducting medium, an excess impedance arises at the solution–mineral interface associated with the charge transfer reactions that are needed to maintain the continuity of the electric current flow. The presence of this impedance and the fact that it is highly frequency–dependant is the basis of the electrode IP method. The concept of using an equivalent circuit to describe electrode impedances was firmly established by the work of Grahame (1952). The environment in the immediate vicinity of the electrode–solution interface must be taken into account. According to an excellent review of the properties of this zone as given by Grahame (1952), this zone is made of two parts as described in the following section.

3.3.1 Fixed Layer

This contains a compact layer of ions and molecules rather rigidly held in place on the electrode by chemical and adsorption forces (Figure 3.1). It also contains a net electric charge and it is within this layer that the charge transfer reaction between the solution and the electrode is assumed to take place. This layer is thin however there is an appreciable electrical capacitance coupling the diffuse zone to the electrodes. This capacitance is known as the **fixed layer capacitance** (CF) whose typical values are in the range of 5–50 μF/cm^2 and this capacitance usually dominates the electrode impedance at frequencies above 30–100Hz.

3.3.2 Diffusion layer

This is adjacent to the fixed layer on the solution side and is considered to be similar to the rest of the solution, except that any net charge in the fixed layer creates an electric field which unbalances the positive and negative ion concentrations in the

zone (Figure 3.1). It has the thickness given by the Debye length, which for room temperatures and .001N salinity is about .01μm. Using a simple model for the conduction phenomenon, the diffusion layer ions can be assumed to move as point charges through a viscous medium under the influence of imposed electric fields or ion concentration gradients or both. The potential drop across the diffuse layer is known as the zeta potential, the effects of which can be directly observed. The value of the Zeta potential is, however, indirectly measured. Note, however, that at high frequencies, when the separation between sites is large compared to the diffusion distance, this acts just like a Warburg impedance. At low frequencies, the impedance acts as a capacitive impedance and is due to the accumulation of the reaction products between the reaction sites.

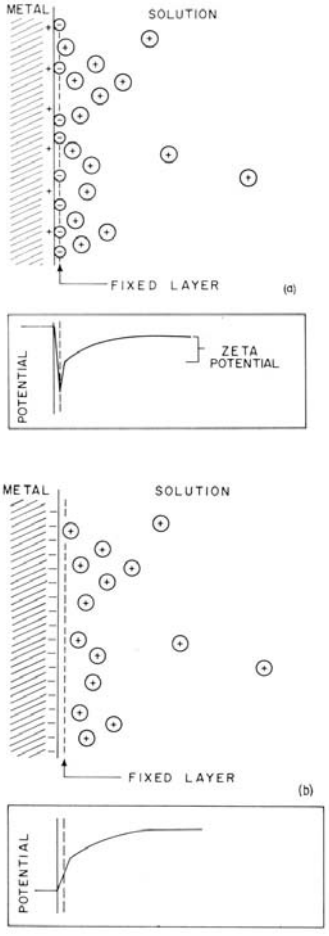

Figure 3.1: Potential across the fixed and diffuse layers with (a) current into and (b) out of the interface ((Sumner, 1976)

3.4 Origin Of Induced Polarization

The phenomenon of induced polarization and its electrochemical mechanisms are extremely complex. Nevertheless, attempts have been made through recent research to establish the important phenomena that cause induced polarization in rocks/soils. These include diffusion of ions next to metallic minerals and ion mobility within pore–filling electrolytes (Sumner, 1976). Most authors agree that these interactions take place at the contact of solid particles and electrolytic solutions which exist in the ground, when a current flow is applied. The surface charges of these particles induce in the solution an ion concentration of opposite sign close to the interface. A double electric layer is formed in which the ions are impeded to be mobilized. When a current is turned off, the initial equilibrium is re–established and the energy consumed in the modification of the occurred interactions is restored. This storage of chemical energy takes place because the mobilities of various ions through the rocks vary from point to point. When a current is applied across such a rock, excesses or deficiencies of certain ions will occur at the boundaries between the zones with different mobilities. The concentration gradients thus developed oppose the current flow and cause a polarizing effect. The **exact causes** of induced polarization are still unclear but most probably, induced polarization results from the combined effects of several physical chemical processes. However, there are two main mechanisms that are reasonably understood:

- Grain (electrode) polarization (overvoltage)
- Membrane (electrolytic) polarization.

They both occur through electrochemical processes.

3.4.1 Electrode polarization (Overvoltage)

In the geological situation, current is conducted through the rock mass by the movement of ions, within groundwater, passing through interconnected pores or through the fracture and micro crack structure within the rock. If the passage of these ions is obstructed by certain mineral particles which, like common metals, transport the current by electrons, ionic charges pile up at particle–electrolyte interface, positive ones where the current enters the particle and negative ones where it leaves as in (Figure 3.2) . The piled up charges create a voltage that tends to oppose the flow of electric current across the interface and the particle is said to be polarized. When the current is interrupted, a residual voltage continues to exist across the particle, due to the bound ionic charges, but it decreases continuously as the ions slowly diffuse back into the pore electrolytes, which process gives the induced polarization effect (Parasnis, 1966).

The induced polarization effect opposes the build up and collapse of the primary potential difference, and is referred to as the *overvoltage* because an extra voltage above that required to overcome the ohmic resistance is required to drive current through the ore zone. The secondary voltage Vs that must be overcome when the current is switched on is the same as the residual value that the potential falls to at switch off (Griffiths and King, 1965). The level of IP is controlled by a number of factors, as each blocked pore becomes polarized the number of pores, hence, the state of dissemination and the volume of the ore will have a large effect. IP is greatly influenced by the total surface of the polarizable material. A disseminated mineralization has a lot of surface (possibly much more than a massive mineralization) and therefore, depending on polarization properties may have a larger IP response than its massive counterpart. However, many massive bodies have a disseminated halo thus increasing the overall surface. High porosity and high groundwater conductivity reduce IP as both lead to a short circuiting of energizing current through unblocked paths (Griffiths and King, 1965).

Foremost among the ore mineral having an electronic mode of conduction and therefore exhibiting strong IP are pyrite, pyrrhotite, chalcopyrite, graphite, galena, bornite, magnetite and pyrolusite.

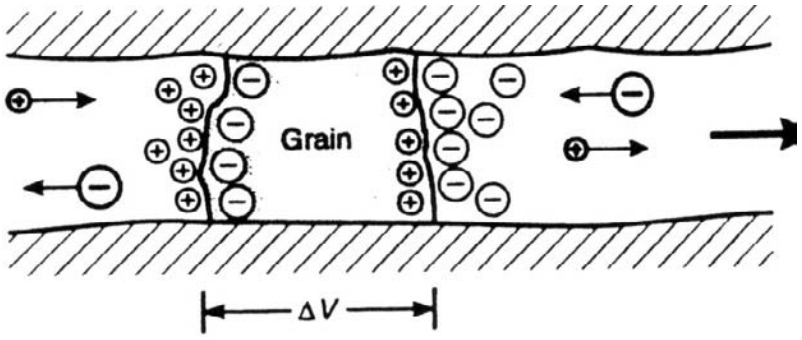

Figure 3.2: Grain electrode polarization (Reynolds, 1997)

3.4.2 Membrane (electrolytic) polarization

This type of polarization explains the IP effects that are observed when no metallic-type minerals are present in the ground. This type of polarization applies to the soil material under this study. There are two causes of membrane or electrolytic polarization:

- **By constriction within a pore channel**
  There is a net negative charge at the interface between most minerals and pore

fluids. Positive charges within the pore fluid are attracted to the rock surface and build up a positively charged layer up to about 100μ m thick, while negative charges are repelled (Figure 3.3) . Should the pore channel diameter reduce to less than this distance, the constriction will block the flow of ions when a voltage is applied. Negative ions will leave the constricted zone and positive ions will increase their concentration, so producing a potential difference across the blockage.

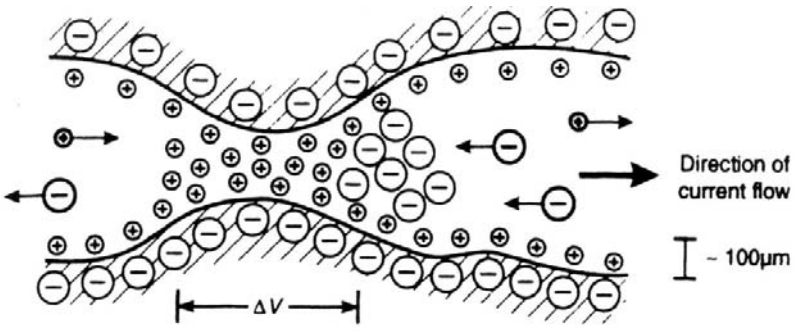

Figure 3.3: Membrane polarization associated with constriction between mineral grains (Reynolds, 1997)

When the applied voltage is switched off, the imbalance in ionic concentration is returned to normal by diffusion, which produces the measured IP response.

- **Presence of clay particles or filaments of fibrous minerals**
  Both of these tend to have a negative charge. In the absence of conductive minerals, IP owes its origin to the existence of clay particles contained within the pore structure of the rock (Parasnis, 1973). The surface of clay particle is negatively charged and thus attracts positive ions from the electrolytes present in the capillaries of a clay aggregate. An electrical double layer is, therefore, formed at the surface of the particle as shown in Figure 3.4, the concentration of the positive ions being the greatest at the surface of the clay particle. If the positively charged zone persists far enough into the capillaries, it effectively repels other positively charged ions and so acts like an impervious membrane impeding their movement through the capillaries.

  Clay minerals have ion–exchange capacities which means that they have cations in ion–exchange positions in the lattice. When they electrolyze (ionize) the exchangeable ions go into solution, leaving behind the clay particle, which carries a net charge. This clay particle then forms a highly charged immobile anion, blocking free ion flow through the pore in which it may be situated. This causes an imbalance in ion concentration along the double layer formed. When an elec-

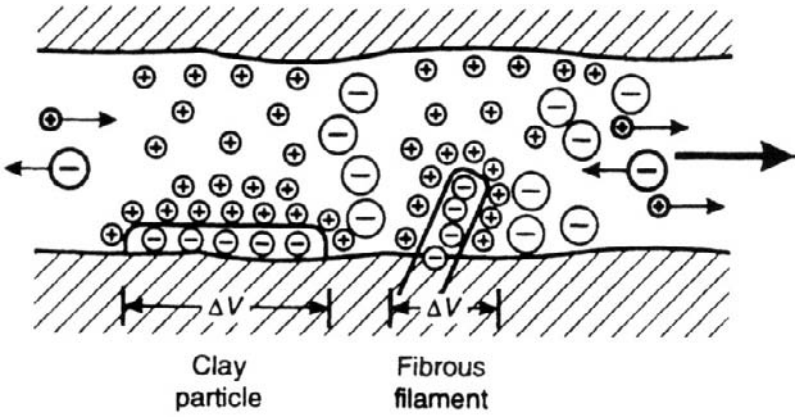

Figure 3.4: Membrane polarization associated with negatively charged clay particles (Reynolds, 1997)

tric current is forced through the clay, the positive ions are displaced (in fact, their displacement constitutes part of the current) and on the interruption of the current the positive charges redistribute themselves in their former equilibrium pattern. The process of redistribution manifests itself as a decaying voltage between two electrodes in contact with the clay as an IP effect.

It might be expected that the amount of polarization in clay bearing rocks and soils increases in direct proportion to the ion exchange capacity. However, this is not true because from experiments done on clay-rich rocks such as shale show relatively little ability to polarize in comparison with siltstone which has a lower content of clay minerals (Keller and Frischknecht, 1966). The explanation to this is that in a rock containing a large proportion of clay, almost all the negative charges may fixed in exchange positions within the lattice with virtually no anions existing in solution. This causes the amount of charge accumulating at a potential barrier in a rock to be small because there are no anions.

The nature of surface conduction in silicates including some clay minerals is a phenomenon that is less known but very important in water bearing rocks. Rock–forming minerals usually fracture in such a way that one species of ion in the crystal is commonly closer to the surface than others. In silicates, the oxygen ions are usually close to the surface. When an electrolyte is in contact with such a surface, it will seem to the ions in solution that the surface is negatively charged . Cations will be attracted to the surface by coulomb forces and adsorbed, while anions will be repelled. The same effect takes place with water molecules, which are polar. The water molecule is not symmetrically

constructed from an oxygen atom and two hydrogen atoms; rather, there is an angle of 105^0 between the bonds from the oxygen to the two hydrogen atoms. As a result, the center of mass of the positive charges (the hydrogens) does not coincide with the center of mass of the negative charges (the oxygen atom). Consequently, when viewed from the oxygen side, the water molecule appears to carry a negative charge; and when viewed from the hydrogen side, it appears to carry a positive charge (Keller and Frischknecht, 1966). When an electrolyte is in contact with such a silicate surface, several layers of water molecules will become adsorbed to the surface. This layer may be several molecules thick since each layer of oriented water molecules absorbs other water molecules. A single adsorbed cation will neutralize a surface charge which would hold several water molecules in a chain. So the conductivity of water in this oriented adsorbed phase is higher than the conductivity of free water and so contributes to the overall conductivity of a rock.

It should be noted, however, that the increased pressure in the adsorbed layers increases the viscosity of water and decreases the mobility of the ions. This means that if many ions are adsorbed, the conductivity of the electrolyte may be significantly reduced.

3.5 Methods of measurement of IP effect

In theory, induced polarization is a dimensionless quantity whereas in practice it is measured as a change in voltage with time or frequency. The time and frequency IP methods are fundamentally similar, however, they differ in a way of considering and measuring electrical waveforms. In the former, a direct current is applied into the ground, and what is recorded is the decay of voltage between two potential electrodes after the cut off of the current (time–domain method). In the latter, the variation of apparent resistivity of the ground with the frequency of the applied current is determined (frequency–domain method).

In another type of frequency method, which is called Complex Resistivity (CR) method, a current at frequency range (0.001 Hz to 10 kHz) is injected in the ground and the amplitude of voltage as well as its phase with respect to the current is measured. That is a phase–angle IP measurement. It is important to note that many CR implementations are measuring the real and quadrature component of the response. Of course it is very easy to transform these two parameters into amplitude and phase as shown in Section 3.5.3.

In Laboratory experiments, either soil/rock samples are used or scale models of typical field situations are simulated as analog models for the measurement of the

IP response. A basic response parameter measured in the IP method is the amount of change of voltage (ΔV) or resistivity ($\Delta\rho$) seen as a function of either time or frequency. The fundamental basic IP function can be written as $\frac{\Delta V}{V}$ or $\frac{\Delta\rho}{\rho}$; this being the basic IP response ΔV or $\Delta\rho$ normalized with respect to Voltage V or resistivity ρ in order to form an independent IP parameter.

3.5.1 Time domain method

One measure of the IP effect is the the chargeability *m* (Siegel, 1959) and is usually expressed as :

$$m = \frac{V_s}{V_p}(mV/V) \tag{3.1}$$

where V_p is the ON–time measured MN voltage, and V_s is the OFF–time measured MN voltage where AB is the current injection dipole and MN is the voltage measuring dipole. Instrumentally, it is extremely difficult to measure V_s at the moment the current is switched off due to electromagnetic effects which produce a transient disturbance on switching , so it is measured at specific times (e.g 0.5s) after cut off. Measurements are then made of the decay of V_s over a very short time period (0.1s) after discrete intervals of time (also around 0.5s). The measured parameter in the time domain is the area under the decay curve of Voltage V(t) corresponding to the time interval (t_1, t_2). The integration of these values with respect to time gives the area under the curve (Figure 3.5) , which is an alternative way of defining the curve. When the integral is divided by V_p, the resultant value is called the chargeability (m) and has units of time (milliseconds). It is expressed as:

$$m = \frac{1}{V_p}\int_{t_1}^{t_2} V_{s_{(t)}}\, dt = \frac{A}{V_p} \tag{3.2}$$

where V_s is the OFF–time measured MN voltage at time t, and V_p the observed voltage with an applied current. Note, however, the major advantage of integration and normalizing by dividing by V_p is that the noise from cross–coupling of cables and from background potentials is reduced. Care has to be exercised in selecting appropriate time intervals to maximize signal to noise ratios without reducing the method's diagnostic sensitivity.

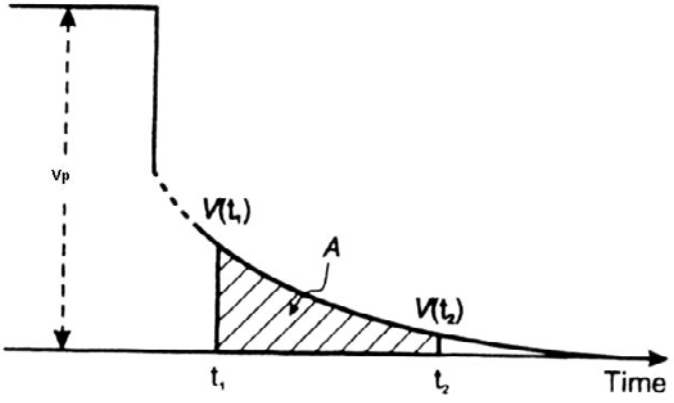

Figure 3.5: The integrated decay voltage used as a measure of chargeability m (Reynolds, 1997)

3.5.2 Frequency domain method

IP effects can be observed using observations in the frequency domain. The IP decay characteristics observed in time domain can be transformed to the frequency domain using Fourier techniques. Frequency domain measurements are made at two different frequencies which are usually less than 10Hz (e.g 0.1 and 5Hz, or 0.3 and 2.5 Hz). The measured parameter is the steady state voltage response after filtering and the derived parameter is the **Frequency Effect** (FE) which is expressed as:

$$FE = \frac{V_{lo} - V_{hi}}{V_{hi}} \tag{3.3}$$

OR

$$FE = \frac{\rho_{lo} - \rho_{hi}}{\rho_{hi}} \tag{3.4}$$

where V_{hi} and V_{lo} are the stead state voltage responses at the filtered high and low frequencies respectively. Since the current is held at a constant peak amplitude while varying the frequency, the FE can as well be expressed as in Equation 3.4, where ρ_{hi} and ρ_{lo} are the respective magnitudes of apparent resistivity at frequencies hi and lo. The apparent resistivity at low frequency (ρ_{lo}) is greater than the apparent resistivity at a higher frequency (ρ_{hi}) because the resistivities of rocks decreases as the frequency of the alternating currents is increased. The two apparent resistivities are therefore used to determine the Frequency Effect (FE) (unitless) which can be expressed, alternatively, as the Percentage Frequency Effect (PFE) (Wait, 959a).

$$PFE = FE * 100\% \tag{3.5}$$

It should be noted that although FE and PFE are defined in terms of two frequencies, modern frequency domain IP surveys are often done either at single frequency (resistivity and phase measurements) or at larger number of frequencies (e.g Zonge offers 5 frequency schemes)

Metal factor (M.F) is another parameter in frequency domain method, which was suggested by Madden to correct (partially) for the resistivity of the country rock (Marshall and Madden, 1959). It is calculated from FE magnitude to compensate for variations in effective resistivity of the host rock including changes in electrolyte, temperature, pore size that are unrelated to the capacitive effect of the metal content (Telford et al., 1976). It is defined as the FE divided by the low frequency apparent resistivity (ρ_{lo}). However, as the number, thus obtained is inconveniently small, it is multiplied by $2\pi * 10^5$, so that the practical definition of the metal factor becomes:

$$MF = A\frac{(\rho_{a0} - \rho_{a1})}{\rho_{a0}\rho_{a1}} = A(\sigma_{a1} - \sigma_{a0}) \tag{3.6}$$

where ρ_{lo} and ρ_{hi} are the apparent resistivities whereas σ_{lo} and σ_{hi} are the apparent conductivities at low and higher frequencies respectively; $\rho_{lo} > \rho_{hi}$ and $\sigma_{lo} < \sigma_{hi}$; and $A = 2\pi * 10^5$.

If the resistivities are expressed in Ω m, the dimensions of the metal factor are Ω^{-1} m^{-1}, which are those of electric conductivity.

In the field, the IP electrode system is the same as the resistivity system, so electrode arrays such as Wenner, Schlumberger, Pole–dipole and double dipole are used. IP field measurements always incorporate resistivity measurements.

Noise sources, besides spontaneous polarization (SP) which is easily compensated for, includes telluric currents, capacitive couple (due to current leakage between current electrodes and potential wires, or between current and potential wires), electromagnetic coupling (due to mutual inductance between current and potential wires) and the IP effect from barren rock (Telford et al., 1976). Other sources of noise include fences, power lines, pipelines and other extensive man made structures with earthed grounds which produce spurious induced polarization anomalies by acting as secondary sources and sinks of current. IP is now a well established technique in exploration geophysics, especially for base metal exploration, as indicated by the extensive use of the metal factor parameter. Both time domain and frequency domain IP are commonly used .

3.5.3 Complex Resistivity (Spectral IP)

This involves taking amplitude and phase measurements, which in IP are defined as the difference in phase angle between the received polarization voltage signal and the

stimulating current signal by Ohm's law, in the case when both are sinusoidal waveforms. If the input current is a square wave, the phase measurement is defined as the phase angle between the fundamental harmonic of the transmitted and received signals.

The phase angle is defined as the angle, whose tangent is the ratio between the imaginary and real components of the received voltage (V) or resistivity and is expressed as:

$$\phi = tan^{-1}\frac{Vimag.}{Vreal} = tan^{-1}\frac{\rho imag.}{\rho real} \tag{3.7}$$

The in–phase (real) and the out–of–phase (imaginary/quadrature) components are more easily measured with modern electronic systems than the phase angle alone and the two components provide additional useful information about IP phenomena.

The magnitude of the complex resistivity ($|Z(\omega)|$) and phase (ϕ) of the polarization voltage are measured over a wide range of frequencies (0.3 to 4 kHz) of applied current. The frequency dependency is usually plotted as a binary function in the form of logarithms to base 2 rather than to base 10. The magnitude is determined from the real and imaginary components of the above mentioned parameters and is expressed as:

$$Z(\omega) = \sqrt{Im^2 + Re^2} \tag{3.8}$$

It has been shown by Zonge et al. (1972) that IP phase angle and frequency domain measurements correlate very well however the difference lies in the fact that by conventional frequency domain IP method, the results are presented in various ways but it is basically only the change in complex resistivity with frequency that is employed.

The complete theory about induced polarization is a subject of further study, however, the chapter has presented what is known so far in regard to the physicochemical basis of the method. An attempt to explain the electrochemical nature of this method is made by use of electrode impedance. This is made possible by use of an equivalent circuit. There are two layers that make up the zone in the immediate vicinity of the electrode–solution interface. These are the fixed and diffusion layers. The origin of induced polarization is complex but two known mechanisms have been presented. Electrode polarization (overvoltage) and membrane (electrolytic) polarization both of which occur through electrochemical processes.

There are three methods of measurement of IP effect that have been discussed. Chargeability being the measured parameter in the Time domain measurements as the Percentage Frequency Effect is for the Frequency domain measurements. Complex Resistivity (CR) is the third measurement method in which the magnitude of the complex resistivity and the phase of polarization voltage are measured over a wide range of frequencies.

The laboratory experiment for which this study is for, applied one of the measurement methods (time domain method) on the soil samples. But where were these soil samples obtained and which factors influenced the choice of the sampling sites, is a question that can be best answered by the next chapter.

Chapter 4

Study areas and soil samples

4.1 Introduction

Study areas are places where soil samples were collected. A description of such places and their soils is the basis of this chapter. In the selection of the soil sampling sites for this research, important consideration was given to the geology, soils and climate of the study area. The sampling locations had to be rich in all the three-targeted mineral types, namely kaolinite, smectites and illites especially for Spain and Kenya.

4.1.1 Spain

The Spain study area shown in Figure 4.1 is located between longitudes $4^0 31' 10''$E and $4^0 51' 10''$E and latitudes $37^0 00' 04''$N and $37^0 10' 04''$N. It is about 45 km north of Malaga in the southern part of Spain and covers the municipalities of Antequera, Campillos and Molina. It spans an area of approximately 30*18 km^2 with varying topography. It is easily accessible by road.

4.1.2 The Netherlands

The Netherlands study area (Enschede) lies in the eastern part of the country (Figure 4.2). It is located between longitudes $6^0 50'$ E and $6^0 55'$ E and latitudes $52^0 10'$N and $52^0 15'$N.

4.1.3 Kenya

The Kenya study area (Nairobi) shown in Figure 4.3 is bounded by $1^0 00'$ to $1^0 30'$S latitudes and $36^0 30'$ to $37^0 30'$E longitudes. It lies in the central part of the country.

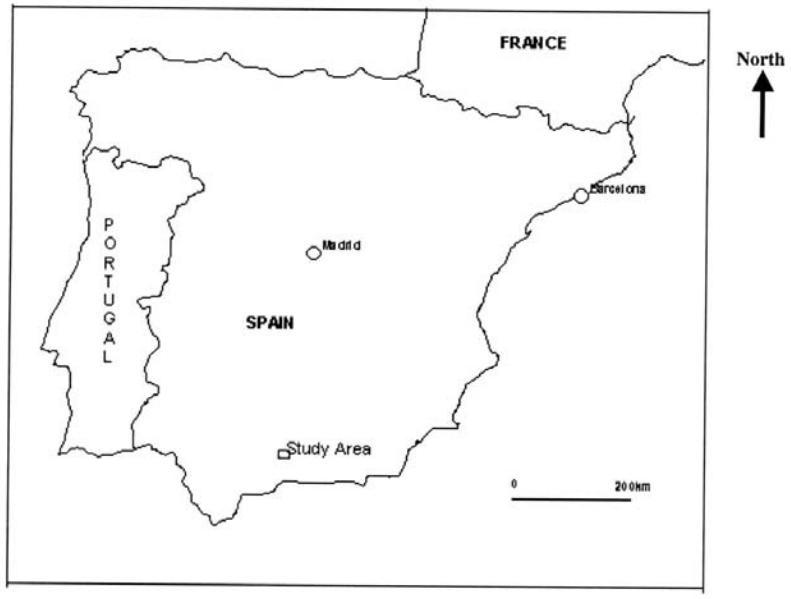

Figure 4.1: Location of study area (Spain) (Dizon-Bacatio, 1992)

Figure 4.2: General map of study area (The Netherlands) (Magellan, 1992)

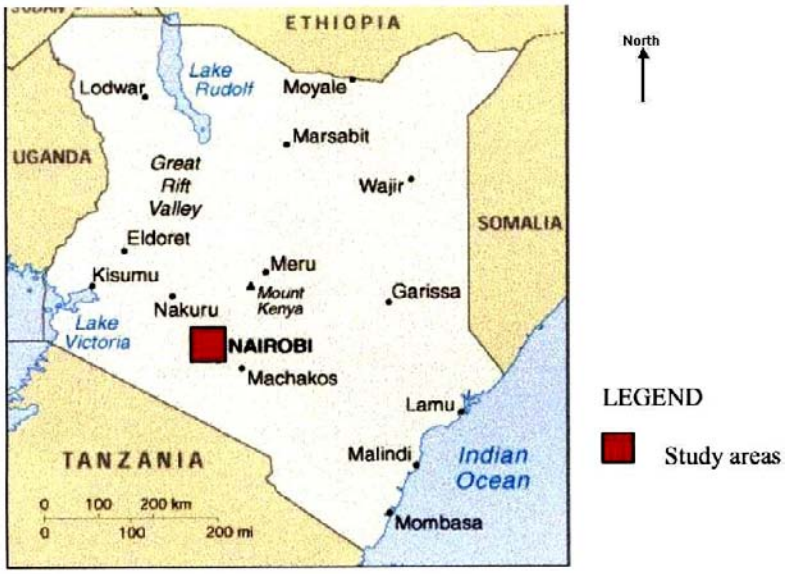

Figure 4.3: General map of study area (Kenya) (Fairburn, 1963)

4.2 Climate

Climate is a composite concept, which includes the temperature, rainfall, humidity and evapotranspiration among other atmospheric variables. Soils and other near surface features are usually determined not only by the current climate but also by the paleo–climate. These factors strongly determine the type of clay mineral formed in an area. The temperature sets the speed of any chemical reaction; rainfall provides a medium in which chemical reactions can take place as well as a medium for the movement of soil constituents. Leaching of calcium carbonate in the soil is rainfall dependant, the higher the rainfall the deeper the horizon where calcium carbonate appears in the soil.

4.2.1 Spain

The study area falls within the Continental Mediterranean type of climate and has a dry summer with an overall mean annual temperature of 17.6^0C. The highest mean temperature is in the month of August at 25.5^0C while the lowest is in the month of January with a mean of 7.5^0C. The rainfall is concentrated between the months of October to April. The month of December receives the highest rainfall averaging 76.8 mm with the lowest being in the month of August averaging 6.1 mm. These climatic conditions have enabled the development of soils rich in clay minerals with a high Si/Al ratio (2:1). Lack of enough rainfall has however led to the calcareous layer to be shallow in the area which leads to less concentrations of bivalent cations (Ca), which

are important for the formation of clay minerals with Si/Al ratio of 2:1.

4.2.2 The Netherlands

The study area has a temperate maritime climate, with temperatures averaging 2^0C in January and 16.6^0C in July. Average annual rainfall is almost 800 mm distributed fairly evenly throughout the year.

4.2.3 Kenya

The study area has got a pleasant climate for most of the year with temperatures ranging between 14 and 28^0C, rainfall is moderate and fairly uniform throughout the year and increases as one moves from the plains at Athi River to the Kikuyu escarpment. Due to the high rainfall and the underlying volcanic rocks, areas to the west of Nairobi City are fertile and well served by streams. To the east, the area is mainly savannah grassland. Deep weathering of the volcanic rocks gives rise to an extremely thick soil cover on the watersheds.

4.3 Geologic setting

4.3.1 Spain

The area under study (Antequera Spain) is situated in the Subbetic zone of the Betic Cordillera, one of the mountain chains of the Iberian Peninsula that is characterized by extensive parallel mountain ranges. According to geological time scale, a geosyncline that encircles the Spanish Meseta, a stable core of the Iberian Peninsula, formed a marine environment in which the sediments were deposited over a very long period of time. A re–orientation and rotation of the Iberian peninsula from the Lias to Cretaceous was followed by an approach of the Iberian Shield to the African shield. During this period, the rather strong forces applied to the geosynclinal sedimentary rocks surrounding the Meseta resulted in their uplifting and subsequent erosion. The by–products of this process, the flysch, form part of the main sequence of the study area.

Another period of compression followed in the Oligocene and Miocene resulting in big overthrusts in which the Triassic evaporites played an important role acting as lubricants. Upper Miocene till late Pleistocene was dominated by deposition of weathered and eroded materials from the uplifted regions into the depressions. These materials have been referred to as Molasse and dominate the study area. They are generally coarse textured occurring as impure sandstone intercalated with marls.

During the periglacial period of the Quaternary, the deposition continued mainly around the hills. Large footslopes from different materials, developed at the foot of the undulating and rolling topography and are referred to as solifluction glacis. The change of climatic conditions since the last geological event has resulted in more stable slopes and the development of deep soil profiles on these glacis (Dizon-Bacatio, 1992).

The geological periods and events had an important bearing on the soil forming processes and properties. This has resulted in 2:1 (silica: aluminium) type of clay domination in the soils due to high concentration of bivalent cations such as Ca and Mg during their formation. The geology of the area consists mainly of marls, limestone, dolomites, gypsum and bioclastic sandstones.

4.3.2 The Netherlands

The rocks that were formed during the Tertiary period are not generally visible on the surface in The Netherlands, but their direction of dip is from the southeast to the northwest. Rocks of this period include limestone, which outcrops in a few places in the southeast and the east of the country (Meijer, 1994).

The surface of the Netherlands consists almost entirely of sediments deposited in the Quaternary period. In the penultimate pleistocene ice age–the Riss or Saale period ice sheets were pushed from Northern Europe on to The Netherlands. In the river valleys of the present provinces of Utrecht, Overijssel and Gelderland (the central Netherlands), which run from south to north, the valley walls were pushed sideways and upwards. This resulted into a series of elongated ice ridges or push moraines, which reach a height of more than 100 meters and are now a popular recreational area.

During the ice ages, the North Sea coast line laid much further to the northwest, due to a considerable drop in the sea level. After the ice had melted, an extensive area in the north of the country was covered with ground moraine, consisting of sand, gravel, glacial till, boulder clay and erratic boulders. Prior to the ice age, the Rhine and Mass rivers had deposited thick layers of sand and gravel from the erosion of Alps and the lower European mountain ranges into the central and southern parts of the country.

After the ice sheets had disappeared, westerly and northwesterly winds, partly blowing across the dry floor of the North Sea, dispersed sand over the Netherlands. The sand largely covered the ground moraines, the ice pushed ridges and the river deposits.

In the period that followed, the Holocene, the climate became warmer resulting into the rising of the sea level. The North Sea flooded the west of The Netherlands up

to the line formed by Groningen, Utrecht and Breda. The cross section of the western Netherlands shows quite clearly that the pleistocene strata dip towards the west. In the low Netherlands, the subsurface consists of Holocene clays, peats and pleistocene sands.

During the period of sea level rise, sand bars were formed in the West running parallel to the present coastline. In the course of time, the sand bars were transformed into low dunes, which are now referred to as old dunes. In approximately AD 1000, dunes were once again formed on top of the old dunes. The younger dunes are higher reaching about 20 to 40 meters above sea level. Behind the old dunes, a lagoon formed, to which the sea could penetrate through gaps in the dune chain. Initially marine clay was deposited in the lagoon but peat formation ensued as the lagoon became increasingly shallow. However the peat was sometimes washed a way by the sea which led to new deposits of marine clay.

Peat formation also occurred in a number of marshy areas of the high Netherlands. During the Holocene period, rivers deposited sediments especially sand and clay, however this was largely restricted to the region of the major rivers.

4.3.3 Kenya

The geology of the study area can be described as succession of lavas and pyroclastics of cainozoic age overlying a foundation of folded Precambrian schists and gneisses of the Mozambique Belt. The crystalline rocks are rarely exposed but occasionally, fragments are found in agglomerates derived from the former Ngong volcano. The geology consists of mainly metamorphic and volcanic rocks namely crystalline rocks (fine grained schists and coarse gneisses), granitoid gneisses, phonolites and phonolitic trachytes, tuffs and lake beds.

4.4 Description of soil samples

The sampling was done by Mr. P. Kariuki [1] and the samples were kindly made available to this MSc research project.

4.4.1 Spain

The selection of these soil samples was aided by an existing soil database that has been built over the years in the soil division of ITC [2]. These soil formations have been described as consisting of mainly the 2:1 clay minerals and greatly affected

[1] PhD student, Department of Earth Systems Analysis

[2] International Institute for Geoinformation Science and Earth Observation

by the geological/geomorphological processes and the climate as well. The degree of development of these soils has a high correlation with the physiographic position and pedogenesis prevailing in the area. Rainfall is enough to wash lime into the soil but not out of the soil. This has resulted in the soil being mainly calcareous (Dizon-Bacatio, 1992). The soils have textures ranging from loamy sand to clay loam on the surface, gravel clay loam to sandy clay loam, silty clay loam to clay in the subsurface horizons, sandy clay to clay. Their colour ranges from dark/dark brown to reddish brown and dark grey to dull yellowish orange.

There was no distinctive spatial sampling interval. The samples were obtained from near surface at a sampling depth as shown in appendix B, which is above the water table. Most of the samples were obtained from areas that are not densely covered with vegetation and others using hand augers because the surface was hard. These soil samples were labelled as 1–24 for the IP/Resistivity measurements.

4.4.2 The Netherlands

As discussed in section 4.3.2, most of these soils contain sands,clays, and Peat. Cover sandy soils were deposited in the period of the last ice ages (Pleistocene). The damp sandy soils are used as meadowland, the high sandy soils as meadows and woodland, whereas the medium high sandy soils are used as arable land. The parental material of these soils is the material mixed up by sub soiling (humose sand, peat and podzolized sand) overlying undisturbed sand (aeolian sand of Weichsel age)
(De Bakker, 1978). Their colour ranges from brownish for sands to dark colour for peat. Soil samples under this category were labelled as 27–30.

4.4.3 Kenya

These soils were selected due to their known richness in both high and low swell potential soils. Soils of this area are products of weathering of mainly volcanic rocks under relatively high temperature and rainfall. The principle soils overlying the trachytic rocks of the northwest part of the area include strong brown to yellow–red friable clay and red friable clays with high humus layer overlying clay. These are developed from lava, volcanic tuff and ash in humid region with rainfall of more than 1000 mm per year and give way southeastwards to red friable clays developed on similar rock types in area where annual rainfall is 762–1000 mm. Where drainage is impeded over the Athi plains, the soils are black to dark grey clays comprising black cotton soils with calcareous and non–calcareous variants. They overlie the Nairobi and Kapiti phonolites, which form impermeable strata. The soils that have been sampled were formed under different conditions but contain clay minerals that

are responsible for swelling especially the 2:1 (Si/Al) ratio. For the experimental procedure, the soil samples were labelled as 25-26 and 31-43 .

The general description of the study areas including location, climate and geological setting has been discussed. The climate has been described as an important factor in the formation of the three types of clays (montmorillonite, illite and kaolinite). The geological setting of the study areas has been characterized by geological periods and events that had an important bearing in the soil forming processes and soil properties. It has been indicated that presence of high concentrations of bivalent cations such as Ca and Mg has resulted into a 2:1 (Si/Al) type of clay dominance in the soils during their formation. The samples that have been obtained from the above mentioned locations were prepared in order to make them suitable for both gravimetric and IP/Resistivity measurements. The next chapter shows the processes and methods used.

Chapter 5

Data acquisition methodology

5.1 Introduction

A great number of laboratory measurements have been made by a lot of investigators to study the basic phenomena of induced polarization using different methods. Under controlled conditions it is possible to examine the influence of different factors such as clay content, clay mineralogy, and moisture content on the IP effect. A set of Laboratory measurements has been done on a suite of near surface soil samples to study their IP response under varying conditions of clay mineralogy, clay content and moisture content. As natural rather than synthetic samples were used, the range of these parameters were limited by the composition of the available samples.

5.2 Sample preparation

Owing to the fact that the IP response of soil depends not only on the mineralogy and moisture content but also on the texture (Klein and Sill, 1982), the sample preparation procedure was made in such way that the original structure of soils was not distorted. To meet this, soil samples were taken with sample rings of known volume and diameter. However, recent comparisons by Vanhala and Soininen (1995) of laboratory measurements of spectral induced polarization with field results suggest that sampling and packaging procedures have minor influence on the electrical response of a soil, particularly the phase spectrum.

The undisturbed soil material from Spain was collected by using a metallic pF ring of dimension (diameter 50 mm and length 50 mm) shown in Figure 5.1. pF rings are sample stainless steel tubes that are smooth inside and out with a bottom, which has got cutting edge for easier soil entry. The pF ring was hammered into the ground using an impact absorbing hammer. The soil samples so obtained were

properly labelled, tightly covered using red caps and insulating tape and then put in a storage box.

The Netherlands samples were collected using a long Polyvinyl Chloride (PVC) tube by hammering it into the ground using the same type of hammer. However, the cutting edge at the bottom of this tube, was done by use of a knife before any soil sample could be collected.

The Kenya samples were collected as loose sediments, and put into plastic bags. Neither the pF rings nor the PVC tubes were used in the collection for this type of soils.

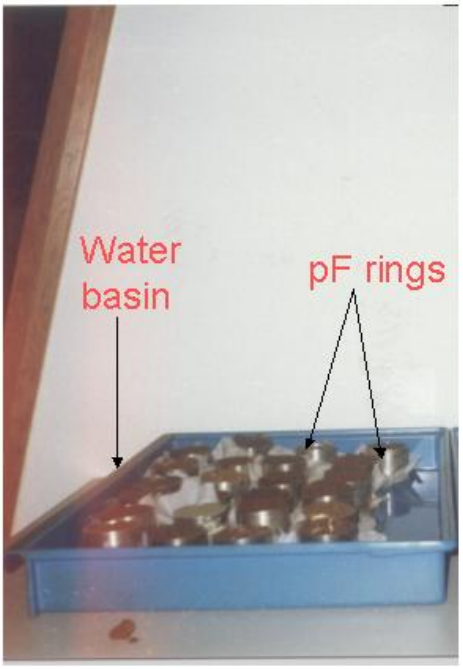

Figure 5.1: pF rings

Sample tubes for the IP measurements were designed from PVC plastic tubes. Several pieces of electrically inactive tubes (50 mm long and 40 mm wide) were cut from a long PVC plastic tube. Figure 5.2 shows the already cut sample tubes with red caps, which were used to prevent soil particles from spilling over.
Holes for potential electrodes were drilled in between the 15 mm and 35 mm marks and temporarily closed with black insulating tape as shown in Figure 5.2 in order to stop loss of soil material.

Figure 5.2: PVC made sample tubes

5.2.1 Saturation of soil samples

In order to use the soil samples for a laboratory experiment, a simple procedure was devised to saturate them using distilled water. This procedure was important because the soil had lost its field moisture. Because the soil samples under study were collected from different locations and by different methods, the procedure of saturating them differed.

The samples that were collected from Spain were being kept in metallic pF rings, and it was by use of these pF rings that the soil was put in a basin containing distilled water. The pF rings were carefully opened, and at one end of the opening of every pF ring, a piece of cloth was wrapped and fastened by use of rubber bands whereas the second opening was left free as shown in in both Figure 5.2 and Figure 5.3. All of these pF rings were then put in a basin containing distilled water to a level of about 3 cm and left to saturate as shown on the left hand side of Figure 5.3. Since the pF rings are metallic and therefore conduct electricity, the soils were resampled and put into standard sample plastic tubes designed for the IP measurement. Resampling involved removing the soil material from the pF rings to the plastic PVC tubes for electrical measurements. For samples from The Netherlands, since they were collected in longer tubes than the standard sample tube size, it was necessary to resample the soil into the standard sample tubes. Both tubes were of the same diameter but with different lengths, therefore, it was a matter of aligning them and with

Figure 5.3: Saturation process

gentle knock on the longer tube, the soil could just collect into the standard sample tube. These were then wrapped with pieces of cloth and put in a basin containing distilled water. The soils were then left to absorb water.

For samples from Kenya, there was a slight change in the procedure in that the soil was first remolded into the specially prepared sample plastic tubes. This involved taking the loose sediments from the big plastic bags by use of a metallic spoon, and physically putting them in the sample tubes. Thereafter, the tubes were wrapped with pieces of cloth and then put in distilled water to saturate as shown on the right-hand side of Figure 5.3.

The process of leaving the above mentioned type of soils to absorb water took seven days.

5.3 Potential electrodes

Non polarizable potential electrodes were locally assembled from transparent ball pen plastic containers, pieces of sisal material, copper wires and saturated copper sulphate solution (Figure 5.4). A transparent model (ball pen plastic container) was used to allow control of the level of the copper sulphate solution and to ensure that

the copper wire is well immersed in it. Epoxy glue was used to fix the movable parts of the plastic ball pen containers.

A piece of sisal material cut from a long one, which was being used to tie a paper box, was used to make a porous contact between the potential electrode and the soil sample. Saturated copper sulphate was then put into the ball pen plastic container. To make sure that the copper sulphate solution is saturated, hot water was used to dissolve the copper sulphate crystals until the color of the solution became dark blue, however the solution was left to cool before use (Scintrex, 1981). In addition, copper sulphate crystals were put inside the plastic ball pen containers before the cold copper sulphate solution was put. A copper wire was then inserted into the container full of copper sulphate solution and then connected to the measuring cables.

Small pieces of sisal material were kept as short as possible in order to keep the contact resistance below 20 kΩ. The potential electrodes were kept damp and an attempt was made to stop them from dripping, as the sample must not be contaminated with the electrolyte. These Cu–$CuSO_4$ non polarisable type of electrodes is known to be stable and establish an almost non–polarizable, somehow low–impedance contact between the sample and the measurement apparatus (Vanhala and Soininen, 1995).

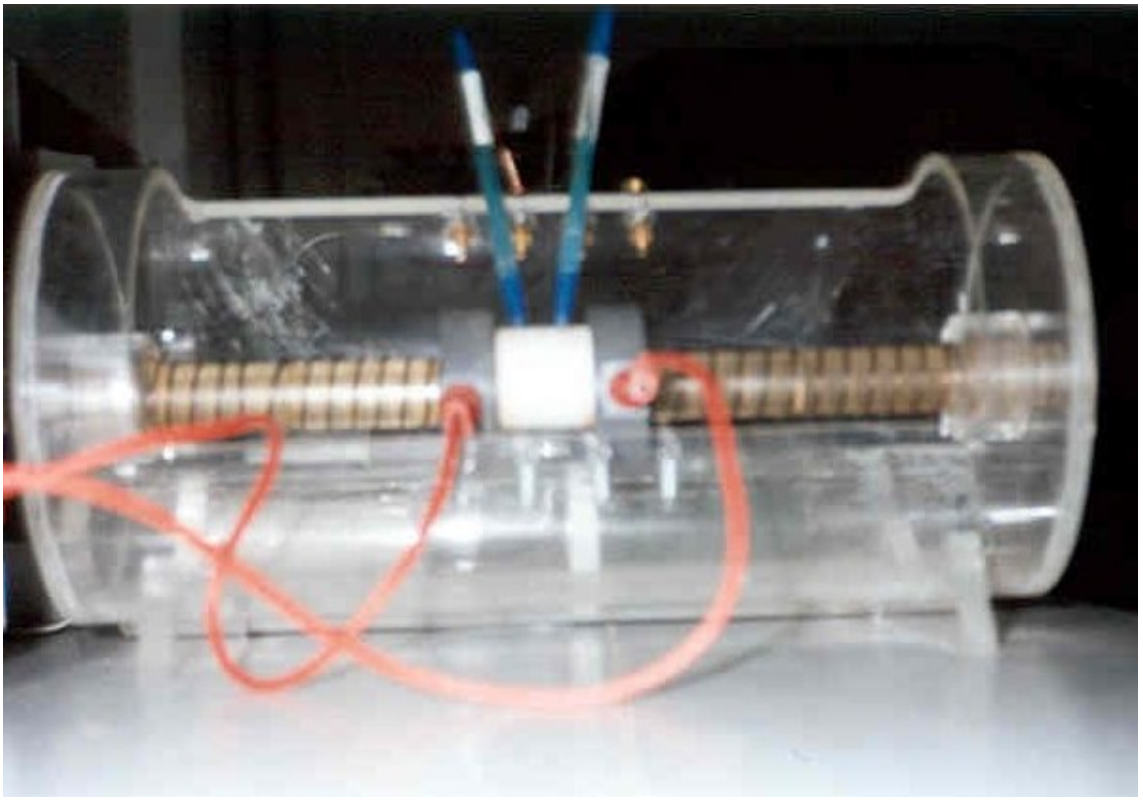

Figure 5.4: Sample holder and potential electrodes

In order to properly use the electrodes, a CTU core sample holder shown in Figure 5.4 was used. It has output terminals to which the potential electrodes were connected and linked to the receiver by measuring cables. It has copper disks at its ends, and for this experiment, acted as the current electrodes.

Wires transmitting current were then fixed to the current electrode terminals of the CTU, which are just on the round disks of the core holder and then connected to the ITC Laboratory Transmitter.

For the IP measurements, the samples were put in the core holder of the same device shown in Figure 5.4. This core holder though designed to accommodate mineral exploration drill hole core sizes, was some how able to accommodate this soil sample size because of the elastic springs around its ends. This would hold the sample during an IP measurement and on change of the sample, one of the handles could just be moved in the opposite direction to the other. The copper contacts were regularly cleaned to ensure good electrical contact.

5.4 Geometric factor K

This is a constant numerical factor, which when multiplied by the measured resistance will convert the resistance to the resistivity for a uniform medium. It is dependant on the type of the electrode array and spacing used. It was essential to determine the K because the experiment involved measurement of resistivity. The sample tubes are considered to be cylindrical, and owing to the electrode array used, the K is computed in the following way:

Consider a cylindrical sample tube as shown in Figure 5.5, (ℓ) being the length between the potential electrodes.

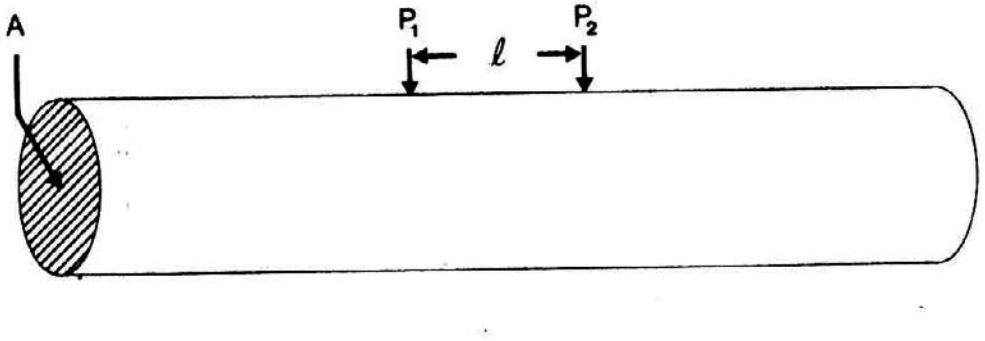

Figure 5.5: Cylindrical sample tube

The area of the circular end (A) of the tube is calculated by the following expression:

$$A = \pi(d/2)^2 \tag{5.1}$$

The following expression is then used to find the geometrical factor K:

$$K = \frac{\pi(d/2)^2}{\ell} \tag{5.2}$$

Where d is the diameter of the circular end and ℓ is the distance between the potential electrodes P_1 and P_2.

For all the sample tubes, the ℓ was measured with a ruler and by use of Equation 5.2, the K values were obtained and are presented in Appendix B.

5.5 Determination of water content

This is a test that is intended to measure the mass of water contained in a soil sample as a percentage of the dry sample mass. In this study, water content of the soil is defined as the ratio expressed as a percentage, of the weight of water to the weight of the dry soil in the given mass. It is required as a guide to classification of natural soils (Franklin and Vogler, 1979) and is a useful property to know as it enables electrical induced polarization to occur once a current is fed into the soil sample.

A standard operating procedure was followed to determine the amount of water in the soil. This involved weighing clean and dry plastic (PVC) containers using a Mettler top pan balance (dynamic range=400g) to the nearest 0.01g as shown in figure 5.6.

The wet soil samples and their containers were weighed again to the nearest 0.01g. The sample tubes were opened, the soil left to dry in air for an overnight and then weighed again the next day. IP measurements were made in between each of these steps. Care was taken when drying the samples not to lose any material as a spill over. The same procedure was repeated 15 times after an interval of 1 day after each balance measurement.

In order to completely dry the sample, a gravimetric method was used in which soil samples were heated and dried in an oven at 105^0C to a constant weight for 24 hours. The sample container was made up of PVC material and resisted the high temperature for 24 hours. The samples were then put in a desiccator for cooling before being weighed. This ensured that no moisture could be absorbed by the soil during the cooling process. A balance of adequate capacity (Figure 5.6), capable of weighing to a resolution of 0.01g of the sample weight was used. The dry weight of the soil was used as the divisor in the calculation because it expresses the absolute

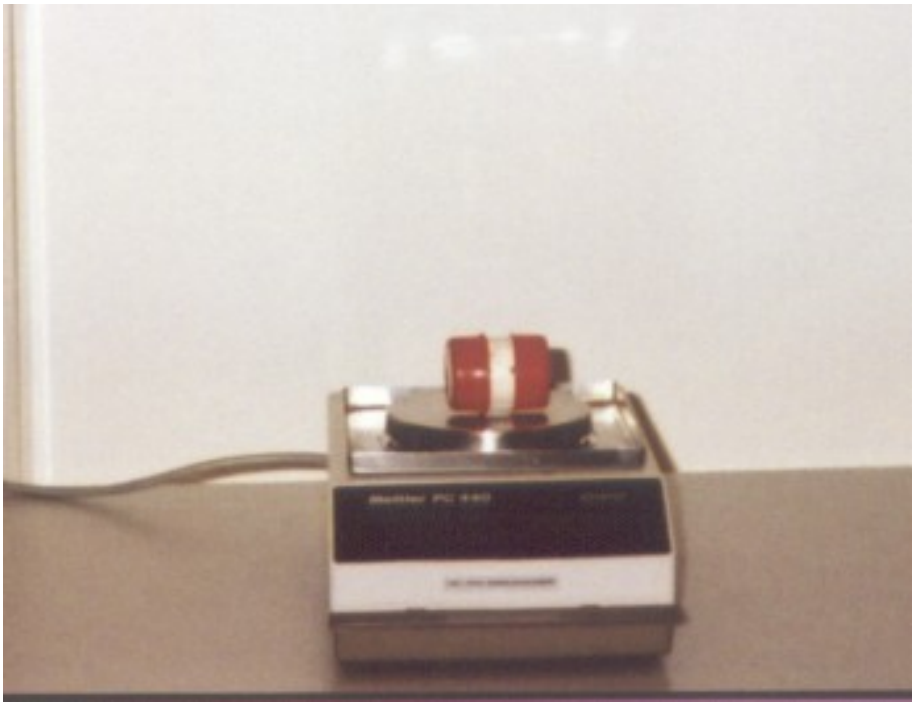

Figure 5.6: Weighing process

quantity of soil present. The following mathematical expression was then used to find the percentage of water that is contained in every sample.

$$W = \frac{M_w}{M_s} * 100 \tag{5.3}$$

Where M_w is the mass of the water
M_s is the mass of the dry soil.

In the same experiment, the degree of water saturation was determined by taking the mass of water (M_w) as obtained from above and dividing it by the total mass of water contained in the pores at saturation. Since 1 g of water is equivalent to 1 cm^{-3} of water, then the expression for the degree of water saturation (S_w) becomes

$$S_w = \frac{V_w}{V_{total}} \tag{5.4}$$

where V_w is the volume of water and V_{total} is the total volume of water in the pores (Franklin and Vogler, 1979).

Volume of cylinder is given by:

$$V = \pi * r^2 * h \tag{5.5}$$

Other measurements involved the determination of porosity for all the soil samples. Porosity is defined as the ratio of the total pore volume that is not occupied

by the solid constituents to the total volume of a representative soil sample. It is a dimensionless quantity and expressed as either a decimal fraction or a percentage. Porosity measurements were made on the soil samples by taking volume of water in the pores of samples at saturation and then dividing it by the volume of the sample tube as determined by Equation 5.5. In particular the following expression was used to compute for the porosity (Φ)

$$\Phi = \frac{V_{water}}{V_{total}} * 100 \tag{5.6}$$

Where V_{water} is the volume of water contained in the soil sample when saturated, and V_{total} being the bulk soil sample volume (Franklin and Vogler, 1979).

5.6 Instrumentation

The laboratory measurement system used in this study was the ITC Laboratory Transmitter and IRIS Elrec–6 Receiver (Figure 5.7) units employing the four–electrode technique similar to that used by (Vanhala and Soininen, 1995). These are respectively a laboratory transmitter and a digital multichannel IP receiver adapted to small–scale laboratory measurements of induced polarization.

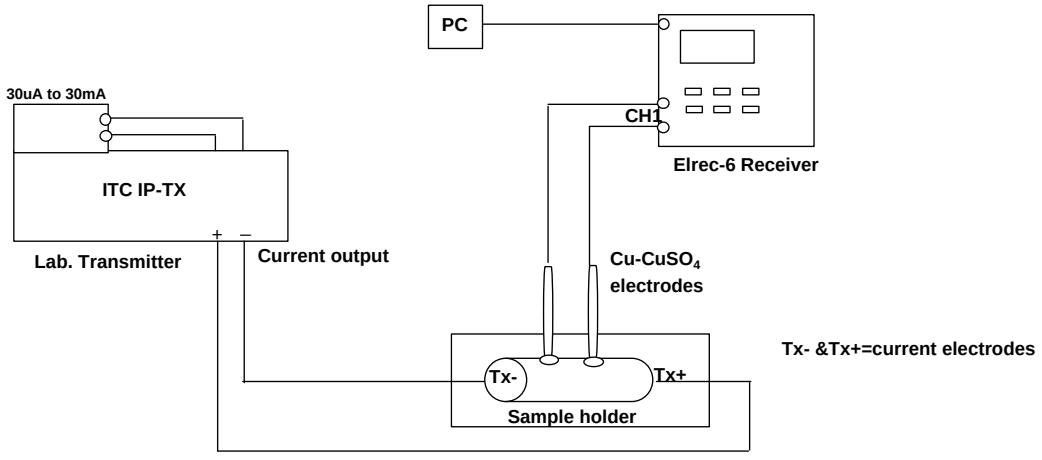

Figure 5.7: Schematic representation of the IP instrumentation set up

Figure 5.7 shows an illustration of the instrumentation employed for the time domain IP measurements in the laboratory. The ITC Laboratory Transmitter was modified to suit laboratory work in addition to the field measurements of small

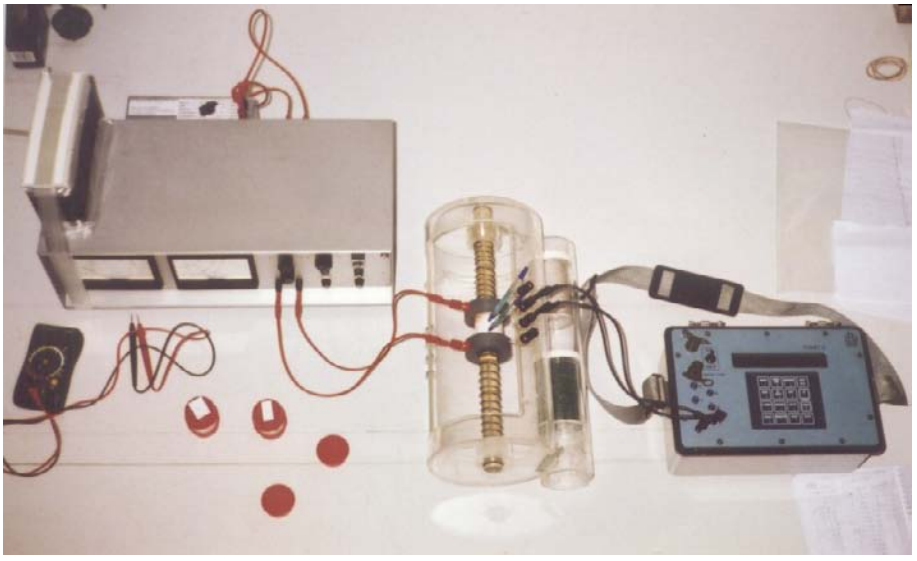

Figure 5.8: IP instrumentation set up

A–MN–B separations. The A–MN–B refers to the arrangement of electrodes where AB are current electrodes between which, are the potential electrodes indicated here as MN.

It consists of two parts:

(a) ITC IP–TX Transmitter which generates a square pulse electric current that is fed to the current electrodes AB. This transmitter has the following specifications: a crystal controlled timer and a relay driver where the On+=Off=On-=Off=2.000 sec with the 'On' time and 'Polarity' relays switching signals. The polarity is automatically changed between the pulses. The waveform shown in Figure 5.9 indicates how the current is usually transmitted. The pulse times as indicated from above are T=2.000 sec. It has a 7 steps current regulator with a nominal range from 30 μA to 30 mA with 9 defined selector switch positions: Battery, Off, 30 μA, 100 μA, 300 μA, 1 mA, 3 mA, 10 mA, 30 mA. The transmitter is powered by batteries with an output voltage of nominally 18 volts because it is made with batteries of 6 Volts.

(b) IRIS Elrec–6 Receiver is a six dipole multiwindow Time domain Receiver designed for induced polarization DC electrical measurements (Figure 5.10). It is powered by either six 1.5 D size alkaline dry cells or one 12 V external battery or two internal rechargeable 6 V batteries connected in series (=12 V). In the time domain mode, and besides the classical logarithmic and arithmetic sampling modes of chargeability, the programmable mode offers 10 fully independent IP windows. It measures the voltage between the receiving electrodes and displays the apparent resistivity and the chargeability values. The measurement is made fully automatically through

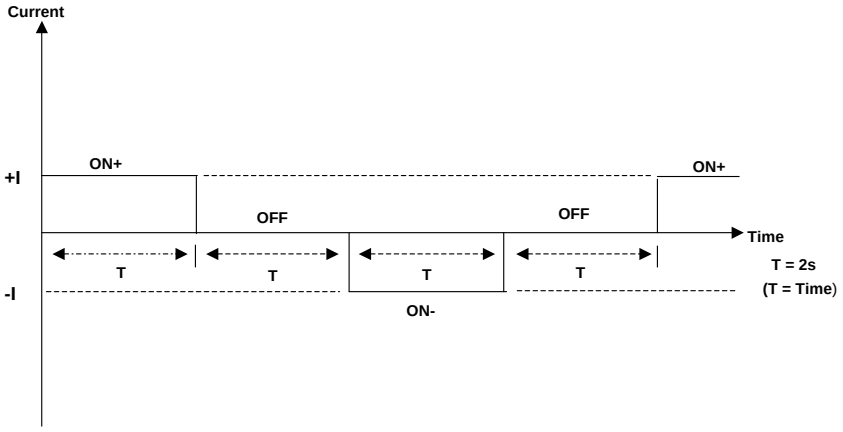

Figure 5.9: Transmitted time domain current wave

the control of a micro processor that does the automatic self potential correction, the digital stacking for signal enhancement and the error display in case of procedure troubles. A real time clock introduced in the instrument permits the recording of each reading with the date and the time of the measurement.

Figure 5.10: IRIS Elrec–6 receiver

5.7 Laboratory techniques and methods of measurement

5.7.1 Time domain method

The IP time domain measurement mode was used in this experiment. After the set up of the experiment as shown in Figure 5.7, the Transmitter had to be calibrated by the following procedure: First the battery voltage reading was recorded using the digital voltage meter (DVM) set at voltage 20 VDC when the switch is put in Battery position as shown in Figure 5.11 . Secondly the current output was measured using the same DVM but using the Ammeter section. The switch was progressively put on each successive current settings and the value was read and recorded with strong attention to the DVM settings at a bigger scale when the range is getting exceeded. When all that was done the system was then connected for IP measurements as shown in Figure 5.8. The calibration of the transmitter was done before every measurement and the values of voltage and current written down (Appendix B, Table 6. The regulator was put in Off position and then two jumpers were connected from the regulator to the back of ITC IP–TX. The terminals in the front of the ITC IP–TX were connected to current electrodes of the sample holder as shown in figure 5.11. An attempt was made to keep the cables as straight as possible to minimize electromagnetic coupling.

Before the actual IP measurements could be made, the Elrec–6 Receiver had to be properly set. The following operations had to be made after the setting up of the experiment and these included: a **BATTERY CHECK** in order to check the voltage of the internal batteries (IRIS, 1998). This was done when the unit (Elrec–6) had been switched on. For proper operation of the instrument , the voltage of its dry cells have to be more than 5.6 V.

In order to select the sampling I.P decay curve, the mode that consists of four types of sampling of Time domain I.P decay curves had to be set. The four modes include the Arithmetic, semi logarithmic, logarithmic and programmable. For this particular study, the **semi logarithmic mode** was selected and according to the charging time which is 2000 ms, this mode shows 10 I.P windows as shown in figure 5.12. Table 5.1 shows the window widths (ms) for the semi logarithmic mode with charging time of 2000 ms.

Due to the fact that for any I.P measurement a certain configuration of electrodes has to be used, it was important to set the **E–array** which is the electrode configuration. For this experiment, the electrode array was described amongst the **"OTHER"** category which includes all those electrode arrangements that are not incorporated into the instrument by the manufacturers.

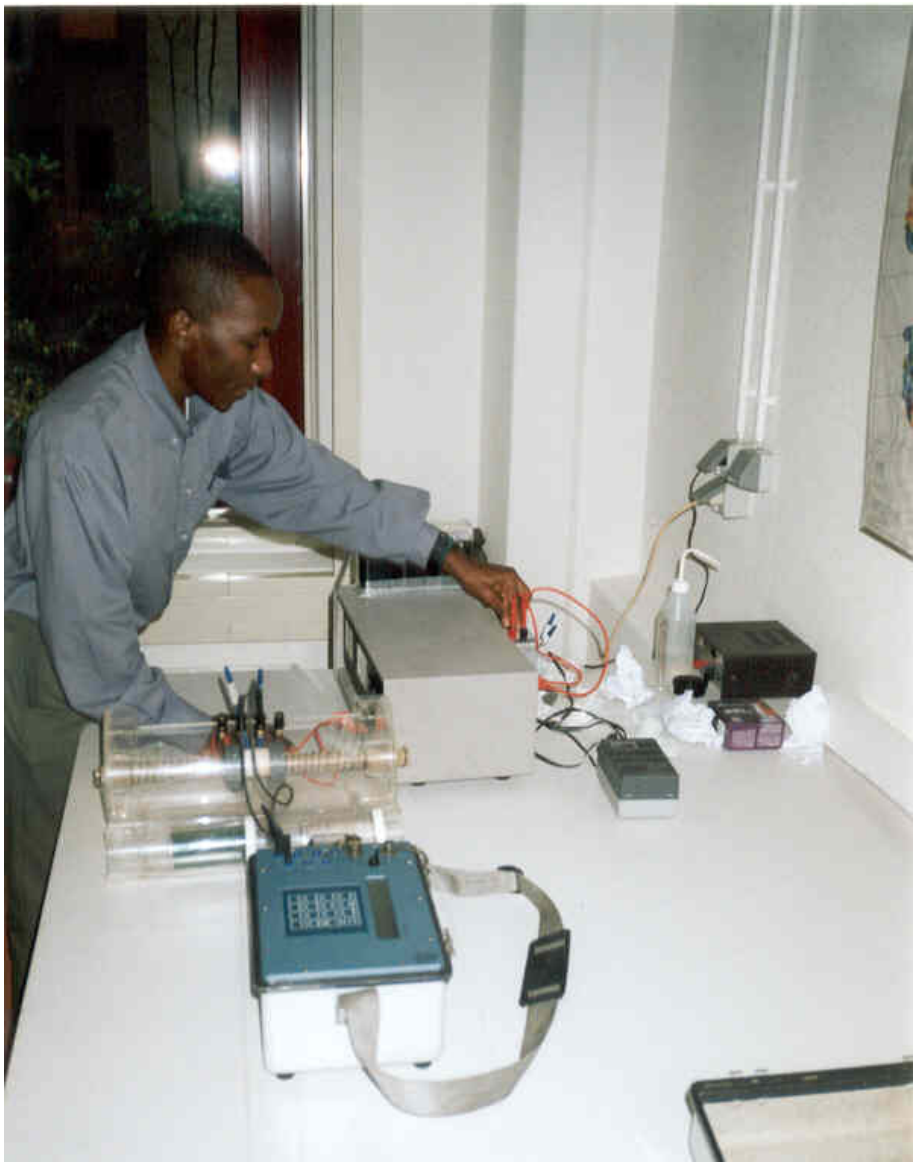

Figure 5.11: Calibration of the transmitter

Other important settings were under the configuration menu which concern the type of IP values, type of readings, sign of voltage, type of grid unit and set date options. Raw values of IP option was selected because it gives the true chargeability values during the measurement as opposed to normalized value option that gives chargeability values according to a standard IP decay curve. The type of readings chosen was the **running readings** whereby the values displayed during the measurements are the average values of the three last consecutive pulses. On the other hand, the cumulative readings show values that are the average of all the pulses received from the beginning of the measurement. For the voltages, it was suitable to

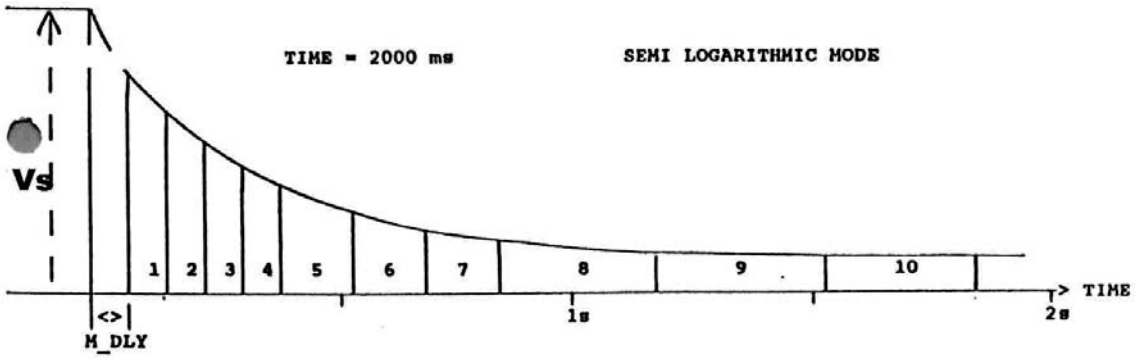

Figure 5.12: Decay curve sampling mode

Table 5.1: Window widths (ms) for the decay curve semi logarithmic mode

	TIME = 2000 ms											
MODE	V_DLY	M_DLY	1	2	3	4	5	6	7	8	9	10
SEMI LOGARITHMIC	1260	80	80	80	80	80	160	160	160	320	320	320

choose the **Unsigned voltage option** because it gives the primary voltages at the end of the measurement in absolute value regardless of the polarity i.e they will always be positive. For the signed voltage option, the voltages are signed with respect to the polarity of the dipole and consequently, the resistivity values are also signed. The **metric grid** was selected as the type of grid unit. This means that some parameters were to be introduced in meters such as the geometrical factor (K) and in this case, the apparent resistivity value was computed by the system in Ohm–meters.

The above described operations do not change so frequently if the experiment is carried out under similar conditions. However, there other operations that have to be changed for every measurement because they are sample specific. This leads to the description of the procedure of the measurement of induced polarization effect.

After putting the soil sample in the sample holder, both current and potential electrodes were connected to the system. From the alphanumeric key board of the Elrec–6 receiver shown in Figure 5.10, the geometrical factor (K) was introduced through the **SPACING** option. The K values were obtained as described in Section 5.4. The introduction of the K value at this point was very important because of the electrode array which was selected with the **E–ARRAY key** and the need for the computation of the resistivity values.

In order to ensure proper connection of the electrodes to the instrument channel (Channel 1) of the receiver before current was transmitted, the ground resistance

Figure 5.13: Measurement process

of the electrodes were checked by use of the **Rs CHECK key**. It is recommended to operate with the lowest possible values of ground resistances preferably around 4 k Ω though a value of 20 k Ω should not be exceeded. For this study, the contact resistance was maintained below 20 k Ω.

The current being transmitted has to be entered into the system and this was done through the **SET UP KEY**. In addition, the measuring domain (TIME) and pulse duration were selected. The current was set in mA and the time was 2000 ms and constant throughout. The measuring domain was selected as Time T. wave which permits to compute the global apparent chargeability and partial chargeabilities by sampling the I.P. decay curve. This option uses a symmetrical Time domain

waveform curve: ON+, OFF, ON-, OFF as shown in Figure 5.9. In this domain, the sampling rate is 10 ms with an accuracy in synchronization of 10 ms. The chargeability values measured have a resolution of 0.1 mV/V with a typical accuracy of 0.6 %, and a maximum of 2 % of reading 1 mV for Vp>10 mV. It was very important before any measurement to control the level of noise by use of the **MONITOR KEY**. This function features a voltmeter that can be used to display the value of voltage coming from the soil sample in mV.

After making all those settings, measurements were taken by pressing the **START key** and after seven pulses, the process was stopped and the readings recorded in the memory of the receiver (Figure 5.13). After the experiment, the data that had been stored in the memory of the receiver, would be transfered into the computer using a serial link and a data transfer software utility provided with the IP receiver as shown in Figure 5.14.

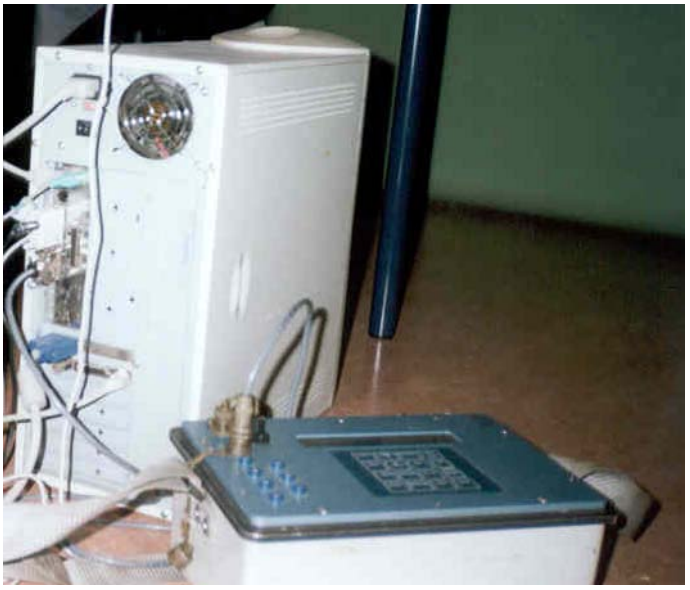

Figure 5.14: Data transfer to a PC

What was given as a result were chargeability values which are described in the following way. In each I.P window (T_{Mi}: width), the value of the partial apparent chargeability (Mi) is computed and these Mi values permit to obtain the weighted value (M) of these partial chargeabilities (Mi).

At the end of the measurement, the average values of partial apparent chargeabilities (Mi) are computed. The weighted average value (M) of these average partial apparent chargeabilities is also computed.

$$M = \frac{\sum_{i=1}^{nip} T_{Mi}.Mi}{\sum_{i=1}^{nip} T_{Mi}} \tag{5.7}$$

Where
nip is the number of I.P. windows: up to 10.
T_{Mi} are the width of the I.P. windows, expressed in ms.
Mi are the average values of the partial apparent chargeabilities, expressed in mV/V
.
M is the weighted average value of the average partial apparent chargeabilities, expressed in mV/V)(IRIS, 1998).

It was observed that as the samples were becoming dry, the chargeability was decreasing. The contact resistance potential electrodes were observed to increase when the samples lost water.

5.8 Test measurements

- Ten pairs of potential electrodes were tested in terms of their contact resistance. It was observed that potential electrodes with match sticks as their porous contacts had contact resistances ranging between 100–350kΩ whereas those with sisal material contacts were below 20kΩ.

- A test run was made to check the effect of a charger connection to the receiver on the chargeability values as compared to its in–built DC voltage output. It was observed that there was no change in the chargeability values given by the same sample under the two conditions e.g sample 1 (Spain) at current of 0.29 mA gave a chargeability value of 0.29 mV/V with and without a charger.

- Measurements were made on the same sample to test the effect of different values of current. The currents used were 0.03mA, 0.10 mA, 0.29 mA and 0.97 mA and the chargeability values given were 2.90 mV/V, 3.77 mV/V, 2.30 mV/V and 2.03 mV/V respectively.

- Soil samples were weighed before they were prepared for IP/Resistivity measurements, to check whether the dynamic range of the Mettler top balance is not exceeded.

5.9 Sources of errors and their magnitude

When performing this experiment, sources of errors were identified and are outlined as follows

1. The samples were dried in air (room temperature) when the caps have been removed. The Oven was not used for the daily drying because the same samples

were to be taken for another test (NMR) and it was thought that heating them before that test would distort the structure of the clay mineralogy. This air drying did not ensure even distribution of water in the samples giving rise to a possible distortion on IP readings.

2. For the IP measurements, all samples were put in a CTU sample holder stand (see Figure 5.4). After the measurements, they were removed and replaced. The problem was that when these samples were still wet, when removing them, they would leave some soil particles on the current copper contacts (current electrodes)(Figure 5.16). A laboratory tissue was used to clean the contacts but it was impossible to recover all the soil from the tissues back to the samples. This gave errors in the procedure for the determination of the water content to the magnitude of 0.80g. When the samples were dry, particles would spill over onto the surface of the sample holder stand, a small brush was used to collect them but it was impossible to get all of them.

3. The potential electrodes used were locally made, which caused problems. The sisal material used as a porous contact between the electrode and the soil sample was dripping and as result contaminating the samples. This means that when measurements are done on the following day, the resistivity and IP values may be different. Owing to this dripping nature, the contact resistance of the potential electrodes was very hard to keep constant. The effect due to this is that chargeabilities may change if contact resistances are not kept constant (Scintrex, 1981). In order to quantify this error, samples were weighed before being put in the experimental set up and then after. This gave an average 0.5 g of extra weight. The contact resistance of the potential electrodes was always above the optimal ceiling ($\leq$ 4 kΩ) but within the acceptable range of 0–20 kΩ (IRIS, 1998).

4. The sample tubes were locally designed from a long Polyvinyl tube to the dimensions mentioned in section 5.2. Cutting these sample tubes was not perfectly done because they did not have flat ends. The ends of some of the tubes were a little bit diagonal (Figure 5.15). The effect due to this is that when the ends are not flat, there is no good current electrode contact. Errors were also given by irregular end surfaces of soils themselves. For example sample number 9, the end surface was irregular and the measurement taken gave with it gave a chargeability value of 0.33 mV/V and after flattening the end surfaces, it then gave a chargeability value of 1.56 mV/V. This is caused by heterogeneous flow of electric current in the sample due to a localized contact.

5. When some samples were saturated with distilled water, they overgrew and

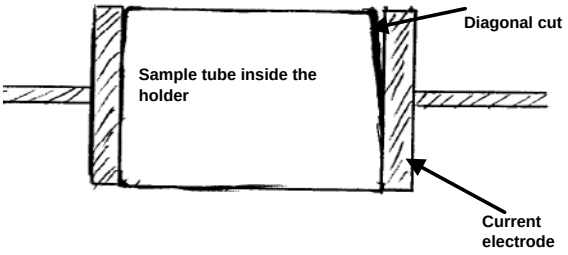

Figure 5.15: illustration of the diagonal cut of the sample tubes

in an attempt to make the surface flat, the overgrown part was trimmed off. On drying, these samples shrunk and became smaller, which provided a poor current electrode contact.

6. The springs on the CTU–2 sample holder were not strong enough to hold the size of sample that was used in this experiment. The problem was easily identified when improvising for the current electrode contact by using the aluminium foil or the old two and half Dutch guilder coins. When the rods bearing the springs are physically pushed towards each other (Figure 5.4), the voltage output from the transmitter and observed with receiver is increased thus indicating a better current electrode contact than before.

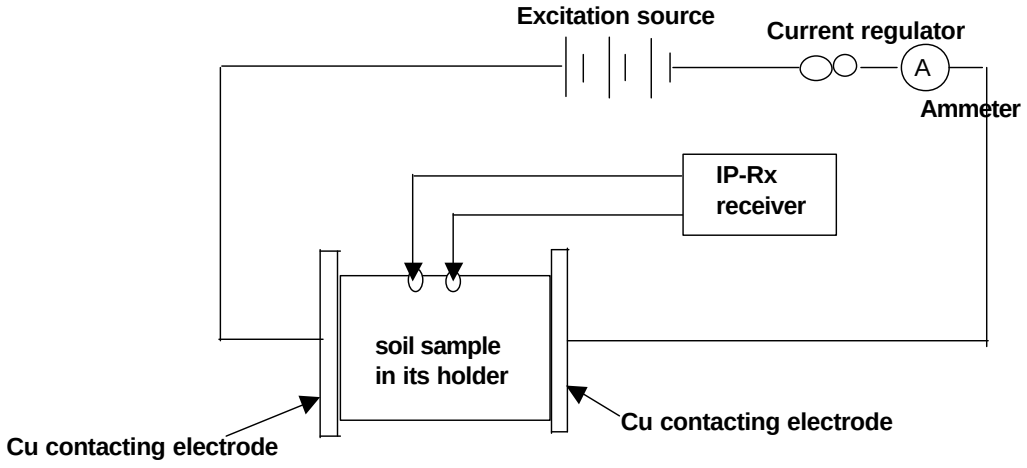

Figure 5.16: illustration of the set up

7. Some IP measurements were carried out when the excitation was not current regulated i.e the regulator not being in its linear range. This was being checked by taking a spot check at the current electrodes (Figure 5.16) and making sure that the voltage across them is less than 5 volts. Because of this error, the

results obtained from samples (13, 28 and 30) were removed from the data set of this study together with half of the results obtained from samples (9, 12 and 27). For the rest of the samples, the last two measurements that were taken when the samples were getting drier were also removed. The requirement of linearity for electrode polarization was only fulfilled with current ($\leq$ 2.84 mA), so IP measurements taken with current (9.07–25 mA) were not considered in this study.

A table of the IP/Resistivity measurements reliability is presented in Appendix B (Table 4). It shows what happened to each of the soil samples during the experiment.

Data acquisition is an important aspect of this research. The chapter has outlined the main steps taken to prepare, saturate and weigh the soil samples. The IP instrumentation (ITC–IP Transmitter and Elrec–6 Receiver) has been described in regard to use, calibration and maintenance. However, there were errors observed during the experiment and these have been clearly stated. The experimental data that has been obtained need to be analyzed in order to acquire more information about soil samples , which is the subject of the next chapter.

Chapter 6

Experimental data and processing

6.1 Introduction

With the main variable parameters of the response obtained i.e chargeability and resistivity, an attempt was made to relate them with the other variables including water content (%), clay content (%), grain size (mm) and CEC (meq/100g). The data /results were displayed using graphs and ternary plots.

6.2 Water content

A standard operating procedure described in Section 5.5 was used to obtain the amount of water contained in the soil samples. A set of data for sample 1 (Spain) is shown in Table 6.1.

Table 6.1: Water content (%) values obtained with sample 1 (Spain)

Field number	Lab. sample no.														
	1	WATER CONTENT DETERMINATION													
		1st reading at saturation	2nd	3rd	4th	5th	6th	7th	8th	9th	10th	11th	12th	13th	14th	15th
Mass of container (g)		17.12	17.12	17.12	17.12	17.12	17.12	17.12	17.12	17.12	17.12	17.12	17.12	17.12	17.12	17.12
mass of wet soil + Container (g)		113.61	113.03	111.91	110.67	108.50	107.67	107.07	105.14	104.13	104.12	103.54	101.7	100.68	99.42	97.35
Mass of wet soil (g)		96.49	95.91	94.79	93.55	91.38	90.55	89.95	88.02	87.01	87.00	86.42	101.7	83.56	82.30	80.23
Mass of Dry Soil + Container (g)		97.35	97.35	97.35	97.35	97.35	97.35	97.35	97.35	97.35	97.35	97.35	97.35	97.35	97.35	97.35
Mass of dry soil (g)		80.23	80.23	80.23	80.23	80.23	80.23	80.23	80.23	80.23	80.23	80.23	80.23	80.23	80.23	80.23
Mass of water (g)		16.26	15.68	14.56	13.32	11.15	10.32	9.72	7.79	6.78	6.77	6.19	21.47	3.33	2.07	0.00
Water content (%)		20.27	19.54	18.15	16.60	13.90	12.86	12.12	9.71	8.45	8.44	7.72	26.76	4.15	2.58	0.00

It was observed that with some soil samples as shown in Appendix B (Table 4) increased in volume on taking up water, and with a gradual loss of water, they decreased in size. This is analogous to clay soils which expand with increase in moisture content whereas moisture loss is accompanied by shrinkage. However, the amount of shrinkage is thought to be effected by the packing arrangement of the particles. It was further observed that the water content of the samples varied depending on the soil type and sampling site.

6.3 Analysis of IP response characteristics

The IP study of samples was developed in successive steps. Initially, a comparative analysis was made of chargeability and resistivity of the different samples. This was followed by a comparative examination of chargeability and water content, chargeability and CEC for fixed clay percentages, and finally chargeability and grain size. This type of analysis provided information regarding the phenomenon of IP in soils under study.

6.3.1 Chargeability and resistivity

From the time domain measurements were obtained readings for the chargeability in mV per volt (mV/V) and resistivity in Ohm–meters (Ω.m). Figure 6.1 shows a graphical display of chargeability (mV/V) against resistivity (Ω.m) at saturation. The legend shows 6 classes of CEC values and the origin of samples. The CEC classes were obtained through grouping the clustered points together after sorting them in an ascending order. A group of sample points of the same origin (Spain) with CEC classes (11–15 meq/100g and 16-22 meq/100g) occupy the lower part of the graph between 0–5 mV/V and 0–200 Ω.m The soil samples that are included in the above CEC classes are number 21 with 27.4% clay content, 31 (71.5%), 6 (44.5%), 15 (33.2%), 5 (42.3%), 7 (37.0%), 14 (38.0%) and number 17 with 48.0% clay content, 34 (27.4%), 8 (44.6%), 3 (46.0%), 33 (70.7%), 23 (41.0%), 20 (50.4%), 25 (41.1%) respectively (Appendix B, Table 1).

In the upper part of the graph, there are samples with higher CEC classes dominated by a single origin (Kenya). For examples, samples in the (23–26meq/100g) CEC class include number 13 with 51.8% clay content, 42 (35.5%), 16 (48.0%), 4 (65.4%), 19 (63.7%), 18 (57.2%), 24 (46.1%),37 (56.0%) whereas in the class (27–30 meq/100g) there are number 1 (57.7%), 2 (61.4%), 9 (67.9%) and 43 (53.7%). This group of samples is characterized by higher chargeability values (13–21 mV/V) but with the same range of resistivity as the first group.

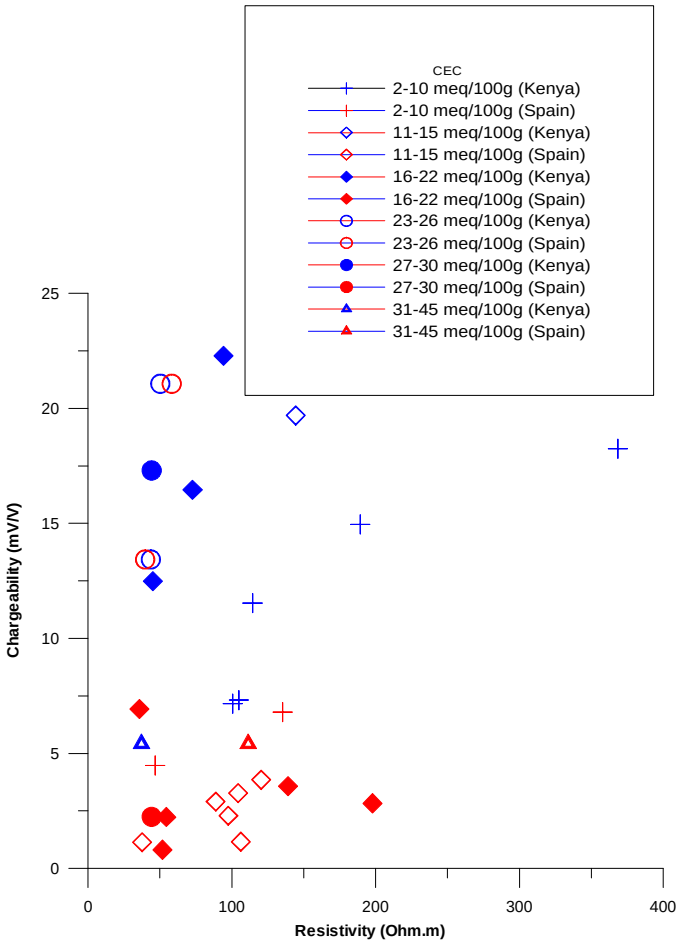

Figure 6.1: A plot of chargeability against resistivity

6.3.2 Chargeability and water content

Figure 6.2 shows the results of measurements done on samples 2, 17, 19 from Spain and 27 from Holland. In general, their chargeability values increase with increasing water content up to a maximum beyond which they decrease. Sample 2 attains a maximum of 1.56 mV/V at 36% water content. It contains 36% of clay with a CEC value of 19.0 meq/100g. It is a type of soil formed from lacustrine sediments (silt (21.8%) and sand (16.8%) and was collected from a lacustrine plain. Sample 17 was formed from colluvium material and collected from a hill land. It's maximum chargeability (7.39 mV/V) is achieved at 23% water content. Its clay content is 48.8% with 16.8 meq/100g CEC. Other materials include silt (19.0%) and sand (32.2%). Sample 19 is formed from bio–sands and was collected from a piedmont. The value of chargeability obtained at its peak is 3.49 mV/V at 27% water content. The CEC value is 24.4 meq/100g and other materials are clay (63.7%), silt (10.3%) and sand (25.9%). And

lastly, sample 27 which is sandy has a maximum of 3mV/V at 30% water content.

Figure 6.3 shows another type of relation between chargeability and water content. For these samples, the chargeability increases with increasing amount of water almost linearly. Sample 25 has the highest value of chargeability (22.28 mV/V). This soil sample was formed from residual soils and collected from low lying land. It has 41.1% clay, 21.1 meq/100g CEC with silt (40.6%), sand (18.3%). Sample 36 attains a maximum of 14.95 mV/V at 48% water. It was formed from residual soils and collected from a hill slope. It is made of 52.3% clay, 4.3% silt and 43.5 % sand with CEC value of 4.3 meq/100g. For sample 38, the clay content is 85.6%, silt (3.6%) and sand (10.8%). However it has got a CEC value of 8.1 meq/100g. It was formed from residual soils and collected from a hill slope. Sample 39 was collected from an undulating plateau, having been formed from residual soils. Its highest value for chargeability is 18 mV/V at 43% water content. Sample 10 has the lowest chargeability value of 5.42 mV/V at 38% water content in this group. It was formed from colluvium material and collected from a piedmont. It has 71.6% of clay, silt (24.7%) and sand (3.7%). The CEC value is 45 meq/100g.

For the rest of the samples, more graphs are presented in Appendix A and their descriptions in terms of particle size constituents and parent materials in Appendix B (Tables 1 and 2).

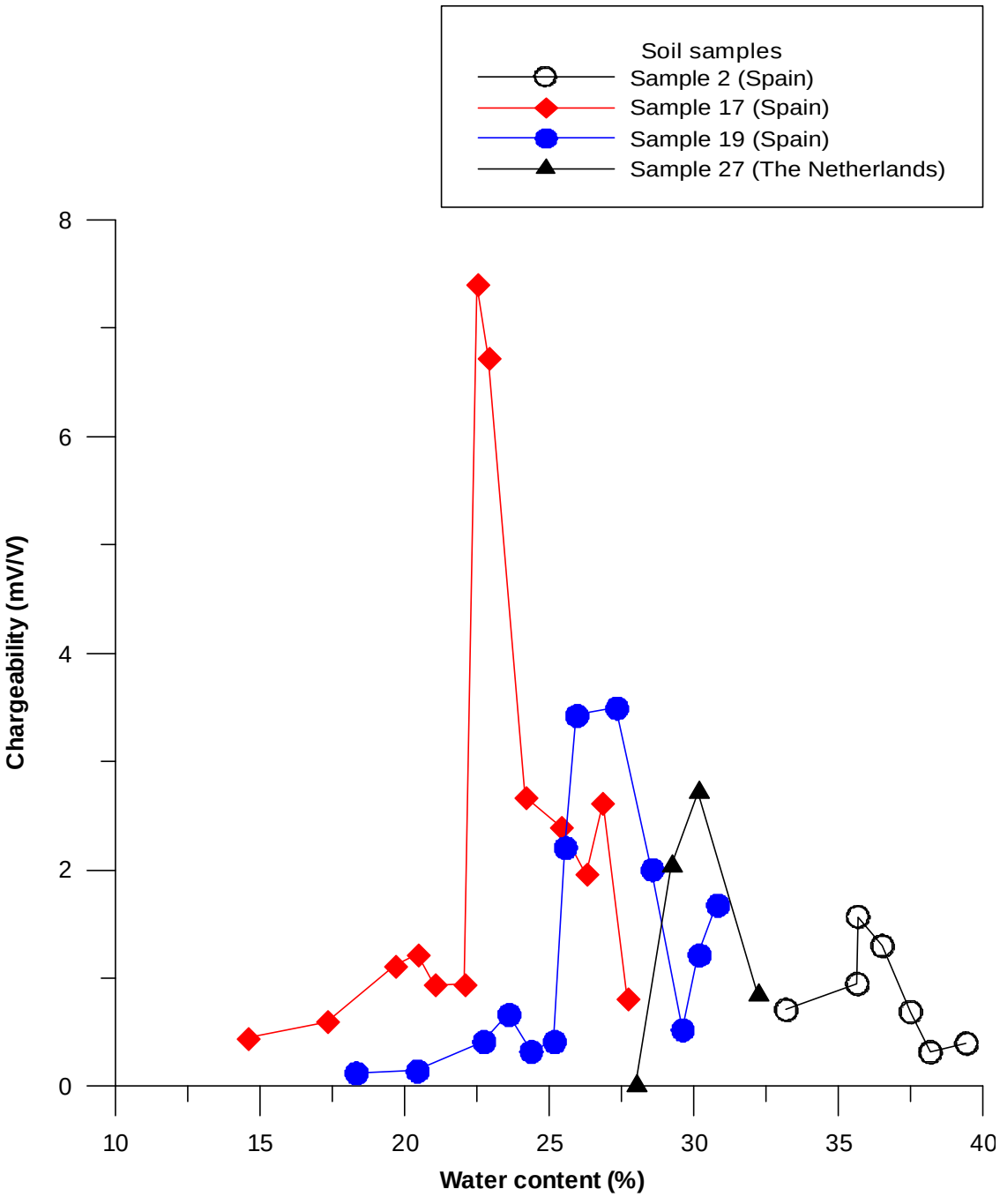

Figure 6.2: A plot of chargeability (mV/V) against water content (%)

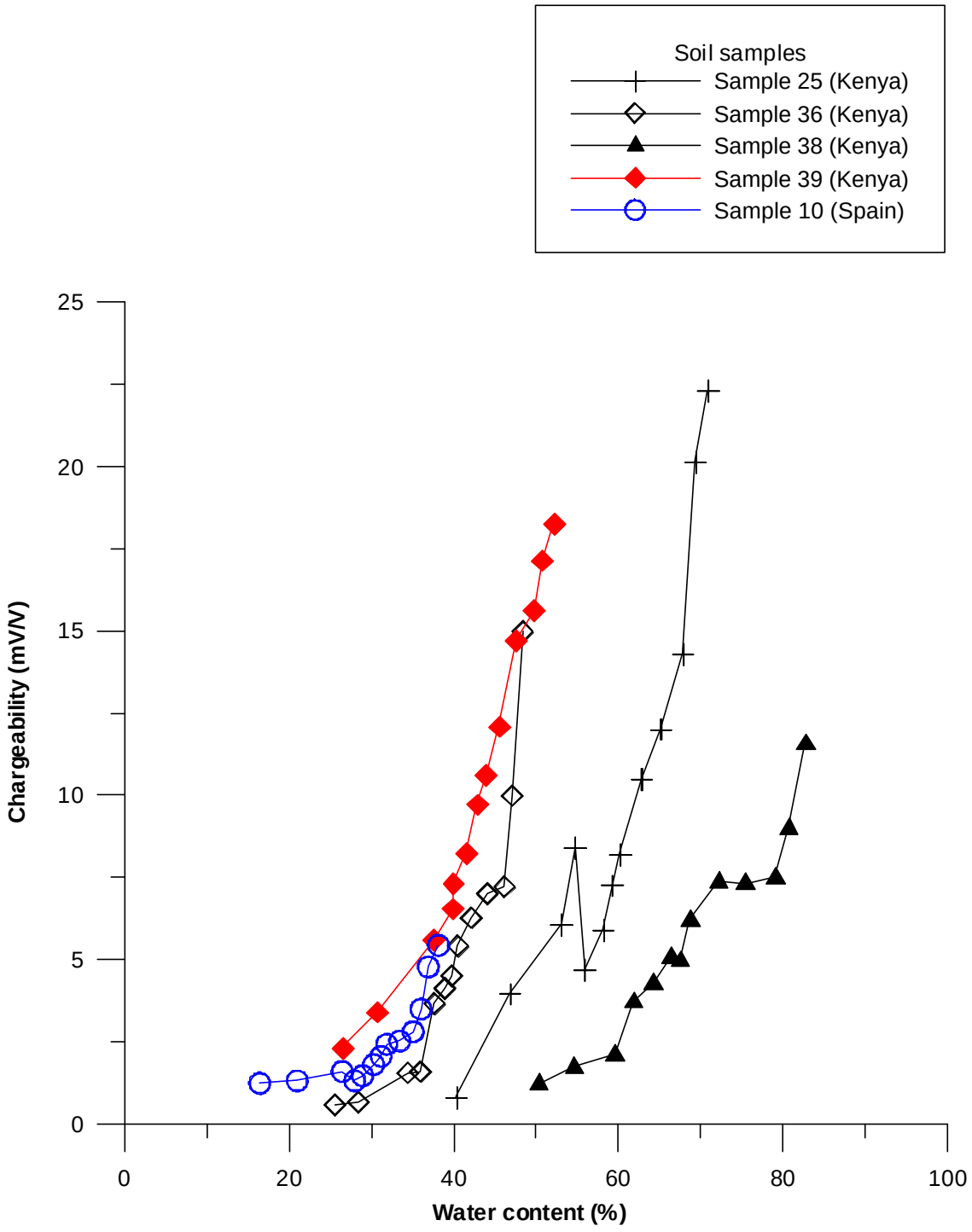

Figure 6.3: A plot of chargeability (mV/V) against water content (%)

6.3.3 Chargeability and clay mineralogy/CEC

In order to study the behaviour of chargeability with clay mineralogy which is characterized here by CEC, a graphical display shown in Figure 6.4 was used. The legend shows the clay percentage classes, which were fixed following a similar procedure as described in Section 6.3.1

Figure 6.4 shows that for a fixed class of clay percentage, the chargeability increases with increasing CEC. With respect to the origin of samples, Kenya samples are represented by higher chargeability values than the Spain samples.

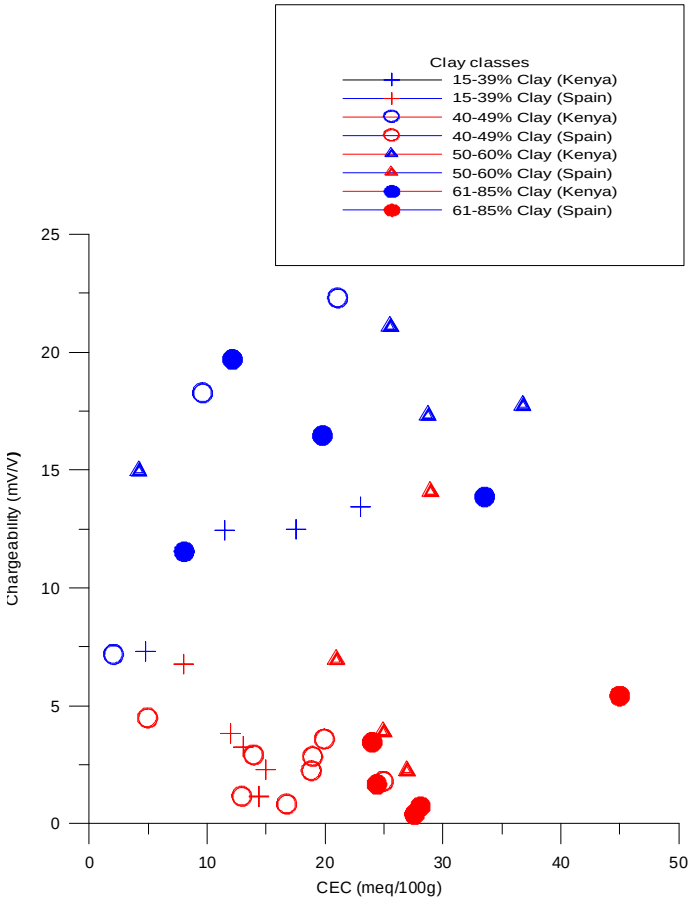

Figure 6.4: A plot of chargeability (mV/V) against CEC (meq/100g)

6.3.4 Chargeability and granulometrical composition of soils

Soils consist of an assemblage of discrete particles of various sizes and so the granulometric composition is made up of separate ranges of sizes that have been determined in relative proportions, by dry mass, of each size range. This grain size classification has a direct application in engineering studies and hydrology.

In an attempt to analyze the relationship between chargeability and the granulometrical composition, a triangular representation was used as shown in Figures 6.5. The corners of the triangle represent the three different grain sizes for Sand ($>$ 0.05 mm), Silt (0.002–0.05mm) and Clay ($<$0.002mm). Each corner of the triangle corresponds to hundred percentage of the respective grain sizes. Samples plotted at the sides of the triangle represent bimixtures of the two grain sizes while any sample lying within the triangle represents a trimixture.

The chargeability of each sample was determined at saturation and plotted in the equilateral triangle according to its grain size. The different symbols represent individual soil samples with the three constituent particle sizes as shown in Figure 6.5. The number written against each of the symbols is the chargeability value in mV/V.

In order to get a close examination, a triangular plot representing samples with CEC values greater than 20 meq/100g was used (Figure 6.6). This was an attempt to fix the mineralogy/CEC and investigate the effect of the individual particle sizes on the chargeability.

Figure 6.6 was divided into two ternary plots according to the origin of the samples. It was observed that samples showed different behavior according to their origin as illustrated below.

Figure 6.7 shows the relationship of chargeability and grain size distribution for both Spain and Kenya samples. The plot shows a loose trend of increasing chargeability from very fine Clay ($<$ 0.002 mm) to less fine fractions (Silt (0.002–0.050 mm) and Sand ($>$ 0.05 mm)) in the case of Spain. However, for Kenya samples, there is no clearly defined trend between their chargeability and particle sizes.

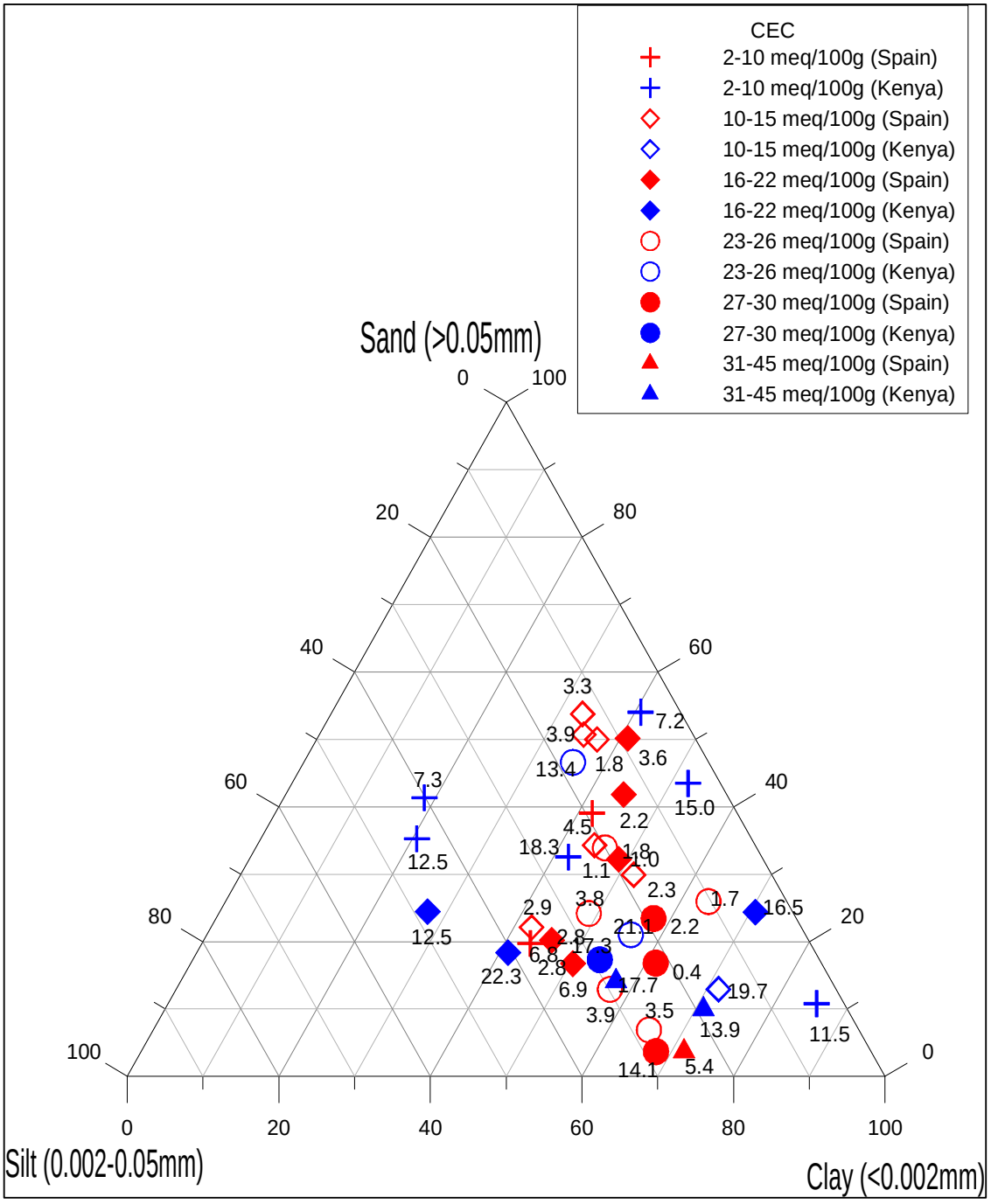

Figure 6.5: Effect of grain size on the chargeability of soil samples

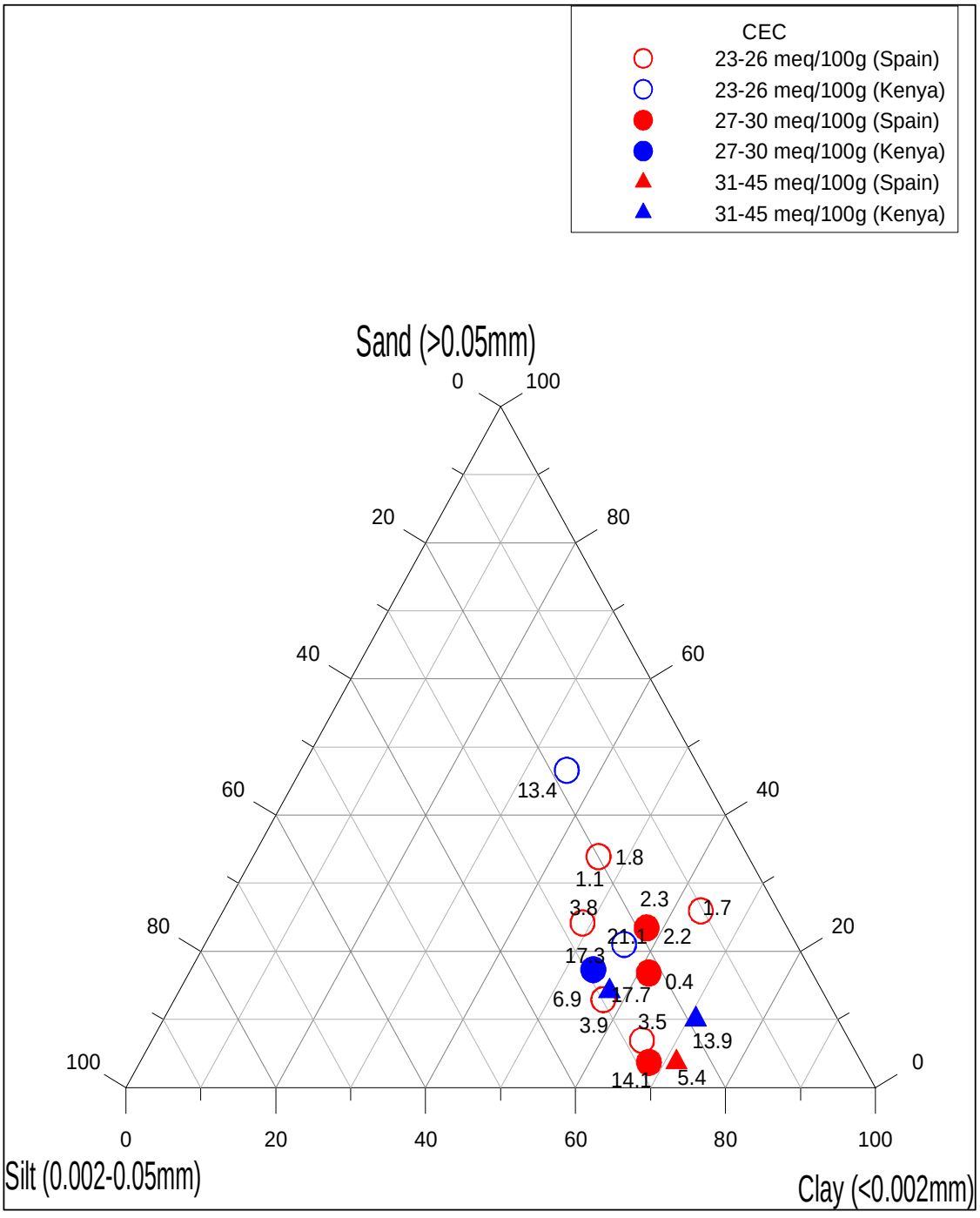

Figure 6.6: Effect of grain size on the chargeability soil samples

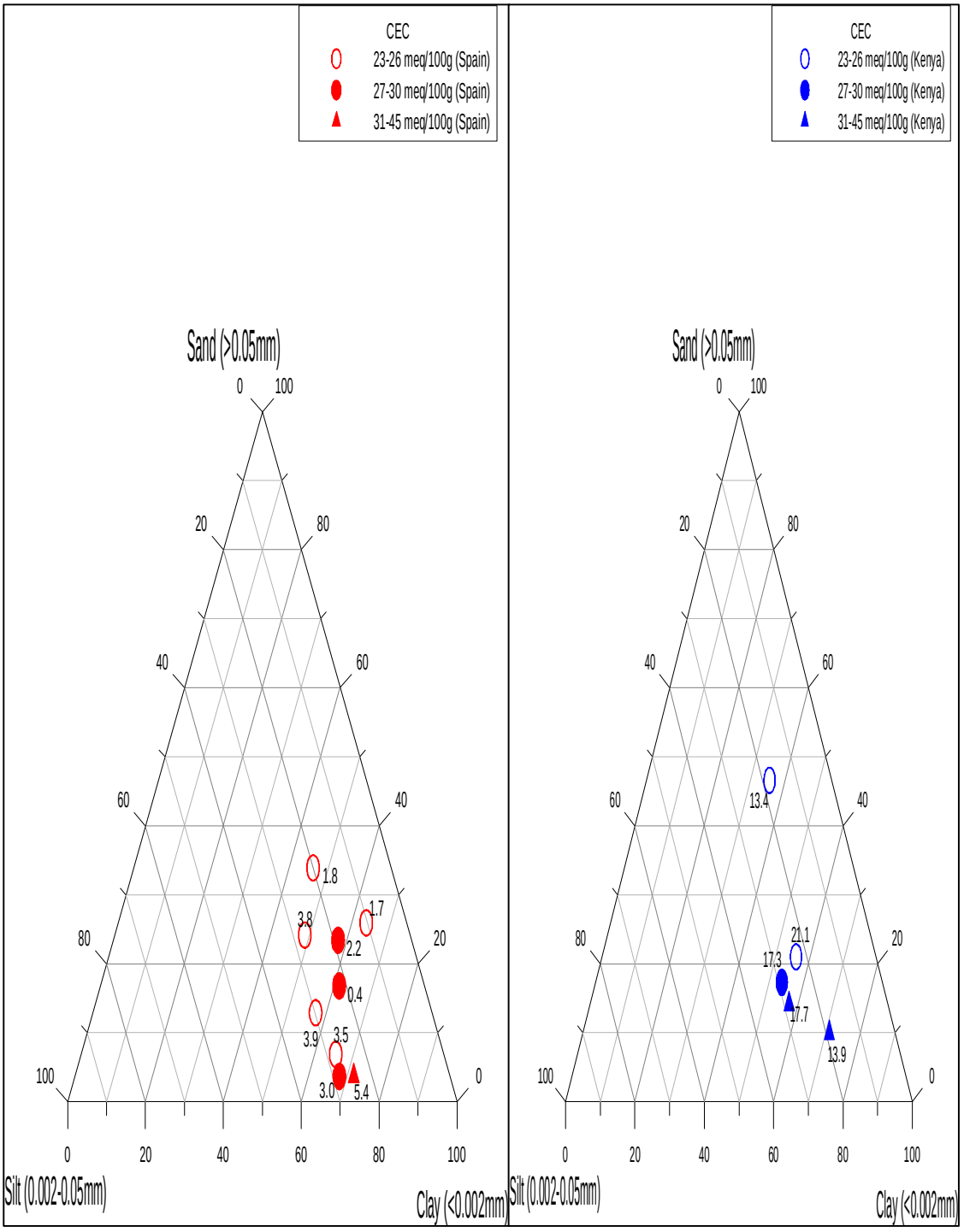

Figure 6.7: Effect of grain size on the chargeability of Spain and Kenya samples

6.4 Decay curve analysis

In order to get more information from the IP response of these soil samples, the exponentials of the individual decay curves were analyzed as suggested in the work of Illiceto et.al (1982), Ogilvy and Kuzmina (1972) and Roussel, 1962. This was made in an attempt to obtain parameters related to granulometry and water content.

The shape of a decay curve or the time dependence of chargeability M(t) may be described as the sum of an exponential function of the form

$$M(t) = \sum_{j=1}^{n} Aj * exp(\frac{-t}{\tau_j}) \tag{6.1}$$

where τ is the time constant of the relaxation mechanism.

The decay curve (Figure 6.8) was constructed from the chargeability values obtained from the IP channels and Time windows. Decay curves that are shown were obtained from soil samples at saturation and at intermediate water content.

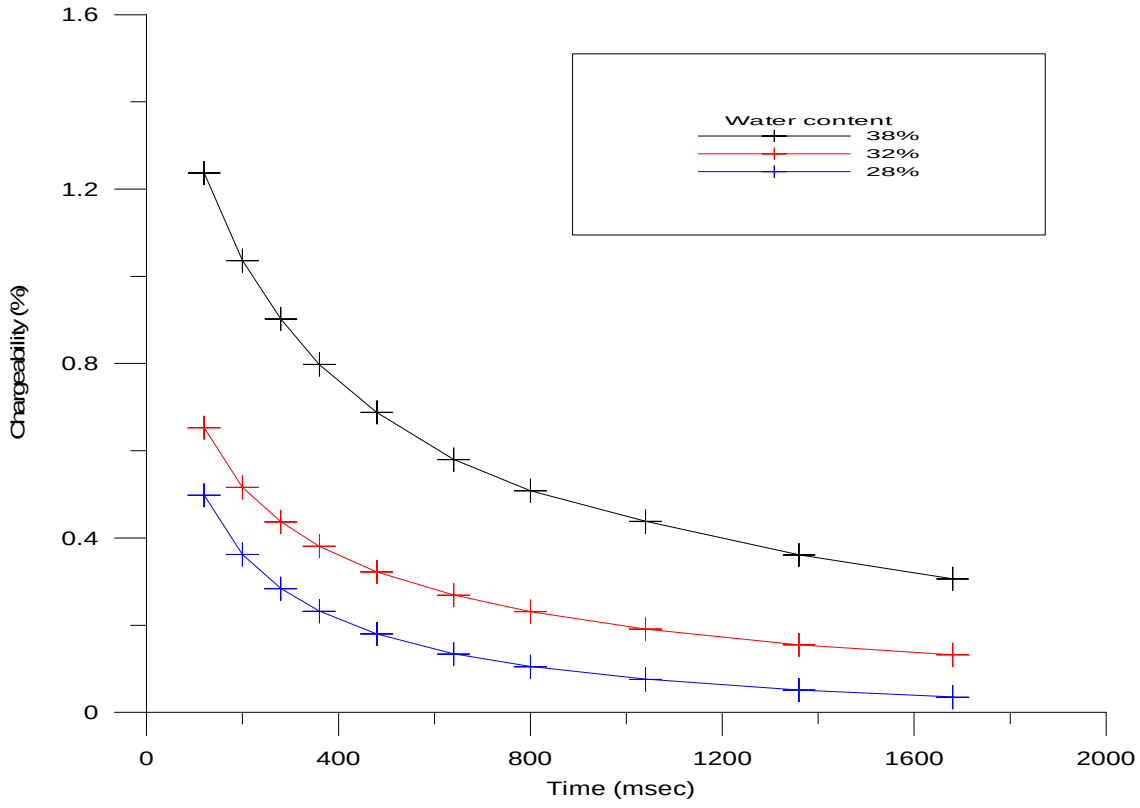

Figure 6.8: Decay curves obtained from sample 10 from Spain at different water contents

The chargeability values were first converted from mV/V to % by dividing them by 10 before plotting them. As mentioned in Section 5.7.1, the semilogarithmic mode

Table 6.2: Typical original receiver readings

V= 525.532	Sp= -12	I= 0.98	Rs= 10.43
Ro= 160.9 Ohm.m	M= 2.24	E= 0.0	
M1= 7.69	M2= 5.77	M3= 4.62	M4= 3.83
M5= 3.04	M6= 2.34	M7= 1.86	M8= 1.43
M9= 1.02	M10= 0.78		
cycl= 8	Time= 2000	V_D= 1260	M_D= 80
T_M1= 80	T_M2= 80	T_M3= 80	T_M4= 80
T_M5= 160	T_M6= 160	T_M7= 160	T_M8= 320
T_M9= 320	T_M10= 320		

of measurement with a time base of 2000 ms was used. This mode measures chargeability in 10 IP windows and these values, referred to as M1...M10 in Table 6.2, make up the Y–axis of the decay graphs.

Consider Table 6.2, V is the average value of voltage, in mV, Sp is the Self Potential at the beginning of the measurement, in mV, I is the introduced value of the current, in mA, Rs is the contact resistance at the beginning of the measurement, in kΩ, Ro is the resistivity value, in Ohm.m, M is the weighted average value of the partial chargeabilities, in mV/V, E is the standard deviation of the chargeability value, M1....M10 are the average values of the partial chargeabilities, in mV/V, V_DLY is the on time delay in ms, M_D is the off time delay in ms, T_M1....T_M10 are the widths of the IP windows, expressed in ms. The time represented on the X– axis corresponds to the delay time plus half time interval of the first window (T_M1) and then for the next time window, it becomes delay time plus the time interval of the first window plus half the time interval for the second IP time window. The same procedure is repeated until the ten time windows are processed. The points effectively represent a digitized decay curve.

In order to extend the IP study beyond the direct chargeability evaluation, decay curves were analyzed using the following interpretation model .

$$m = \sum_{j=1}^{3} Aj * exp(\frac{-t}{\tau_j}) \tag{6.2}$$

The constants A_j and τ_j were determined by least–squares non–linear regression and the Levenberg–Marquardt version of this algorithm was used (Marquardt, 1963).

The three exponential model gives three values of co-efficients (A_1, A_2, A_3) and

three time constants (τ_1, τ_2, τ_3). The advantage of fitting a curve with three exponentials is that it fits the data points well compared to a fit with one exponential as illustrated in Figure 6.9

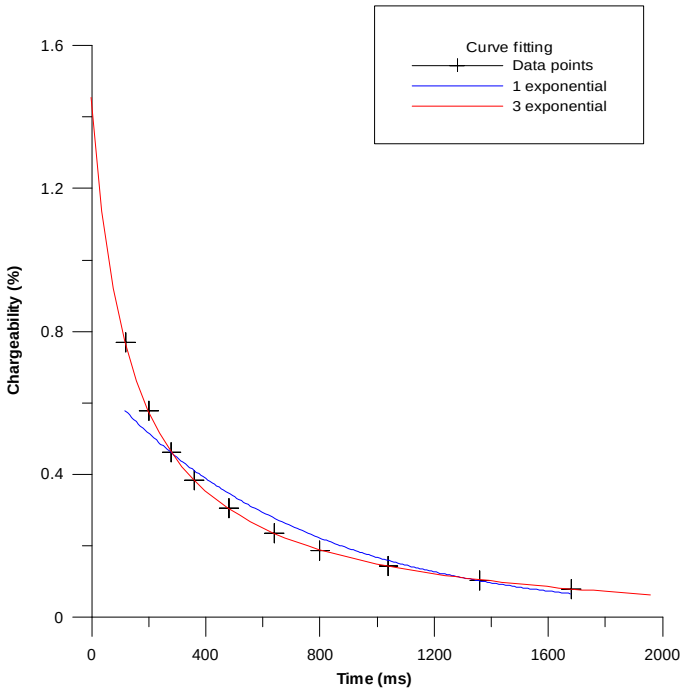

Figure 6.9: Illustration of fits of one exponential and three exponentials to the data points

The initial estimates of $A_j^{(0)}$ $\tau_j^{(0)}$ of the parameters in the model 6.1 were deduced from a mean of values graphically determined from some decay curves. The set of data that was considered for decay curve analysis involved 251 readings.

It was observed that some values of A_j and τ_j for 127 readings obtained from soil samples were not reliably determined by the algorithm due to un regular distribution of current inside the sample due to a localized contact with current electrodes, sample cohesion due to loss of water and lack of proper electrical contact during the IP measurements . By applying a percentage of good fit, it was observed that a half of the 251 readings had a fit of 99.998%, one sixth of the 251 had a moderate fit (95.5%), whereas a a third of the readings were unreliable. An outline of the causes for the unreliable determination for the three exponentials (Amplitude and decay time constants) in regard to the individual samples whose part of the readings were problematic, has been given (Appendix B, Table 5)

However, for the remaining 124 readings, the values of the constants were determined and the following observations made:

1. The shortest time constants for τ_1, τ_2 and τ_3 were 25 ms, 199.1 ms and 500 ms

respectively.

2. The co-efficients A_1, A_2, and A_3 were observed to vary as a function of water as shown in Figure 6.10 and others in Appendix A.

Graphical analysis of the A_1 constant and the amount of water was performed and analyzed statistically for increasing or decreasing trends. The trends were tested for significance using the F–statistic (Draper and Smith, 1981).
The F statistic is defined as the ratio

$$F = \frac{MSQ_r}{\sigma_r} \tag{6.3}$$

where MSQ_r= mean square due to regression; and σ_r= residual variance. The mean square due to regression is the component of total variance that can be explained by the linear trend. As such, trends with greater significance have a higher F. The significance level value p was used in assessing the significance of the trends. And this is the probability that the trend is deemed erroneously significant. The significance of a trend increases as p becomes smaller.

Fig 6.10 shows a plot of A_1 against water content for all the samples from the three locations. The plot visibly indicates a trend of increasing A_1 with an increase in water content. To ascertain the significance of this trend, the A_1 constant values were regressed linearly on the water content values (SPSS., 1998). The F statistics, F=168.635 and p value=0.000, were obtained, which means that the trend is highly significant because the p value for the F is less than 0.0005 (Table 6.3).

Table 6.3: Results of statistical analysis

ANOVA

Model	Sum of Squares	df	Mean Square	F	Sig.
Regression	90.052	1	90.052	168.635	0.00
Residual	55.537	104	0.534		
Total	145.589	105			

a Predictors: (Constant), Water content
b Dependent Variable: A1

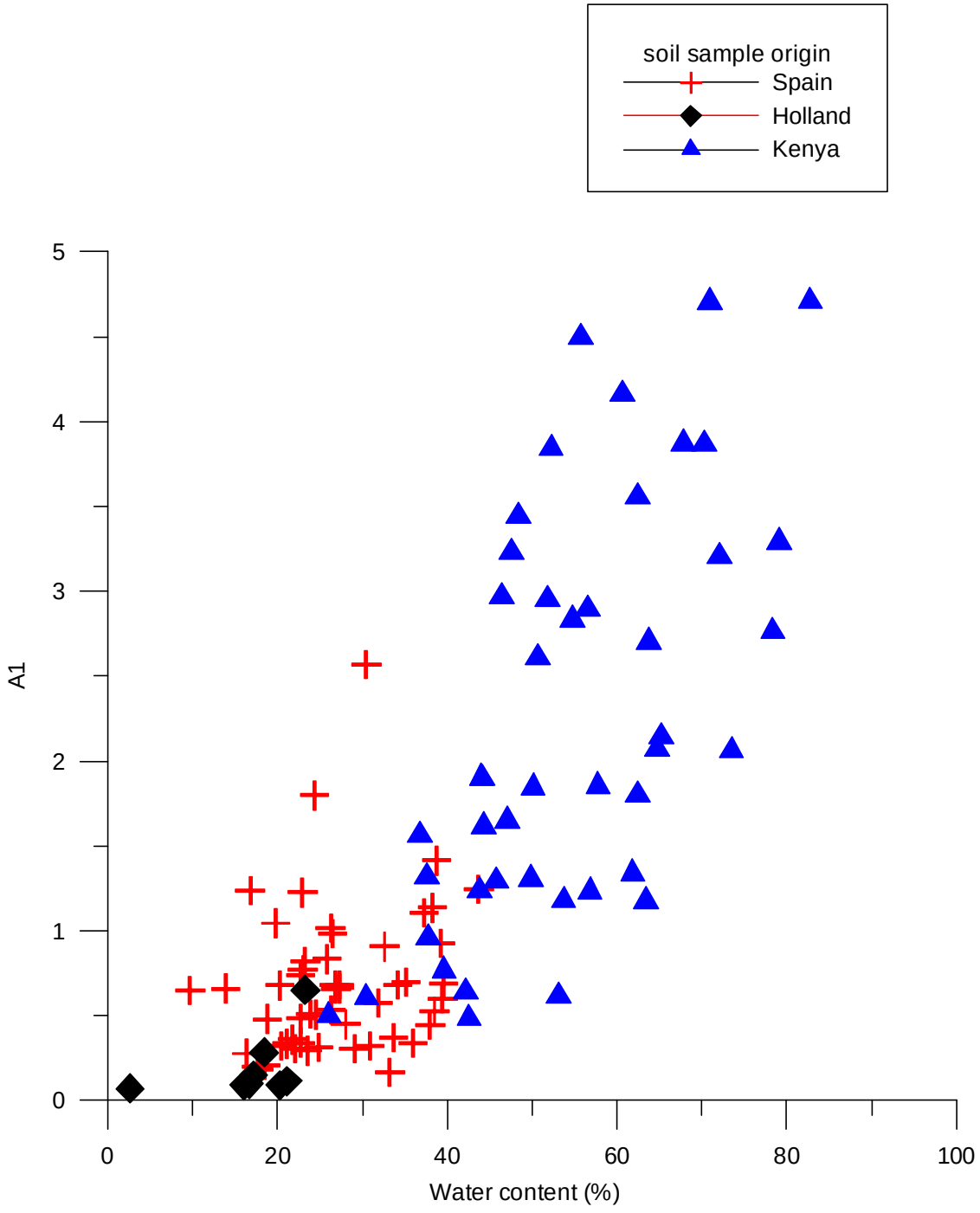

Figure 6.10: A plot of A1 against water content

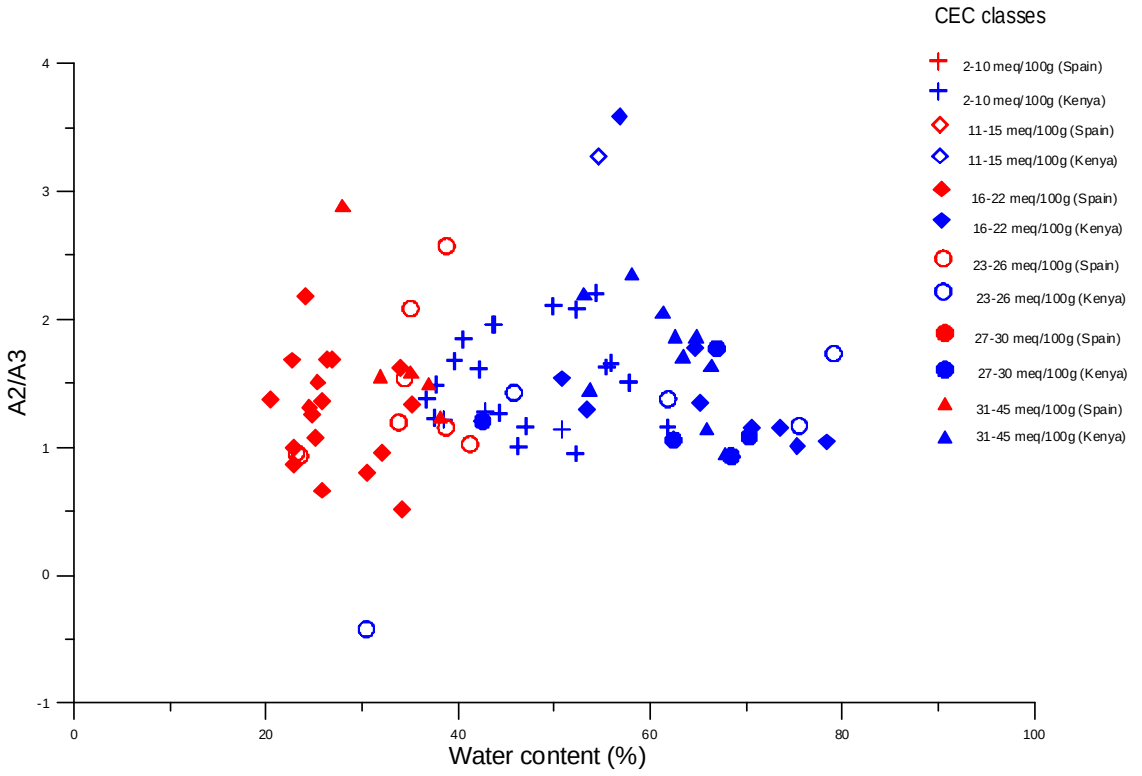

Figure 6.11: Ratio A2/A3 against water content

The A_j were found to vary as a function of water however the ratios between any pair of the co-efficients were observed as not depending on the water content. Therefore, an attempt was made to utilize these ratios for the purpose of differentiation between soil types .

Figure 6.11 shows the ratios obtained from the analysis of decay curves from the samples. The values of this parameter range between 0.5 and 3 for all samples. After plotting various ratios of A_j as a function of water content, ratio A2/A3 was found to have the least spread of values and represented a distinction between samples according to their origin (Figure 6.11).

Figure 6.12 shows a comparative analysis of the three parameters (chargeability, electrical resistivity, ratio A2/A3) as a function of water content.

The following can be noted:

1. Samples cluster in groups according to their origin

2. The range of water content of samples from the same origin can be determined from this graph. This information is also useful for the evaluation of porosity of samples.

3. The clusters according to CEC classes occur in the same places with regard to origin and it is not possible to isolate the different classes. However, there are imperfect clusters that can be observed.

More graphs of the A_j ratios are presented in Appendix A.

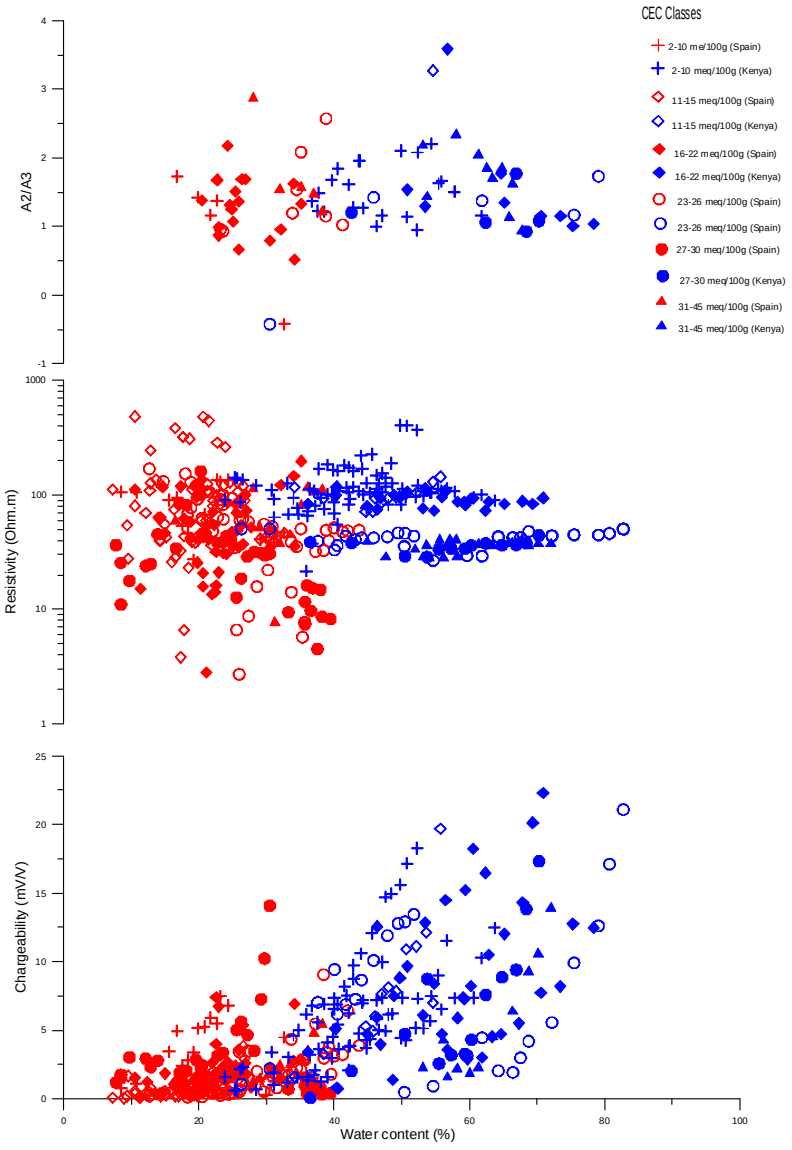

Figure 6.12: Chargeability, Resistivity and Ratio A2/A3 from the analysis of decay curves against water content

6.5 Interpretation and discussion of results

The observations made during the saturation process of soil samples can be explained in the following way. The properties of clay soils are effected by the total water content and by the energy by which that water is held. Due to changes in temperature, extent of saturation and chemical composition or concentration of pores solutions, effects such as shrinkage on drying and swelling on water uptake are observed. However, the magnitudes of these changes depend upon interrelated variables of geological history, fabric, extent of consolidation /cementation, mineralogical composition and nature of exchange ions (Gillot, 1968). The high porosities observed with samples from Kenya are indication of the presence of high swelling clay minerals such as Montmorillonite. This has an expanding lattice when hydrated. Secondly, porosity also depends on other factors such as shape, arrangement and degree of sorting of the constituent particles, cementation and compaction. As illustrated in Section 5.2.1, the Kenya samples were not highly compacted, so this contributed partly to the high porosities. The range of water content for the different soil samples is an indication of the difference in soil types.

Figure 6.1 shows points with low resistivity and chargeability values as indicated in section 6.3.1. This is due to the presence of ions that raise the conductivity of pore filling water. The conductivity of the water distributed within the soil pores is increased by the ionization of the clay and surface conductance as discussed in Section 2.3.2. The ions that are adsorbed by the clay surface may be desorbed in a percentage depending on a particular clay mineral, the concentration of clay in water and the particular cation involved in the desorption (Keller and Frischknecht, 1966). Therefore, the conductivity of water in the pore structure will always be increased by those ions supplied. This makes those soil samples to have low resistivities. This observation agrees with the data obtained from the drill hole geophysical and lithology well logs presented by Draskovitis and Smith (1990) . This is an attempt to investigate correlations between IP/Resistivity parameters and reservoir properties such as Clay content. The difference in range of chargeability values given by Spain and Kenya samples is explained by the type of clay and the manner in which it is distributed within the pore structure. The IP response given will depend on those two conditions in that if the clay occurs in small clumps in the pores, it produces a smaller IP effect than when the clay is lining the pore structure uniformly.

The relationship between chargeability and water content within the pore structures of soil is based on the availability of ions for ion exchange, which result into an IP response. The behavior between the chargeability of samples in regard to water content in this research, manifests itself in two ways: There are those that give a bell shaped chargeability curve and others a linear relationship (Section 6.3.2). The

bell shape type of behavior is explained by presence of fixed sites on the clay surface that are responsible for active IP. When these sites are all occupied by water, the IP response obtained is small, however, as the water gets decreased, the sites become available for ion exchange which gives a marked increase in the response up to the maximum. When the water decreases further, there is a decrease of mobile ions due to the fact that they are now closely attached to the clay surface and as result the IP response decreases as well.
For the linear relationship, it is because the right side of the curve (bell-shape curve) is not reached .i.e water contained in the soil samples does not occupy all the fixed sites. The observation in Figure 6.2 is in agreement with what Parkhomenko (1971) noted. The same behavior was also observed by Ogilvy and Kuzmina (1972) in shaly sands.

Another explanation is that with the introduction of water and mixing with materials inside the soils, the mobility of the ions is changed by increasing the viscous drag as it moves through water (Keller and Frischknecht, 1966). This is a result of the fact that many layers of water molecules are normally attached loosely to the walls of the pore. When an ion migrates through a fine pore, the forces holding these layers of water to the soil increase the viscosity, which in turn decrease the mobility of ions travelling through the pore. There will be a tendency for ionic charge to pile up on the upstream side of such constrictions, forming an anion concentrations on one side and cation concentrations on the other side, therefore, when an electric current is applied, there will be movement of ions but on withdrawal of the electric current, equilibrium is attained through diffusion processes, which gives an IP response which decreases with a decrease in the amount of water.

The linear increase of the IP response with water (Figure 6.3) has also been observed by Fraser and Ward (1965) . This is in response to increased production of membrane barriers because the IP effect depends partly on the degree to which the pore structure in the soil is filled with water.

All samples from Kenya show a linear relationship between chargeability and water content (left part of the active IP curve) whereas Spain samples are showing a bell shape type of relationship . This is attributed first to the formation conditions of these soils. The Kenya soils were formed as a result of intense weathering of volcanic rocks under high temperature and rainfall. These type of soils have high presence of active aluminium and Iron oxides that cause isomorphic substitution in clay mineral structures hence giving rise to high CEC due to high amounts of exchangeable Al ions. This is further depicted in the highest values of chargeabilities that are given by these soils. Soils formed by weathering are the residual clay containing materials rich in high swelling clay minerals (Gillot, 1968). Soils from Spain are formed under different climatic conditions from Kenya, Continental Mediterarranean type and lack

of enough rainfall leads to calcareous layers to be shallow which impedes the production of bivalent cations like Ca that are used for ion exchange in the inter layer clay mineral structures, which process gives rise to IP response. It should, however, be noted that the parent material effects soil formation and has particularly important influence on the origin of the clay minerals. In that regard, the porosity and water holding capacity of the parent material effect the concentration of solutions and it is further responsible for what ions are available to go into solution (Gillot, 1968).

The observed trend in chargeability and CEC values with soils in Figure 6.4 at a fixed clay content classes agrees with observations made by Parkhomenko (1971) . CEC refers to the quantity of negative charges on clay surface in soil, thus the capacity to attract positively charged ions (cations). It is by this analogy that the more the ions that are available for attraction, the higher the IP response . It was shown by Sill (1964) that as CEC increases, membrane polarization increases too. With high CECs, the free mobility of ions is restricted locally and as a result, membrane blockage is caused, thus blocking the flow of negative charge carriers on the application of an electric field. However, when the electric field is eliminated, all the charges return to equilibrium positions by a diffusion process, which gives IP effect proportional to the number of exchangeable ions and available ions in the electrolyte. Montmorillonite is one of the clay minerals with a high CEC value (Section 2.3.1)

The observation made in regard to granulometrical composition of Spain samples is in agreement to what most investigators notably Keller and Frishknecht, 1966; Ogilvy and Kuzmina,1972 found when considering a much wider range of grain size parameters, however, they both worked with artificial samples. Samples from Kenya (Figure 6.7) do not show any relationship between the chargeability and the grain sizes indicating that in some natural samples, there are other variables that contribute to the chargeabilities, an observation also made by Illiceto et al. (1982) when working with fine sediments.

The decay curve analysis showed that A_1, A_2, A_3 depend on water content and soil type. This is in agreement with what Illiceto et al. (1982) observed when working with fine sediments. The use of ratios of Aj is, however, to remove the influence caused by the on time inducing of the voltage and investigate the response due to membrane barriers in the soil. Therefore, these ratios attempt to normalize fundamental discrepancies and enhance the response due to the property of the soils. The use of ratios in this research was able to differentiate soil samples according to their origin and give imperfect clusters of soils in regard the same CEC class. However, the ratios were not able to differentiate samples perfectly according to their lithotype as observed by Illiceto et al. (1982) . This is due to the fact that though Illiceto et al. (1982) worked with natural soil samples, they carried out specific tests where they separated samples into discrete classes according to granulometric con-

stituents, which was made possible by natural processes that made sediments more or less sorted depending on the horizon and locations sampled. This enabled them to get materials with dominant lithotype. Whereas for this research, the soil samples were a mixture of grain sizes and there was no control over their constituents particles, possibly contributing to the failure of identifying lithotypes by use of ratios.

The results show that IP depends on water content, cation exchange capacity and clay content. The dependency of polarizability of soils upon their lithological composition and hydrologic properties favours the applicability of IP method in studying the composition, hydrologic and strength properties of soils/rocks, which is important for engineering–geologic investigations. Therefore, the IP technique can be used as a parameter for establishing correlative relations between geophysical and strength parameters of soils. The polarization parameter makes it possible to differentiate soil with respect to the lithology and characterize its particle size distribution which is crucial for engineering purposes. Therefore, it is essential that polarizability data be compared with mineralogical and chemical analysis as well as porosity and other hydrologic and granulometrical properties. Such comparisons are of interest in establishing correlations between IP parameters and parameters related to engineering geologic investigations.

It should be noted that IP techniques can not be applied independently of other electrical, mineralogical–chemical analysis, porosity determination, compressive strength, particle size analysis, remote sensing techniques and seismic methods for engineering geologic studies. The comprehensive solution to the problem of soil swelling as confronted by foundation engineers can be achieved by comparing the parameters obtained from the analysis of various physical fields.

Chapter 7

Models

7.1 Introduction

The use of IP in this research is an attempt to find an in–situ information provider for the detection/identification of clay minerals as regards their swelling potential in soils. Having carried out laboratory measurements on a suite of near surface soil samples, the goal was to attempt to obtain an empirical relationship, which can give a quantitative estimation of the CEC from chargeability values, water content, resistivity and clay content. However, this chapter attempts to describe the concepts of various models.

7.2 Theoretical aspects of model development

Soils are inhomogeneous systems that consist of macropores filled with one or more pore fluids and macrograins of different sizes with or without clay coating. Movements of free and bound ions in the vicinity of the interface between ionic solution and ion exchange competent (clay) particles cause electrical (induced) polarization and to a lesser extent also electrolyte/grain interface.

Experimental investigations relating rock properties and electrical parameters in regard to electrolytic polarization have been restricted to sedimentary rocks e.g Archie, (1942) ; Waxman and Smits, 1968 and Knight and Nur, 1987 although studies related to microcracks involved igneous and metamorphic rocks as well as for electrode polarization. For the whole spectrum of rocks, resistivity has been used. There have been attempts to use IP measurements to estimate hydraulic permeability as first envisaged by Vacquier et al. (1957) . In this regard, Oluronfemi and Griffiths, 1985 described an empirical relation between time domain IP parameters and permeability of the Sherwood sandstone formation.

The Cole–Cole dispersion is the spectrum of a model first proposed by Cole and Cole (1941) to describe the complex dielectric behavior and has been used by Pelton et al. (1978) to describe complex resistivity behavior of rocks. The Cole–Cole expression for the impedance of the equivalent circuit is then given by Pelton et al. (1978) as:

$$Z(\omega) = Ro\left[1 - m\left(1 - \frac{1}{1 + (j\omega\tau)^c}\right)\right] \tag{7.1}$$

Where Ro is the resistance that simulates the continuous pore paths, *m* is the chargeability of the rock, τ is the relaxation time constant, *c* is the frequency dependency, ω is the angular frequency and j=$\sqrt{-1}$. This is one of the most known and used models, however, the ion trap model by Keller and Frishcknecht, 1966 is important especially in this type of study.

Keller and Frischknecht, 1966 described a relation between induced polarization and clay content. He began by approximating that in a rock containing clay, the number of polarization centers (fixed clay anions) will be proportional to the density of fixed charges on the rock frame work, a_0. This density of fixed charges was considered to be the ion exchange capacity of the rock expressed in chemical equivalents per unit pore volume. The constant of proportionality between number of clay particles and total exchange capacity would then depend on the type of clay and the manner in which it was distributed in the rock. This is supported by the fact that if clay occurs in small clumps in the pores, it will form fewer potential barriers than if the clay lines the pore structure uniformly. It was also assumed that the polarization was approximately proportional to the number of anions in solution which are free to accumulate at the potential barriers, $(a - a_0)/a$. Using the cation exchange capacities for the various clay minerals, an estimate of the clay content that would cause the maximum amount of induced polarization to take place in a rock could be obtained. It follows that the amount of polarization should be proportional to the number of potential barriers formed by the clay and to the fraction of the anions free to collect at such barriers:

$$Polarization \propto \frac{a_0(a - a_0)}{a^2} \tag{7.2}$$

where $\frac{a_0(a-a_0)}{a^2}$ is the anion trap number.

The expression 7.2 models a rock when it is saturated with water containing dissolved salts .i.e having a concentration of ions in ppm and in which one of the three minerals may occur, illite, montmorillonite or kaolinite.

Keller and Frischknecht, 1966 calculated curves showing the relationship between the fractional volume of clay within a reservoir rock and a factor proportional to induced polarization (anion trap number). Figure 7.1 shows three clay minerals that were considered separately, illite, montmorillonite and kaolinite. The calculations were made for a 20% porosity and an electrolyte salinity of 100 ppm. Maximum

polarization was observed for small amounts of montmorillonite clay in a rock, from 0.1 to 0.4 %, while in the case of kaolinite, which has a much lower exchange capacity than montmorillonite, maximum polarization was observed for clay content between 3 to 12%. However, these figures were considered to be only qualitative. In case a higher water salinity could be assumed, then larger amounts of clay would be required to cause a maximum polarization.

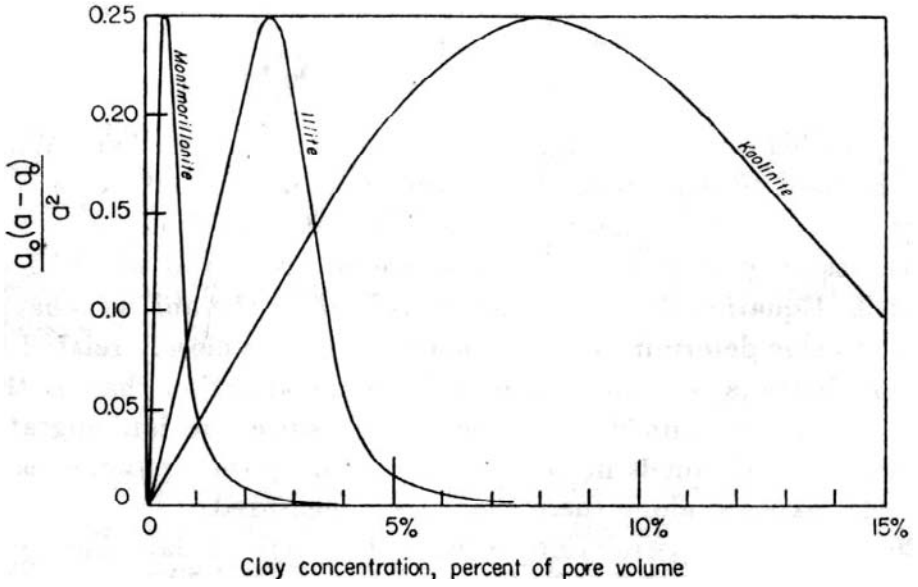

Figure 7.1: Anion trap number against clay concentration (Keller, 1966)

It is upon this that the highly idealized model of a clay bearing rock is based because the induced polarization observed in such rocks correlates with the ion–trap ratio defined in Equation 7.2. This ratio can be computed for a given rock and a given water salinity, a, if the cation exchange capacity, a_0 is known. Though the model has been applied to rocks, it allows for the derivation of most of the essential features of the IP phenomenon observed in the field and in the laboratory with unconsolidated samples like soils. From expression 7.2, the chargeability (polarization) depends on the amount of clay present in isolated selective zones and the cation exchange capacity. Then the co-efficient of proportionality between the number of clay particles and the total exchange capacity depends on the type of clay and the manner in which it is distributed within the soil.

At this stage, it would be logical to fit a model that can in turn be used to get an estimator for CEC. The Cole–Cole model would not be adequate in describing these soils compared to the model by Keller and Frischkneit (1966). This model (the ion trap model) is useful because it explains from a physicochemical perspective the bell shaped response of most of the factors influencing IP response: CEC, Clay concentra-

tion, electrolyte concentration and water saturation.

According to the observations made in this research, the model that could fit or describe the results would be a modification of the Keller model but an attempt to do so was not possible because part of the data set was noisy due to errors that have been mentioned in Section 5.9. The remaining part of the data set did not yield a good fit for the model. Therefore, the CEC estimator was not obtained when non linear least square fitting algorithm (Levenberg–Marquardt) was applied on this data. However, the idea was to obtain a CEC estimator from IP/Resistivity measurements so as to be able to obtain information that can be applied by foundation engineers as regards the subsurface information before any engineering project could take foot. It has been clearly shown in Section 6.3.3 that IP depends on CEC and from earlier discussion, CEC has been shown to represent clay mineralogy, so this estimator would have been an added advantage for the potential evaluation of this approach (detection of clay minerals by IP technique).

Chapter 8

Conclusion and Recommendation

To detect and map the effect of the presence of clay minerals, several attempts have to be made in order to find ways that can be used. However this has been the first time, the IP technique has been tried at ITC for this purpose and therefore it has been a learning process. Through this attempt, the IP technique has showed promise of being an effective tool in attempting to detect clay mineralogy though it requires some improvements.

8.1 Conclusions

- It was observed that the subject of IP in regard to identification of clay minerals is not in common use. So this has made this study a try and error way of learning. But since the presence of clay particles significantly intensifies the on set of induced potentials, then the potential of using the IP technique for detecting the presence of clay minerals is viable.

- Experimental investigation in the laboratory led to a better understanding of the fundamental relationship between soil properties and the electrical parameters (IP and Resistivity), however, their usage and application of their information content needs to be improved.

- The task of interrelating variables like chargeability, resistivity, water content, cation exchange capacity, grain size and clay content using graphical display has been shown in this research. This inter relationship provided a better understanding of the IP technique and ways of approaching the subject.

- The results have demonstrated that the IP response is possible when soils contain some water as opposed to being completely dry. The IP response depended highly on the amount of water. The Kenya samples showed higher chargeability values than Holland and Spain samples.

- A model of 3 exponentials fitted to the decay curves led to the use of ratios of the Amplitude (co-efficients), which provided a clear distinction of samples according to their origin but not according to their lithotype.

- Through this experimental study, all sources of errors and their magnitude have been identified. Personal experience in carrying out laboratory experiments, proper reading and recording of results has been acquired.

- IP/Resistivity measurements on soil samples have shown that characterization of the subsurface for engineering purposes is possible but more studies and experiments in this regard are required.

- Results presented in this research are of an academic nature in the sense that they evaluate potential approaches to the IP technique rather than provide ready to use applications.

8.2 Recommendations

The results that have been obtained, so far, have created confidence in the possible use of the technique in clay swelling potential evaluation, however, the following considerations have to be noted:

- In an attempt to improve the IP technique for clay mineral identification, due attention has to paid on the sampling procedure. Special sample tubes should be used in the sampling procedure and subsequently used for the IP measurements in order to reduce the disturbance within the soil.

- The soil samples should specifically be prepared for one set of measurements e.g water content and IP/Resistivity measurements. This is meant to keep polarization properties of materials intact, for example, when membrane polarization materials, such as clay, are heated or dried and then water is subsequently reintroduced into the pores, they lose most of their polarization properties.

- For any further research in this field of of laboratory IP, it is recommended to use more than one charging time (T) in order to fully examine the IP characteristics due to a wide variety of charging times (e.g T=4s, 8s, 16s)

- For any future experiment, care should be taken with the non polarizable potential electrodes. They should be assembled properly without any possible dripping. Preferably, they should be factory made or locally assembled from good porous materials. This would prevent the flow of copper sulphate solution into the soil, thus reducing the contamination of the samples. Secondly, this would reduce the amount of work involved in filling these electrodes with copper sulphate solution on a daily basis.
- In order to improve the signal to noise level, higher input voltages should be used, considering the maximum input voltage of the receiver in use, however, this should satisfy the requirement of linearity, therefore, sufficiently low current densities should be used.
- When using the CTU sample holder for any other experiment, the springs should first be oiled in order to allow easy movement of the current electrode extensions.
- In order to evaluate how well these laboratory measurements represent in situ IP response of soils, it is strongly recommended that for any further research on this topic, these small scale laboratory measurements should be accompanied by field measurements that are carried out at the same sampling sites.

Bibliography

Angoran, Y. and Madden, T. R. (1977). Induced polarization: a preliminary study of its chemical basis. *Geophysics*, 42:788–803.

Archie, G. E. (1942). The electric resistivity log as an aid in determining some reservoir characteristics. *Am. Inst. Mining Matall. Engineers Trans.*, 146:54–62.

Bertin, J. and Loeb, J. (1976). *Experimental and Theoretical Aspects of Induced Polarisation*, volume 1 of *1*. Gebruder Borntraeger, Berlin.

Bioag (2001). http://bioag.byu.edu/aghort/282pres/claychem/s1d019.htm. Chemical and colloidal properties of soil.

Bleil, D. F. (1953). Induced polarization, a method of geophysical prospecting. *Geophysics*, 18:636–661.

Boadu, F. K. and Seabrook, B. (2000). Estimating hydraulic conductivity and porosity of soils from spectral electrical response measurements. *JEEG*, 5(4):1–9.

Bolt, G. H. and Bruggenwert, M. G. (1978). *Soil Chemistry, Part A, Basic elements*. Elsevier, Newyork.

Borner, F., Gruhne, M., and Schon, J. (1993). Contamination indications derived from electrical properties in the low frequency range. *Geophysical Prospecting*, 41:83–98.

Borner, F. D. and Schon, J. H. (1995). Low frequency complex conductivity measurements of microcrack properties. *Surveys in Geophysics*, 16:121–136.

Borner, F. D., Schopper, J. R., and Weller, A. (1996). Evaluation of transport and storage properties in the soil and groundwater zone from the induced polarisation measurements. *Geophysical Prospecting*, 44(4):583.

Cohen, M. H. (1981). Scale invariance of the low–frequency electrical properties of inhomogeneous materials. *Geophysics*, 46:1057–1059.

Cole, K. S. and Cole, R. H. (1941). Dispersion and adsorption in dielectrics. *Alternating current field. J. Chem. Phys.*, 9:341.

Dakhnov, V. N. (1962). Geophysical well logging. *Q. Colo. Sch. of mines*.

Dankhazi, G. (1993). A new principled approach to induced polarization in porous rocks. *The Log Analyst*.

De Bakker, H. (1978). *Major soils and soil regions in the Netherlands*. Dr. W. Junk B. V. Publishers.

Dizon-Bacatio, C. R. (1992). A study on mapping unit composition and map evaluation in the Antequera area, Malaga, Spain. Msc, ITC, Enschede, The Netherlands.

Draper, N. and Smith, H. (1981). *Applied regression analysis*. Wiley, New York.

Draskovits, P. and Smith, B. D. (1990). Induced polarisation surveys applied to evaluation of groundwater resources, Pannonian Basin, Hungary. In Ward, S. H., editor, *INDUCED POLARISATION: Applications and Case histories*, volume 4. Society of Exploration Geophysicists.

Edge, A. B. and Laby, T. H. (1931). The principles and practice of geophysical prospecting. Technical report, Imperial geophysical Experimental Survey, Australia.

Fairburn, W. A. (1963). Geology of the North Machakos–Thika area. Technical report, Geological Survey, Kenya.

Franklin, J. A. and Vogler, U. W. (1979). Suggested methods for determining water content, porosity, density, absorption and related properties and swelling and slake–durability index properties. *Int. J. Rock Mech. Min. Sci. and Geomech*, 16:141–156.

Fraser, D. C. and Ward, S. H. (1965). Electrical properties of clay contaminated sandstone. *Geophysics*, 30:1233–1234.

Gillot, J. E. (1968). *Clay in Engineering Geology*. Elsevier Publishing Company, Amsterdam London New York.

Grahame, D. C. (1952). Mathematical theory of faradaic admittance. *J. Electrochem. Soc.*, 99:370.

Griffiths, D. H. and King, R. F. (1965). *Applied Geophyiscs for Engineers and Geologists*. Pergamon Press, London.

Grim, R. E. (1968). *Clay mineralogy*. McGraw-Hill, New York.

Head, K. H. (1992). *Manual of Soil Laboratory Testing*, volume 1. Pentech Press, London.

Henkel, J. H. and Collins, T. C. (1961). Induced polarization in electrolyte saturated earth plugs. *Geophysics*, 26:205–210.

Illiceto, V., Santarato, G., and Veronese, S. (1982). An approach to the identification of fine sediments by induced polarization laboratory measurements. *Geophysical prospecting*, 30:331–347.

IRIS (1998). ELREC–6 IRIS Receiver. User Manual.

Keller, G. V. and Frischknecht, F. C. (1966). *Electrical Methods in Geophysical Prospecting*, volume 10. Pergamon Press Inc.

Klein, J. D. and Sill, W. R. (1982). Electrical properties of artificial clay-bearing sandstone. *Geophysics*, 47(11):1593–1605.

Knight, R. and Nur, A. (1987). The dielectric constant of sandstones. *Geophysics*, 52:644–654.

Magellan (1992). http://www.unctad.org. 1992 Magellan Geographix SM Santa Barbara.

Marquardt, D. W. (1963). An algorithm for least squares estimation of non–linear parameters. *Journal of the Society of Industrial and Applied Mathematics*, 2:431–441.

Marshall, D. J. and Madden, T. R. (1959). Induced polarisation, a study of its causes. *Geophysics*, 24:790–816.

Mazac, O., Kelly, W. E., and Landa, I. (1985). A hydrogeophysical model for relations between electrical and hydraulic properties of aquifers. *Journal of Hydrology*, 79:1–9.

Meijer, H. (1994). *Compact Geography of the Netherlands*. The Information and documentation center for the Geography of the Netherlands, Utrecht.

Mitchel, J. K. (1993). *Fundamentals of soil behaviour*. John Wiley and Sons, New York, second edition.

Mohamed, S. S. (1970). Induced polarisation, a method to study water collecting properties of rocks. *Geophysical Prospecting*, 18:654–665.

Nelson, P. H., Hansen, W. H., and Sweeney, M. J. (1982). Induced–polarization response of zeolitic conglomerate and carbanaceous siltstone. *Geophysics*, 47:71–88.

Ogilvy, A. A. and Kuzmina, E. (1972). Hydrogeologic and engineering-geologic possibilities for employing the method of induced potentials. *Geophysics*, 37(5):839–861.

Olhoeft, G. R. (1985). Low frequency electrical properties. *Geophysics*, 50:2492–2450.

Olorunfemi, M. O. and Griffiths, D. H. (1985). A laboratory investigation of the induced polarization of the Triassic Sherwood sandstone of Lancashire and its hydrogeological applications. *Geophysical Prospecting*, 33:110–127.

Parasnis, D. S. (1966). *Mining Geophysics*. Elsevier Publishing Company, Amsterdam.

Parasnis, D. S. (1973). *Mining Geophysics*. Elsevier Publishing Company, Amsterdam London New York.

Parkhomenko, E. I. (1971). *Electrification phenomena in rocks*. Plenum Press, New York.

Pelton, W. H., Ward, S. H., Hallof, P. G., and Nelson, P. H. (1978). Mineral discrimination and removal of inductive coupling with multifrequency IP. *Geophysics*, 43:588–609.

Reeuwijk, L. P. V. (1995). Procedures for soil analysis. Technical report, International Soil Reference and Information Center.

Reynolds, J. M. (1997). *An introduction to Applied and Environmental Geophysics*. John Wiley and Sons.

Roussel, J. (1962). Etude sur modeles reduit des phenomenes de polarisation provoquee. *Annales de Geophysique*, 18:360–371.

Roy, K. K. and Elliot, H. (1980). Model studies on some aspects of resistivity and membrane polarisation behaviour over a layer Earth. *Geophysical prospecting*, 28:759–775.

Schlumberger, C. (1920). Etude sur la prospection electrique du sous–sol. *Gauthier–Villars, Paris*.

Schon, J. H. (1986). *Physical Properties of Rocks; Fundamentals and Principles of Petrophysics.* Elsevier Science Limited, Amsterdam.

Scintrex (1981). CTU–2: Physical Property Testing System. User Manual.

Sherman, D. M. (1997). http://mineral.gly.bris.ac.uk/mineralogy/clayminerals.html. Phyllosilicates I–The clay minerals.

Siegel, H. O. (1959). Mathematical formulation of type curves for induced polarization. *Geophysics*, 24(3):546–565.

Sill, W. R. (1964). Induced polarization in clay bearing sandstones and effects of oil saturation. *Inst. of Geoph. and Plan. Physics, Univ. of California, San Diego*.

SPSS. (1998). *SPSS Base 8.0: Application Guide*. Marketing Department, SPSS Inc., Chicago.

Sternberg, B. K. and Oehler, D. Z. (1990). Induced polarisation in hydrocarbon surveys: Arkoma basin case histories. In Ward, S. H., editor, *INDUCED POLARISATION: Applications and Case histories*, volume 4. Society of Exploration Geophysicists.

Sumner, J. S. (1976). *Principles of Induced Polarisation for Geophysical Exploration*. Elsevier Scientific Publishing Company, Amsterdam.

Sumner, J. S. and Zonge, K. L. (1980). Induced polarisation for exploration geophysics–short course. South African Geophysical Association, The University Of Witwatersrand, Johannesburg, South Africa.

Telford, W. M., Geldart, L. P., Sheriff, R. E., and Keys, D. S. (1976). *Applied Geophysics*. Cambridge University Press.

Towel, J. N., Anderson, R. G., Pelton, W. H., Olhoeft, G. R., and LaBrecque, D. (1985). Direct detection of hydrocarbon contaminants using induced polarisation method. *SEG meeting*, pages 145–147.

Vacquier, V., Holmes, C. R., Kintzinger, P. R., and Lavergne, M. (1957). Prospecting for groundwater by induced electrical polarisation. *Geophysics*, 23:660–687.

Van der Meer, F. (1999). Can we map swelling clays with remote sensing? and discussion by Dr. Jean Roy (p233–234). *International journal of Applied Earth Observation and Geoinformation*, 1:27–35.

Vanhala, H. (1997). Mapping oil contaminated sand and till with the spectral induced polarization (SIP) method. *Geophysical prospecting*, 45:303–326.

Vanhala, H. and Peltoniemi, M. (1992). Spectral ip studies of Finnish ore prospects. *Geophysics*, 57:1545–1555.

Vanhala, H. and Soininen, H. (1995). Laboratory technique for measurement of spectral induced polarization response of soil samples. *Geophysical prospecting*, 43.

Vinegar, H. J. (1984). Induced polarization of shaly sands. *Geophysics*, 49(8):1267–1287.

Wait, J. R. (1958). Discussions on a theoretical study of induced electrical polarization. *Geophysics*, 23:144–154.

Wait, J. R. (1959a). Overvoltage research and geophysical application. In *International series of monographs on earth sciences*, volume 4, pages 22–83. Pergomon press, Oxford, England.

Wait, J. R. (1959b). A phenomenological theory of overvoltage for metallic particles. In *Overvoltage research and geophysical application*, volume 4, pages 22–28. Pergomon press, Oxford, England.

Wait, J. R. (1959c). The variable–frequency method. In *Overvoltage research and geophysical application*, volume 4, pages 29–49. Pergomon press, Oxford, England.

Waxman, M. and Smits, L. J. M. (1968). Electrical conductivities in oil–bearing shaly sands. *Soc. Pet. Eng. J*, 243:107–122.

Waxman, M. H. and Thomas, E. C. (1974). Electrical conductivities in shaly sands. *J. Petr. Tech.*, 257:213–225.

Weller, A. and Borner, F. D. (1996). Measurements of spectral induced polarization for environmental purposes. *Environmental Geology*, 27:329–334.

Worrall, W. E. (1968). *Clays, their nature, origin and general properties*. Maclaren and Sons, London, first edition.

Worthington, P. A. and Collar, F. A. (1984). Relevance of induced polarisation to quantitative formation evaluation. *Marine and Petroleum Geology*, 1.

Zonge, K. L., Sauck, W. A., and Sumner, J. S. (1972). Comparison of time frequency and phase measurements in induced polarisation. *Geophysical Prospecting*, 20:626–648.

Appendix A

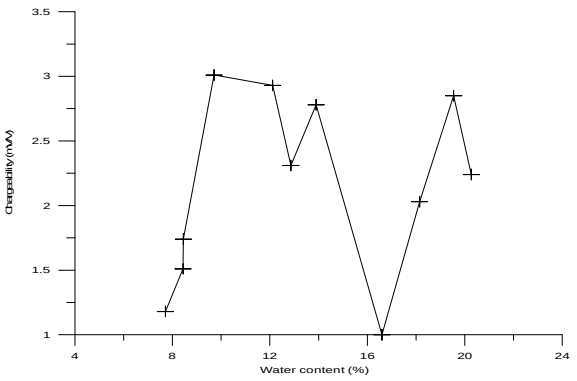

Figure 1: Chargeability against water content for sample 1

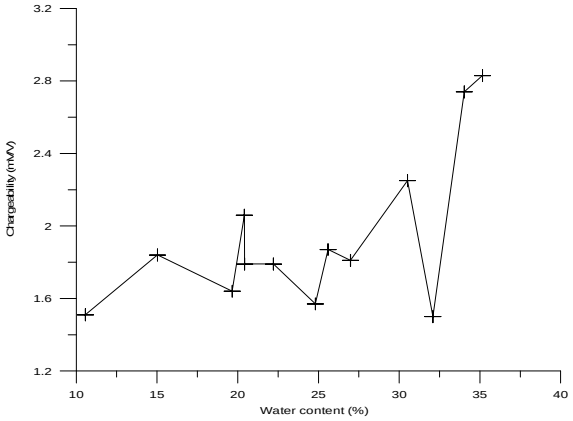

Figure 2: Chargeability against water content for sample 3

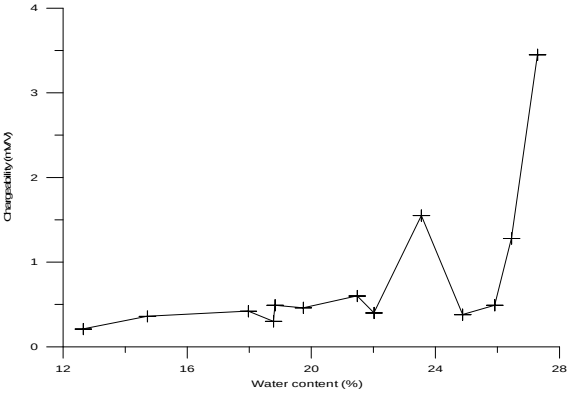

Figure 3: Chargeability against water content for sample 4

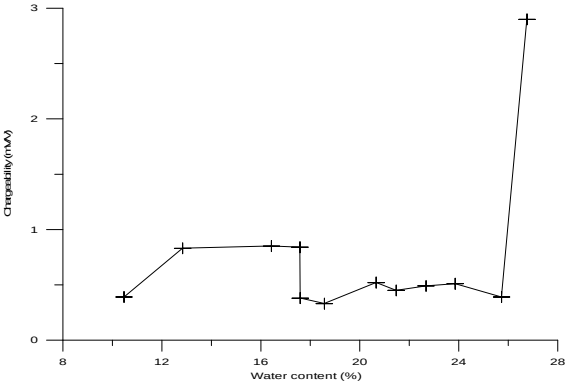

Figure 4: Chargeability against water content for sample 5

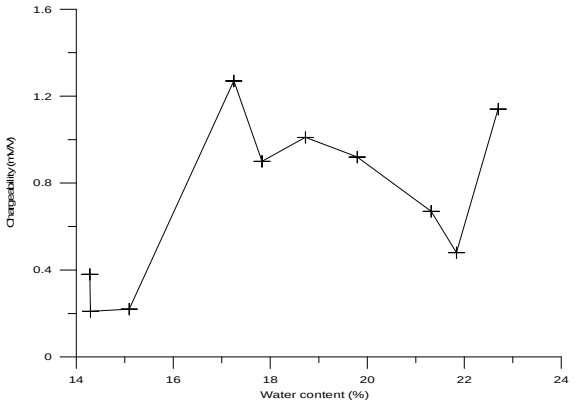

Figure 5: Chargeability against water content for sample 6

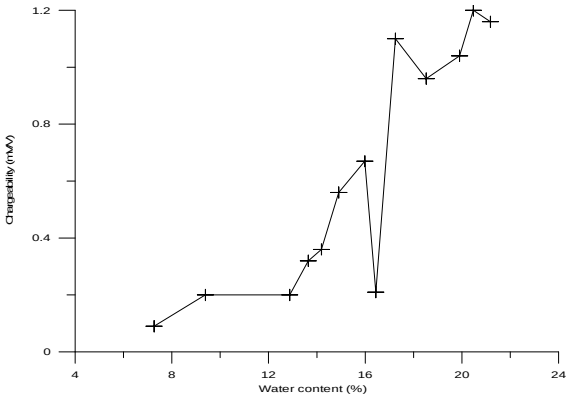

Figure 6: Chargeability against water content for sample 7

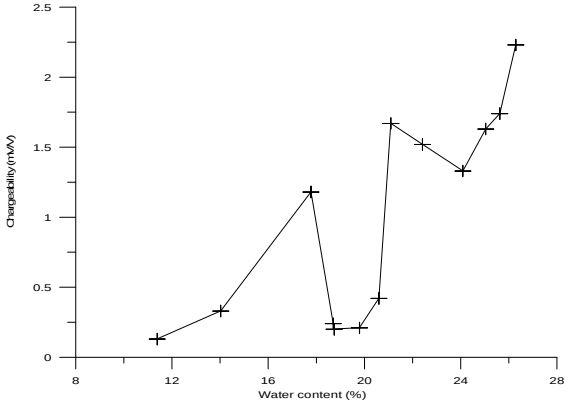

Figure 7: Chargeability against water content for sample 8

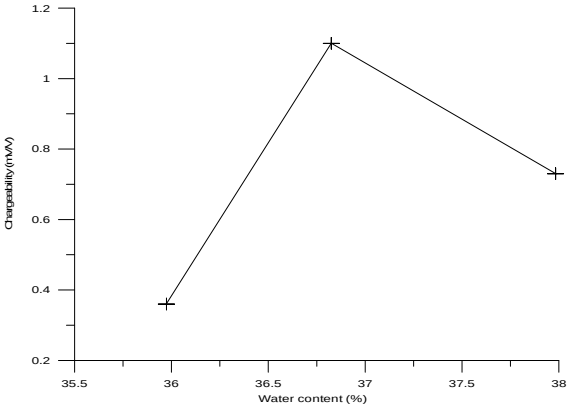

Figure 8: Chargeability against water content for sample 9

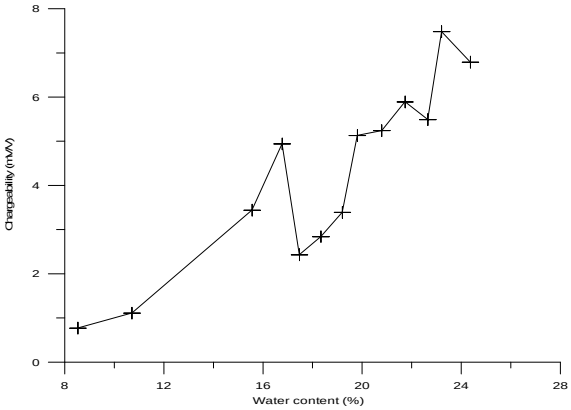

Figure 9: Chargeability against water content for sample 11

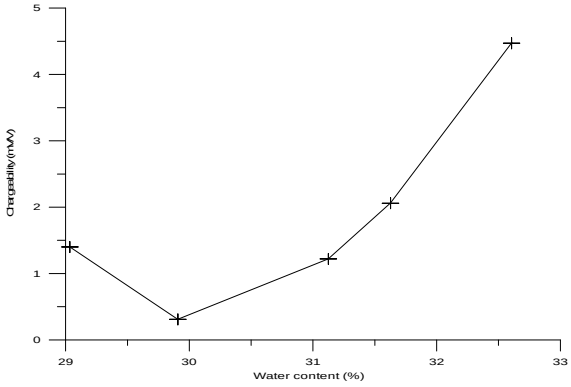

Figure 10: Chargeability against water content for sample 12

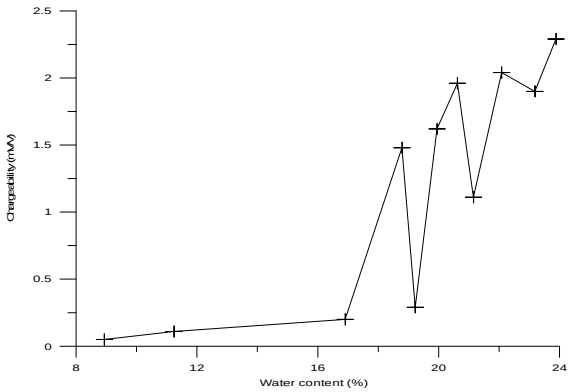

Figure 11: Chargeability against water content for sample 1

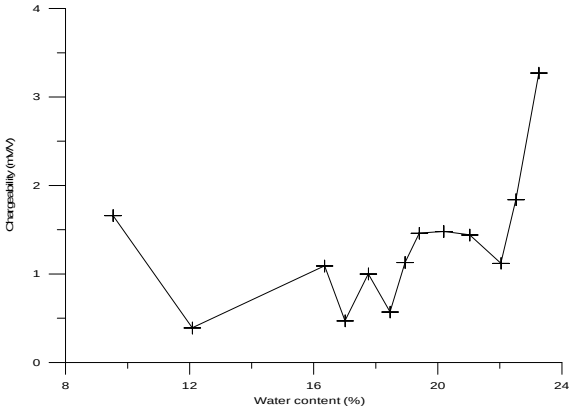

Figure 12: Chargeability against water content for sample 15

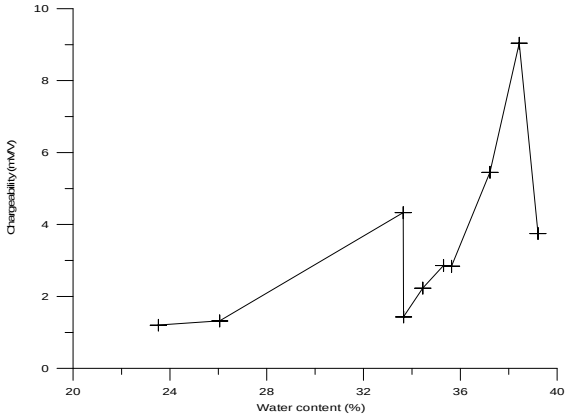

Figure 13: Chargeability against water content for sample 16

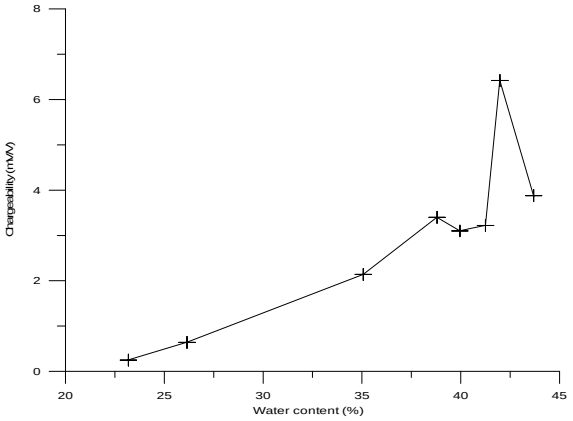

Figure 14: Chargeability against water content for sample 18

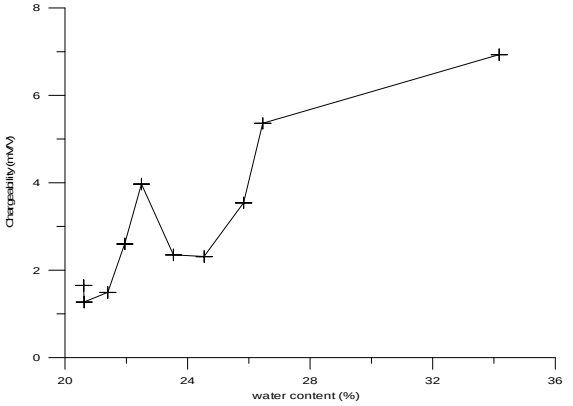

Figure 15: Chargeability against water content for sample 20

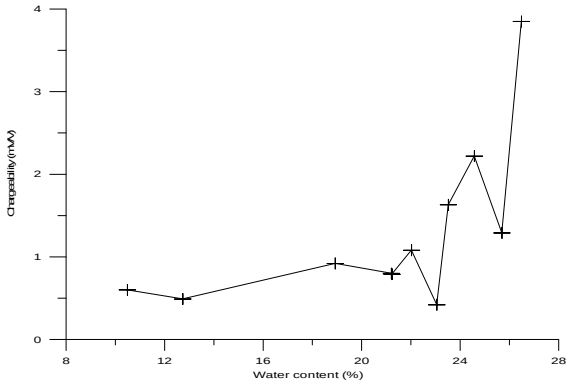

Figure 16: Chargeability against water content for sample 21

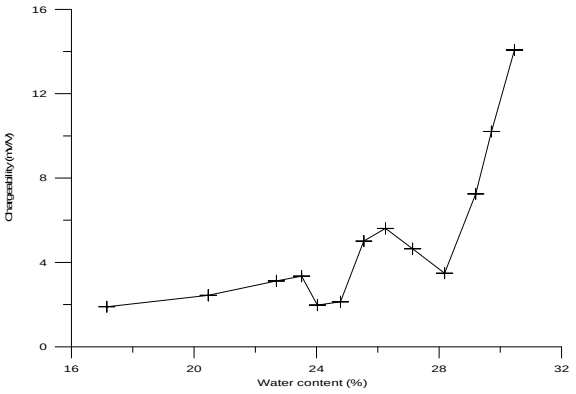

Figure 17: Chargeability against water content for sample 22

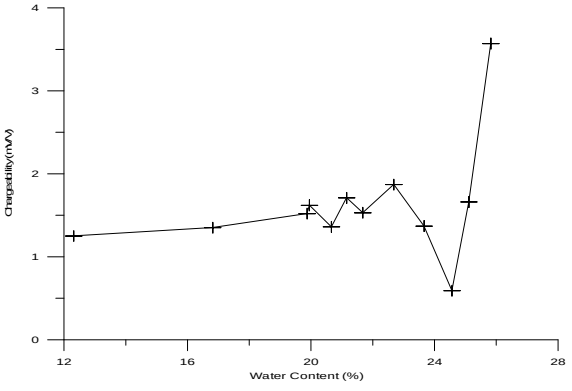

Figure 18: Chargeability against water content for sample 23

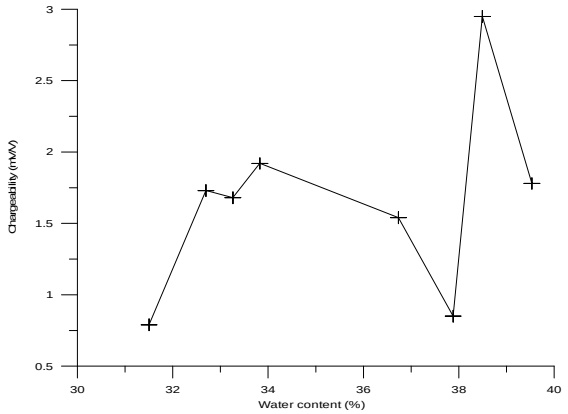

Figure 19: Chargeability against water content for sample 24

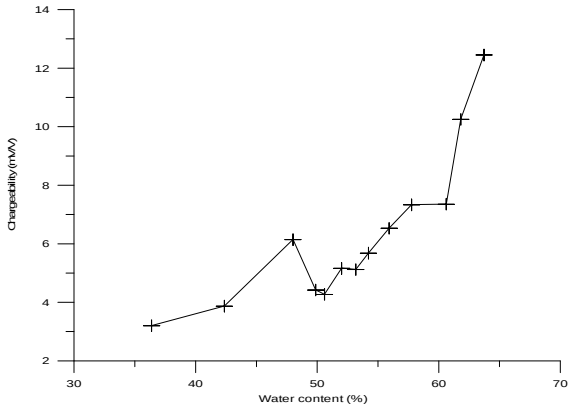

Figure 20: Chargeability against water content for sample 26

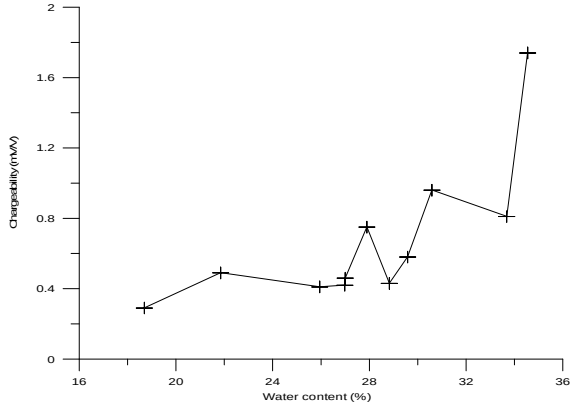

Figure 21: Chargeability against water content for sample 29

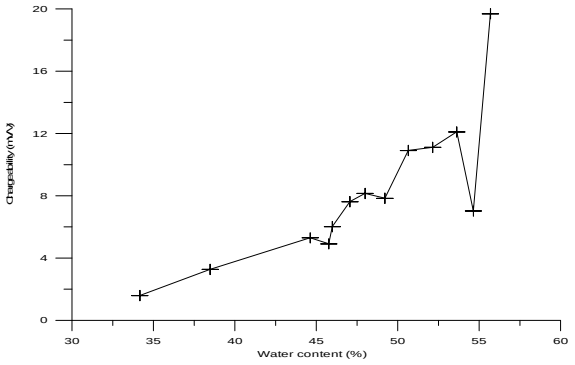

Figure 22: Chargeability against water content for sample 31

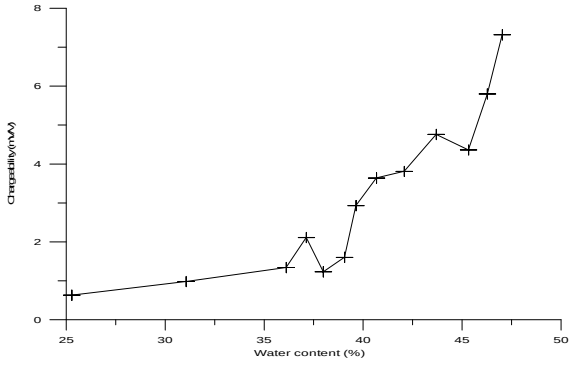

Figure 23: Chargeability against water content for sample 32

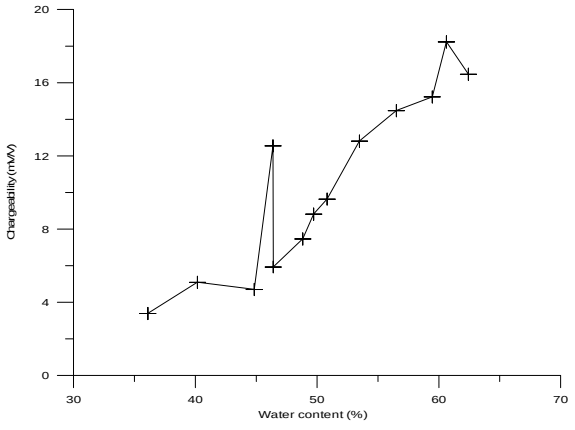

Figure 24: Chargeability against water content for sample 33

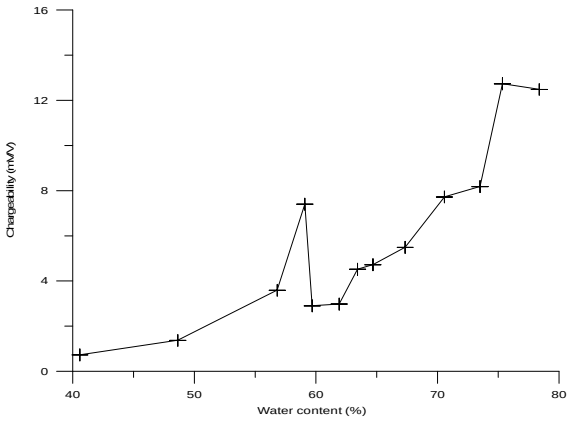

Figure 25: Chargeability against water content for sample 34

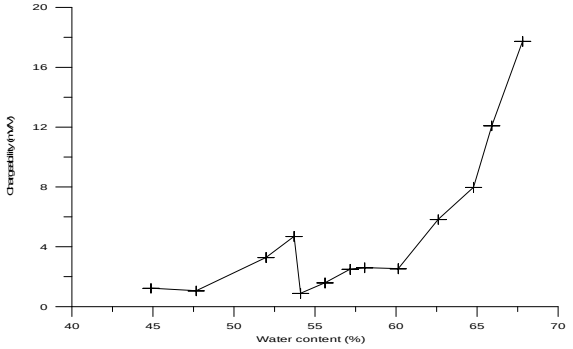

Figure 26: Chargeability against water content for sample 35

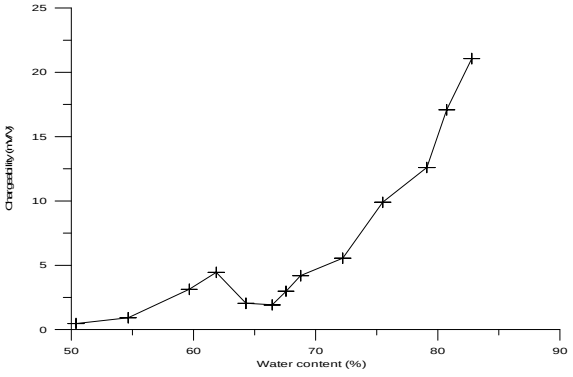

Figure 27: Chargeability against water content for sample 37

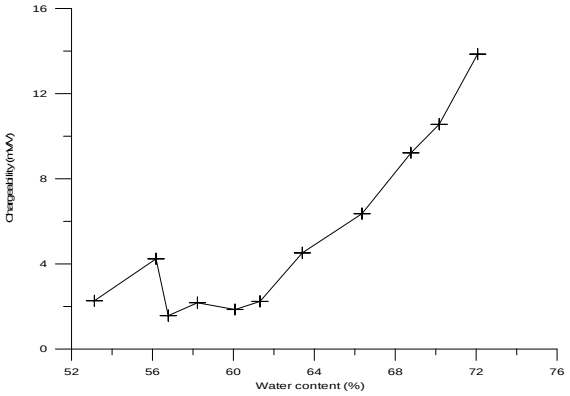

Figure 28: Chargeability against water content for sample 40

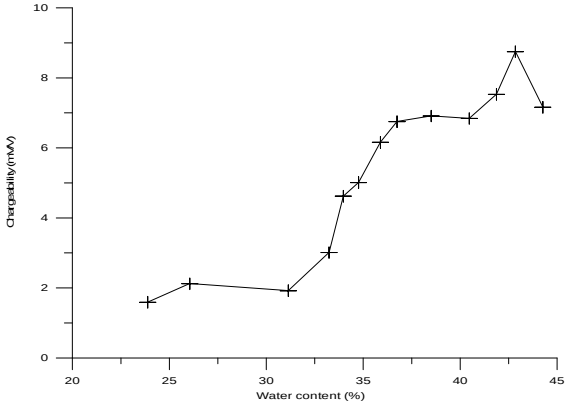

Figure 29: Chargeability against water content for sample 41

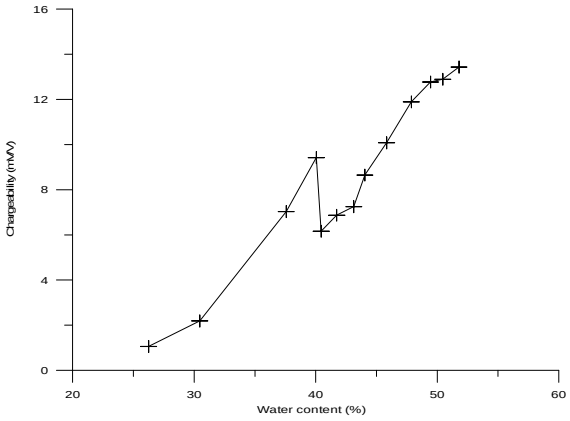

Figure 30: Chargeability against water content for sample 42

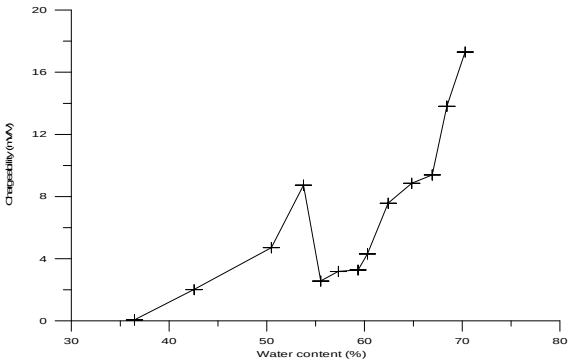

Figure 31: Chargeability against water content for sample 43

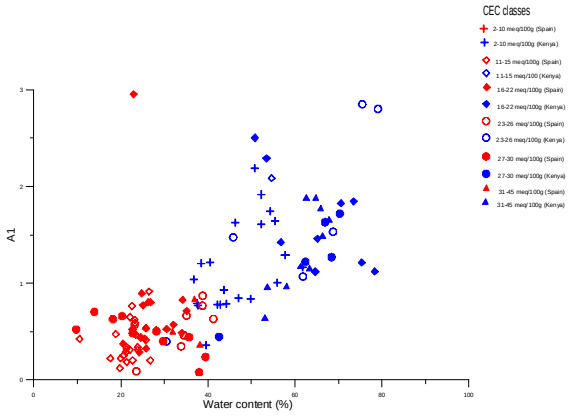

Figure 32: A1 against water content

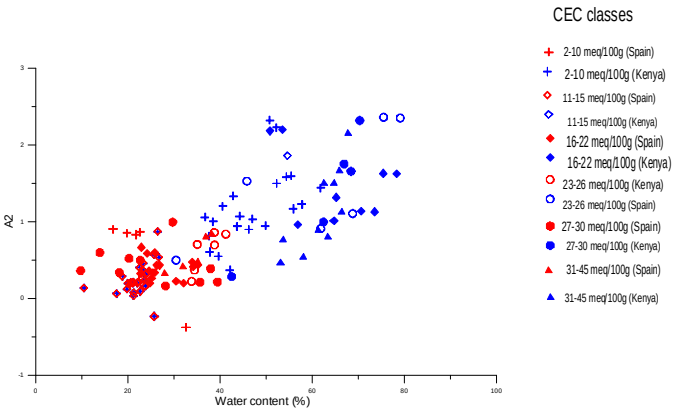

Figure 33: A2 against water content

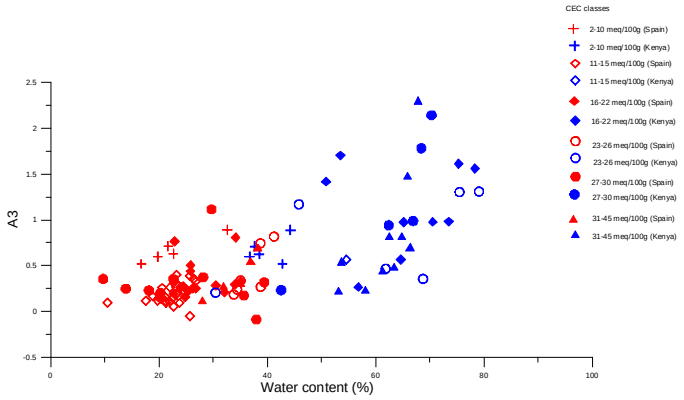

Figure 34: A3 against water content

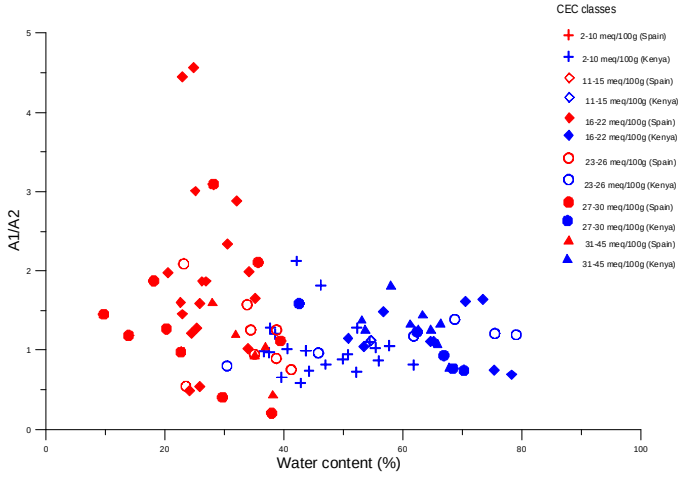

Figure 35: Ratio A1/A2 against water content

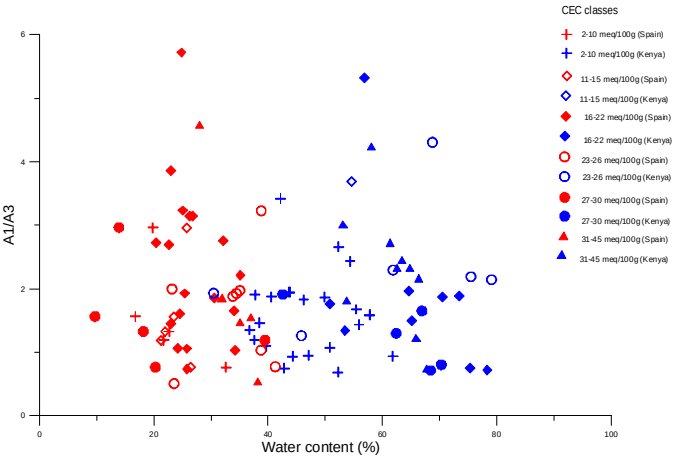

Figure 36: Ratio A1/A3 against water content

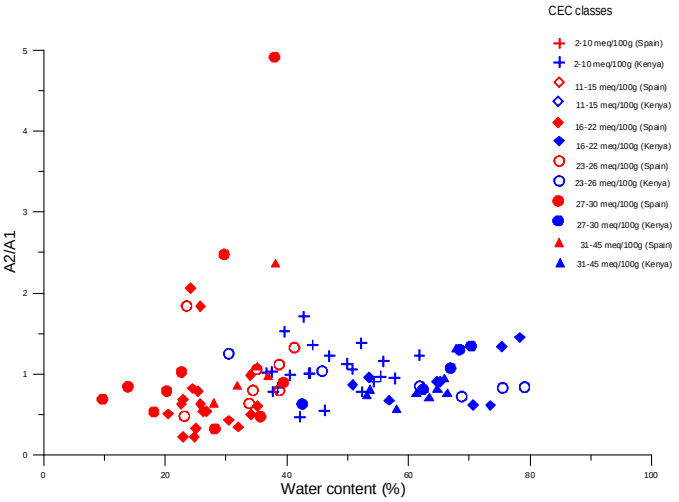

Figure 37: Ratio A2/A1 against water content

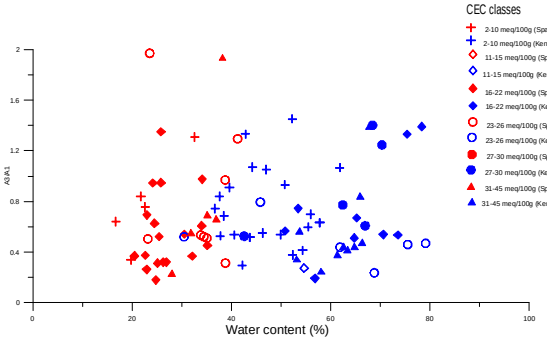

Figure 38: Ratio A3/A1 against water content

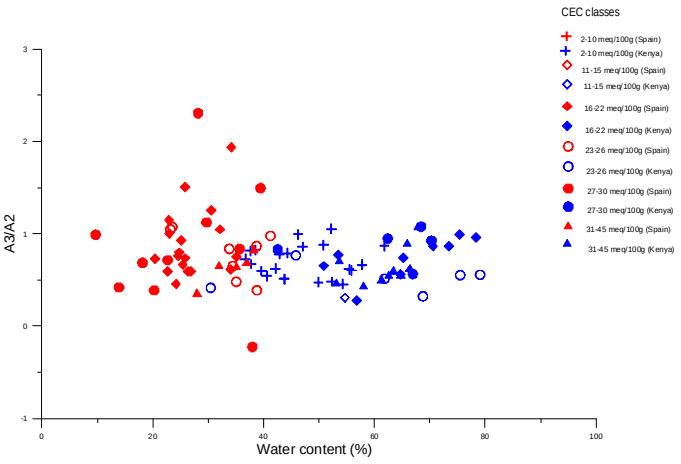

Figure 39: Ratio A3/A2 against water content

Appendix B

Table 1: Soil sample description 1

Soil sample	Easting	Northing	Altitude (m)	Depth (cm)	Sand (>0.05mm) (%)	Silt (0.05-0.002mm) (%)	Clay (<0.002m) (%)	CEC (meq/100g)	Porosity (%)
1	344031	4106293	429	0-15	23.4	18.8	57.7	27.0	34
2	348375	4103048	397	0-10	16.8	21.8	61.4	27.6	54
3	340931	4112753	472	0-30	20.2	33.9	46.0	19.0	45
4	336625	4113242	431	0-15	6.9	27.7	65.4	24.0	46
5	346680	4098593	377	0-27	22.1	35.6	42.3	14.0	41
6	347177	4098651	378	0-25	34.3	21.2	44.5	13.0	39
7	345970	4096777	389	0-10	50.0	13.0	37.0	14.4	38
8	342670	4105921	411	0-18	41.8	13.6	44.6	18.9	42
9	340750	4106908	423	0-10	3.7	28.4	67.9	28.1	57
10	339034	4112378	480	0-10	3.7	24.7	71.6	45.0	51
11	345749	4097693	389	0-35	12.6	23.6	27.7	8.0	39
12	343763	4103538	411	0-10	39.0	19.1	41.8	5.0	51
13	343700	4103799	424	0-9	29.9	18.2	51.8	23.0	56
14	342784	4102307	430	0-23	13.7	11.7	38.3	15.0	42
15	345898	4100861	396	0-10	53.8	13.0	33.2	13.1	38
16	343137	4103236	412	0-10	24.2	27.0	48.8	23.4	52
17	347665	4098906	393	0-10	32.2	19.0	48.8	16.8	43
18	340595	4107443	429	0-10	12.9	29.9	57.2	25.0	55
19	344998	4099693	397	0-10	25.9	10.3	63.7	24.4	45
20	349800	4101000	397	0-15	16.7	32.8	50.4	21.0	53
21	344081	4103485	434	0-18	39.8	11.3	27.4	12.0	42
22	345223	4097321	383	0-25	3.9	25.1	57.3	29.0	43
23	344711	4102189	432	0-18	50.2	8.9	41.0	20.0	42
24	348664	4106126	456	0-10	33.9	20.0	46.1	25.0	54
25	275749	9868317	1519		18.3	40.6	41.1	21.1	63
26	298966	9864174	1508		35.2	44.2	20.6	11.5	64
27	243056	477543	38						67
28	234166	472713							58
29	227323	467414							72
30	243830	461320	28						54
31	267127	9866234	1610		13.0	15.5	71.5	12.2	59
32	316690	9860366	1590		41.3	40.1	18.5	4.8	56
33	305381	9878366	1464		24.4	4.9	70.7	19.8	63
34	298956	9862549	1525		24.5	48.1	27.4	17.6	65
35	267342	9851174	1661		14.1	28.4	57.4	36.8	63
36	309676	9845664	1563		43.5	4.3	52.3	4.3	60
37	284203	9856308	1540		21.0	23.0	56.0	25.6	73
38	243495	9855571	1969		10.8	3.6	85.6	8.1	62
39	271639	9843357	1583		32.6	25.5	41.9	9.7	56
40	242698	9843620	1882		10.0	19.0	71.0	33.5	65
41	319892	9835487	1322		54.0	5.2	40.8	2.1	54
42	301416	9857980	1519		46.6	17.9	35.5	23.0	57
43	282637	9881266	1557		17.3	29.0	53.7	28.8	66

Table 2: Soil sample description 2

Soil sample	Parent material	Landscape	Soil sample	Parent material	Landscape
1	Lacustrine sediments	lacustrine plain	**20**	Alluvium	alluvial plain
2	Lacustrine sediments	lacustrine plain	**21**	Marls & Gypsum	hilland
3	Colluvium	piedmont	**22**	Colluvium	hilland
4	Lacustrine marls	lacustrine plain	**23**	Colluvium	hilland
5	Alluvium	alluvial plain	**24**	Colluvium	piedmont
6	Colluvium	glacis	**25**	Residual soil	lowland
7	Colluvium	footslope	**26**	Residual soil	undulating
8	Lacustrine deposits	piedmont	**31**	Residual soil	undulating lowland
9	Lacustrine sediments	lacustrine plain	**32**	Residual soil	foothill
10	Colluvium	piedmont	**33**	Residual/Transported	foothill
11	Bios sands	hilland	**34**	Residual soil	undulating
12	Colluvum	piedmont	**35**	Residual soil	lowland
13	Colluvium	piedmont	**36**	Residual soil	hillslope
14	Colluvium	piedmont	**37**	Residual soil	lowland
15	Bios sands	piedmont	**38**	Residual/Colluvial	hillslope
16	Bios sands	piedmont	**39**	Residual soil	undulating lowland
17	Colluvium	hilland	**40**	Residual/Transported	foothill
18	Lacustrine sediments	lacustrine terrace	**41**	Residual soil	flat hillslope
19	Bios sands	piedmont	**42**	Residual soil	lowland
			43	Residual soil	tophill

Table 3: Geometric constant (K) values

Soil sample	Spacing between potential elctrodes (cm)	K value	Soil sample	Spacing between potential elctrodes (cm)	K value
1	1.5	0.3	**31**	1.5	0.3
2	1.7	0.2	**32**	1.5	0.3
3	1.6	0.3	**33**	1.5	0.3
4	1.6	0.3	**34**	1.8	0.2
5	1.6	0.3	**35**	1.8	0.2
6	1.7	0.3	**36**	1.7	0.2
7	1.5	0.3	**37**	1.8	0.2
8	1.8	0.2	**38**	1.6	0.3
9	1.5	0.3	**39**	1.5	0.3
10	1.6	0.3	**40**	1.8	0.2
11	1.5	0.3	**41**	1.7	0.2
12	1.5	0.3	**42**	1.7	0.2
13	1.6	0.3	**43**	1.7	0.2
14	1.5	0.3			
15	1.7	0.2			
16	1.6	0.3			
17	1.6	0.3			
18	1.6	0.3			
19	1.7	0.2			
20	1.7	0.2			
21	1.7	0.2			
22	1.7	0.2			
23	1.7	0.2			
24	1.7	0.2			
25	1.8	0.2			
26	1.8	0.2			
27	1.7	0.2			
28	1.7	0.2			
29	1.7	0.2			
30	1.7	0.2			

Table 4: IP/Resistivity measurements reliability

Soil sample	Comment
1	Okay but shrunk on drying (Aluminium foil used)
2	Sample tube diagonally cut, no proper electricl contact, shrunk (Aluminium foil used)
3	No proper contact on drying (Aluminium foil used)
4	Okay but shrunk on drying (Aluminium foil used)
5	Okay
6	Okay but shrunk on drying (Aluminium foil used)
7	Okay but shrunk on drying (Aluminium foil used)
8	Overgrew and shrunk, no proper electrical contact on drying (aluminium foil used)
9	Overgrew and shrunk, no proper electrical contact on drying, irregular surface
10	Sample tube diagonally cut (Aluminium foil and old 2.50 guilder coins)
11	Sample tube diagonally cut (Aluminium foil used)
12	Okay
13	Sample tube diagonally cut (Aluminium foil used)
14	Sample tube diagonally cut (Aluminium foil used)
15	Okay but shrunk on drying (Aluminium foil used)
16	Sample tube diagonally cut (Aluminium foil used)
17	Sample tube diagonally cut (Aluminium foil used and old guilder coins)
18	Sample tube diagonally cut (Aluminium foil used)
19	Okay but shrunk on drying (Aluminium foil used)
20	No proper contact on drying (Aluminium foil used)
21	Okay
22	Sample tube diagonally cut (Aluminium foil used)
23	Okay but shrunk on drying (Aluminium foil used)
24	Okay but shrunk on drying (Aluminium foil used)
25	Overgrew and shrunk, no proper electrical contact on drying (Aluminium foil used)
26	Overgrew and shrunk, no proper electrical contact on drying (Aluminium foil used)
27	Sandy, lost water fast and was spilling out of the tube
28	Sandy, lost water fast and was spilling out of the tube
29	No proper electrical contact on drying
30	sandy, lost water fast and was spilling out of the tube
31	Sample tube diagonally cut, overgrew and shrunk (Aluminium foil used)
32	Okay
33	Overgrew and shrunk, no proper electrical contact on drying
34	Overgrew and shrunk, no proper electrical contact on drying
35	Overgrew and shrunk, no proper electrical contact on drying
36	Okay
37	Overgrew and shrunk, no proper electrical contact on drying (Aluminium foil used)
38	Overgrew and shrunk, no proper electrical contact on drying (Aluminium foil used)
39	Overgrew and shrunk, no proper electrical contact on drying (Aluminium foil used)
40	Overgrew and shrunk, no proper electrical contact on drying (Aluminium foil used)
41	Overgrew and shrunk, no proper electrical contact on drying (Aluminium foil used)
42	Overgrew and shrunk, no proper electrical contact on drying (Aluminium foil used)
43	Overgrew and shrunk, no proper electrical contact on drying (Aluminium foil used)

Table 5: Causes for the unreliable determination of Aj and τ_j constants

Soil sample	Reason
1	Aluminium (Al) foil used, current density inhomogeneity
2	Al foil used, current density inhomogeneity, sample tube diagonally cut
3	All were determined
4	Al foil used, sample cohesion, current density inhomogeinity
5	All were determined
6	Al foil used, current density inhomogeneity
7	Al foil used, current density inhomogeinity, sample cohesion
8	Irregular surface, sample cohesion
10	Al foil and 2 guilder coins used, current inhomogeinity
11	Current inhomogeinity
12	Current density homogeinity
13	Not included because of non linear current regulation
14	Sample tube diagonally cut, no poper contact
15	Al foil used, current density inhomogeinity
16	All were determined
17	All were determined
18	Sample tube diagonally cut, current density inhomogeinity
19	Al foil used, current density inhomogenity
20	All were determined
21	Unregular distribution of current inside the sample
22	All were determined
23	Al foil used, current inhomogeinity
24	Al foil used, current density homogeinity
25	Sample cohesion, Al foil used, current density inhomogeinity
26	Localized current source
27	Irregular distribution of current in the sample.
28	Irregular distribution of current in the sample.
29	Irregular distribution of current in the sample.
31	Al foil used, sample tube diagonally cut, unregular distribution of current in the sample
32	Al foil used, sample tube diagonally cut, unregular distribution of current in the sample
33	Sample cohesion, Al foil used, current density inhomogeinity
34	All were determined
35	All were determined
36	Unregular distribution of current inside the sample
37	Sample cohesion, Al foil used, current density inhomogeinity
38	Sample cohesion, Al foil used, current density inhomogeinity
39	Sample cohesion, Al foil used, current density inhomogeinity
40	Sample cohesion, Al foil used, current density inhomogeinity
41	Sample cohesion, Al foil used, current density inhomogeinity
42	Sample cohesion, Al foil used, current density inhomogeinity
43	Sample cohesion, Al foil used, current density inhomogeinity

Table 6: Calibration of the transmitter

IP Reserch project/2001/if$r/imk

IP calibration and usage data sheet

Transmitter: ITC laboratory TX **Receiver: IRIS Elrec-6** **DVM**

Date	Start time	Strt-Bat-Volt	Current calibration: 30 uA	100uA	300uA	1mA	3mA	10mA	30mA	End-Bat-Volt	Endtime	User	Remarks
8-10-2001	9:00	19.57	31.5	102.7	294	0.98	2.84	9.09	25.9	19.54	6:30PM	JMK	Good
9-10-2001	9:00	19.53	31.5	102.5	293	0.98	2.84	9.03	25.8	19.51	6:30PM	JMK	Good
10-10-2001	9:00	19.52	31.4	102.3	293	0.98	2.84	9.03	25.8	19.46	4:30 PM	JMK	Good
12-10-2001	9:00	19.50	31.5	102.5	294	0.98	2.84	9.08	25.8	19.45	6:30 PM	JMK	Good
13-10-2001	9:00	19.48	31.5	102.5	294	0.98	2.84	9.08	25.8	19.45	6:30PM	JMK	Good
14-10-2001	9:00	19.46	31.5	102.5	293	0.98	2.84	9.08	25.8	19.44	3:30 PM	JMK	Good
15-10-2001	9:00	19.43	31.4	102.0	293	0.97	2.83	9.07	25.5	19.42	6:30 PM	JMK	Good
26-10-2001	9:00	19.40	31.5	102.4	293	0.97	2.83	9.07	25.8	19.40	2:45 PM	JMK	Good
27-10-2001	9:00	19.40	31.5	102.3	293	0.97	2.83	9.07	25.8	19.37	2:00PM	JMK	Good
28-10-2001	9:00	19.28	31.4	102.2	293	0.97	2.83	9.07	25.7	19.35	1:10 PM	JMK	Good
31-10-2001	9:00	19.25	31.4	102.2	293	0.97	2.83	9.07	25.7	19.34	1:25 PM	JMK	Good
1-11-2001	9:00	19.34	31.4	102.2	293	0.97	2.83	9.07	25.8	19.33	6:30 PM	JMK	Good
5-11-2001	9:00	19.34	31.5	102.4	293	0.97	2.84	9.07	25.8	19.30	4:10PM	JMK	Good
9-11-2001	11:15	19.31	31.5	102.3	293	0.97	2.83	9.07	25.8	19.29	4:25PM	JMK	Good
9-11-2001	10:10	19.29	31.4	102.2	293	0.97	2.84	9.07	25.8	19.28	2:15PM	JMK	Good
12-11-2001	10:15	19.28	31.3	102.2	293	0.97	2.83	9.07	25.7	19.25	3:00PM	JMK	Good
14-11-2001	9:30	19.27	31.4	102.2	293	0.97	2.84	9.08	25.7	19.26	3:00PM	JMK	Good